UNIVERSITÀ POLITECNICA DELLE MARCHE

DIPARTIMENTO DI SCIENZE DELLA VITA E DELL'AMBIENTE

Corso di Laurea Magistrale in Biologia Marina

Classe LM-6 – Biologia

Individuazione di onde di calore nel Mar Adriatico da osservazioni satellitari di temperatura superficiale: applicazione di due diversi approcci.

Detection of marine heatwaves in the Adriatic Sea from satellite observations of sea surface temperature: application of two different approaches.

Tesi di Laurea Magistrale
Di: Giulia Radi

Relatore:
Pierpaolo Falco

Correlatore:
Francesco Memmola

Sessione Straordinaria

Anno Accademico 2022/23

Riassunto

Le onde di calore marino (Marine Heat Waves, MHWs) sono eventi estremi locali, prolungati e insolitamente caldi (Oliver et al., 2021). A seconda della loro intensità e durata, possono avere impatti moderati o dannosi sugli ecosistemi marini e sui relativi servizi che forniscono (Smith et al., 2023). Le MHWs possono derivare da processi atmosferici, oceanici o una combinazione di entrambi e il contributo di questi fattori può variare da evento a evento a seconda della stagione e della posizione geografica (Vogt et al., 2022).

Dalla prima definizione statistica formale (Hobday et al., 2016) che ha permesso uno studio sistematico delle MHWs, un crescente interesse tra la comunità scientifica ha consentito la comprensione dei loro meccanismi, considerando anche che il riscaldamento globale degli oceani sembra rafforzare il verificarsi e la gravità di questi eventi (Holbrook et al., 2019). Una delle regioni particolarmente sensibili alla variabilità climatica e al riscaldamento globale è il Mar Mediterraneo (Pisano et al., 2020). Tale bacino può fornire opportunità per strategie di monitoraggio delle MHWs e mitigazione dei relativi impatti sul comparto biotico.

Da osservazioni satellitari giornaliere della temperatura superficiale del Mar Adriatico rileviamo le MHWs negli ultimi 41 anni (1982-2022) e valutiamo gli effetti indotti dal trend di temperatura sulle proprietà delle MHWs,

analizzandone l'evoluzione in termini di frequenza, intensità e durata. A questo scopo, il metodo di rilevamento delle MHWs viene applicato sia ai dati originali di temperatura superficiale del mare che a quelli cui il trend è stato sottratto.

I nostri risultati mostrano che la presenza di un trend nella temperatura superficiale del mare determina delle MHWs più intense, frequenti e durature. Al contrario, lo stesso metodo di rilevazione applicato ai dati SST a cui il trend è stato sottratto, non presenta cambiamenti significativi nelle caratteristiche delle MHWs nel tempo. In particolare, l'uso dei dati SST originali sottostima il numero di eventi all'inizio del periodo in esame e li sovrastima alla fine. La rimozione del trend permette così di distinguere il riscaldamento a lungo termine da transitori e bruschi cambiamenti della temperatura superficiale del mare evitando di sovrastimare le proprietà delle MHWs nel tempo (Amaya et al., 2023; Martínez et al., 2023).

CONTENTS

ABSTRACT

Ocean temperature variability is a fundamental component of the Earth's climate system, and extremes in this variability affect the health of marine ecosystems around the world. The study of marine heatwaves (MHWs) has emerged as a rapidly growing field of research, given notable extreme warm-water events have occurred against a background trend of global ocean warming. Hence, their correct detection and characterization is crucial to define future impact scenarios, along with adaptation and marine management approaches.

Here, using daily satellite observations of Adriatic Sea surface temperature we detect MHWs over the last 41 years (1982-2022) and evaluate the trend-induced effects on MHWs properties by analysing their evolution in terms of frequency, intensity, and duration. Our results show that the presence of a trend in surface seawater temperature can drive MHW detection toward more intense and frequent MHW events. Conversely, the same detection method applied to detrended SST data do not present any significant change in MHW characteristics over time. Detrending thus allows to distinguish long-term warming (i.e., trend) from transient and abrupt SST changes without overestimating MHW properties over time.

1. INTRODUCTION

1.1 Definition of marine heatwaves (MHWs)

Marine heatwaves (MHWs) - a term first used by Pearce et al. (2011) - are anomalous warm sea-water events that can substantially affect marine ecosystems (Bond et al., 2015; Frölicher and Laufkötter, 2018; Sen Gupta et al., 2020). The study of MHWs have recently become a major concern in climate change research (Marx et al., 2021; Mohamed et al., 2022a) because of their ecological and socioeconomic impacts, including coral bleaching, mortality of benthic communities, decrease in sea surface productivity, and loss of seagrass beds and kelp forests (Garrabou et al., 2009; Eakin et al., 2010; Hughes et al., 2017; Le Grix et al., 2021).

A MHW is qualitatively defined as a discrete period of prolonged anomalously warm water at a particular location. The qualitative definition does not assume any heatwave driver or any specific impact, it can be applied to ocean regions (including subsurface waters, estuarine, or enclosed sea such as the Mediterranean Sea), but may have limited applications in intertidal zones, where ecological responses to high sea temperatures are mediated by air temperature, precipitation and atmospheric conditions (Helmuth et al., 2006). Moreover, this qualitative definition provides flexibility in the way which a

MHW can be defined across multiple end users for their application, but it does not allow for empirical comparisons of the characteristic of MHWs across different events in space and time (Hobday et al., 2016).

Despite the growing scientific interest, there is still not a unique definition of MHW as in each study the definition used may depend upon the parameters selected to define it and the final objectives of the studies. Previous ecological studies defined different approaches to characterize high SST impact on coral reefs (Maynard et al., 2008; Selig et al., 2010). Most marine extreme climate event metrics have been developed to monitor and predict coral bleaching, which is the most advanced field of thermal stress-related marine ecology (Donner et al., 2005; Spillman and Alves, 2009).

More recently, methods for detecting ocean temperature extremes have used a threshold above which any contiguous days of temperature are a single event. In this analysis, the important choice is in defining the threshold, either fixed in time or allowed to vary seasonally or on longer timescales. Hence, MHW quantitative definitions are based on ocean temperatures exceeding a fixed (Frölicher et al., 2018), seasonally varying (Hobday et al., 2016), or cumulative (Eakin et al., 2010) threshold.

Fixed thresholds can be defined by an absolute temperature, based on the thermal limits of marine species (the temperatures above which biological functions become impaired). For example, cumulative temperatures above an absolute threshold have been used for coral bleaching studies (e.g., degree heating days, weeks, and months; Liu et al., 2014). Temporally fixed thresholds can be defined using a relative measure of the temperature variance (e.g., quantiles). While these thresholds are fixed in time, like the absolute thresholds, this measure allows the definition of extreme to come from the time series data distribution itself (Oliver et al., 2021). This approach may be less applicable to a single species, but the results represent a more general quantification of what is extreme in the local context. Fixed thresholds typically only identify warm-season MHWs (Fordyce et al., 2019), therefore they are poor indicators of anomalous warm conditions in other seasons, which may have important consequences for the life cycle and survival of marine species (Ling et al., 2009).

A more versatile method to identify MHWs uses a seasonally varying climatological threshold (Oliver et al., 2021). The climatology is the statistical properties of a time series calculated over a chosen baseline period, preferably a 30-year temperature time series (WMO 2018), including the mean, seasonal

cycle, variance, and quantiles. The method defined by Hobday et al. (2016) uses a local daily upper-percentile climatology as the threshold above which MHWs are detected, coherent with atmospheric heatwave definitions (Perkins & Alexander, 2013). When assessing climate extremes, statistical thresholds have a major advantage over absolute thresholds when analysing the geographical and temporal extent of these events, as they are expressions of anomalies relative to the local climate and thus enable extreme events in different locations to be compared on an equal footing (Rossello´ et al., 2023). On the other hand, absolute SST thresholds can be more suitable for marine science if defined by case-specific environmental metrics to assess ecological impacts. Absolute threshold would only be relevant in terms of impacts in some regions but not in others due to species acclimation (Hobday et al., 2016).

Hobday et al. (2016) offered a MHW definition that has now become the standard among marine scientists. It is based on a seasonally varying statistical threshold set to be the 90th percentile of a local SST calendar-day probability distribution. Moreover, MHWs are defined to be prolonged in time, lasting for 5 or more days and gaps between events of two days or less with subsequent five day or more events will be considered as a continuous event. More recently, some authors (Frölicher et al., 2018; Darmaraki et al., 2019b) have introduced

changes in this definition by using the 99th percentile, allowing the characterization of more intense MHWs.

Various definitions of marine heatwaves as extreme sea temperature events exist to account for its broad applicability, with statistical definitions based on percentile-based thresholds being widespread in the use. The research questions and their application are important factors for selecting a definition, and the availability of long time series data is important for determining reference periods and thresholds (Oliver et al., 2021).

1.2 Dynamical understanding of marine heatwaves

Despite a growing appreciation of their importance, scientific understanding of marine heatwaves is in its infancy compared to that of atmospheric heatwaves. There is limited understanding of the physical processes that give rise to MHWs (Hobday et al., 2016; Perkins-Kirkpatrick et al., 2016), and how large-scale climate variability modulates the likelihood and severity of these events (Holbrook et al., 2019).

The physical processes responsible for MHWs can be explored through the analysis of the heat sources and sinks within the surface mixed layer, which are

reflected in SST variations (Alexander et al., 2000; Deser et al., 2010). To understand the MHW formation, evolution and decay (Benthuysen et al., 2014; Chen et al., 2014; Kataoka et al., 2017) a mixed-layer temperature budget has been used to describe the local processes responsible for changes in surface ocean temperatures. The rate of change of vertically averaged seawater temperature in the mixed layer, or the temperature tendency, is given by the following equation (Moisan & Niiler, 1998)

$$\frac{\partial T_{\mathrm{mix}}}{\partial t} = \frac{Q_{\mathrm{net}}}{\rho c_{\mathrm{p}} H} - u_{\mathrm{mix}} \cdot \nabla_{\mathrm{h}} T_{\mathrm{mix}} + \mathrm{residual} \qquad (1)$$

The left-hand side of the equation (1) shows the rate of change of the temperature in the surface mixed layer (T_{mix}) with time (t). The right-hand side of the equation (1) consists of three terms: air-sea heat flux into the mixed layer, convergence of heat in the mixed layer due to horizontal advection, and a residual term that includes horizontal eddy heat fluxes and the heat flux at the bottom of the mixed layer owing to radiative heat loss, vertical diffusion, entrainment of deeper waters, and vertical advection (Figure 1).

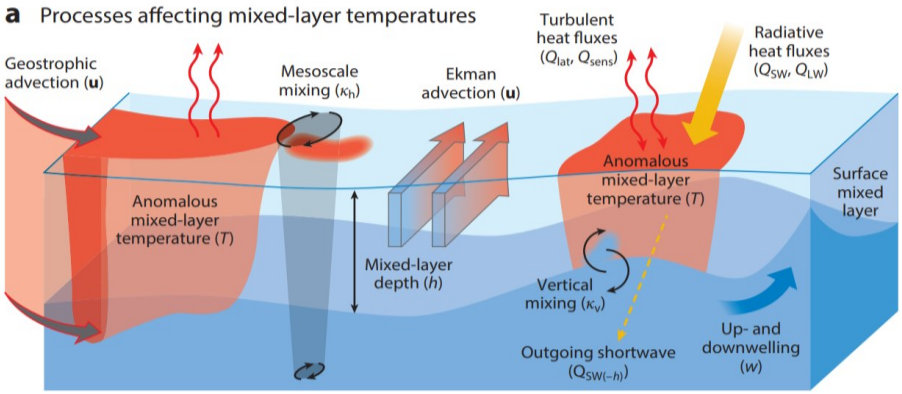

Figure 1. *Physical processes affecting mixed-layer temperatures include the transfer of heat by horizontal advection, air–sea heat flux, lateral and vertical mixing, and entrainment of deeper waters into the mixed layer (Oliver et al., 2021).*

The air–sea heat flux term shows that temperature changes are driven by the net downward heat flux (Q_{net}) scaled by the average seawater density (ρ), the specific heat capacity of seawater (c_p = 4000 J kg^{-1} $°C^{-1}$) and the mixed layer depth (H). The variable Q_{net} itself is composed of the sum of the net shortwave (Q_{SW}) and longwave (Q_{LW}) radiative components minus the fraction of shortwave radiation that escapes out the bottom of the mixed layer [$Q_{SW(-h)}$], as well as the net latent (Q_{lat}) and sensible (Q_{sens}) turbulent heat fluxes (positive into the ocean; Cronin et al., 2019). Except for shortwave radiation, which has a depth structure, these heat fluxes are distributed through the whole mixed layer, and so their effect on temperature tendency is inversely related to the mixed-layer depth (H). MHWs are often associated with anomalous air–sea heat fluxes, which can include abnormally high Q_{SW}, because of less cloud cover and greater insolation, or Q_{sens} when the surface air is warm. Often, both scenarios occur during an atmospheric high-pressure system and coincide with reduced wind speeds that suppress vertical mixing, thereby reducing mixed layer depth. Meanwhile, unusually low latent heat loss from the ocean (negative Q_{lat} anomalies), due to weak surface winds, may also contribute to temperature increases. These processes, which may act independently or simultaneously, are responsible for air–sea heat flux–type MHWs, such as the 2003 Mediterranean Sea MHW (Sparnocchia et al., 2006; Olita et al., 2007).

The horizontal advection term is given by the product between the depth-dependent horizontal velocity vector (u_{mix}) and the horizontal gradient of the mixed layer temperature ($\nabla_h T_{mix}$). Oceanic advective fluxes can drive local temperature changes through horizontal flows across a temperature gradient; examples include strong poleward geostrophic flows in a western boundary current extension region and strong Ekman flows associated with changes in wind stress (Rebert et al., 1985). Anomalous ocean currents or, less often, anomalous temperature gradients are responsible for advective-type MHWs, such as the 2015–2016 Tasman Sea MHW (Oliver et al., 2017).

Vertical temperature advection results from vertical flows in the presence of thermal stratification and is often related to upwelling and downwelling processes. Schaeffer & Roughan (2017) showed subsurface coastal warming associated with downwelling-favourable winds, and Benthuysen et al. (2018) showed warm anomalies and a subsurface MHW owing to anomalous downwelling via a reduction in the expected upwelling for that time of year. Upwelling can also inhibit MHWs by bringing cool water to the surface (DeCastro et al., 2014; Gentemann et al., 2017; Fewings & Brown, 2019).

The remaining terms of the equation are associated with mixing due to horizontal diffusive flux, mixing due to vertical turbulent flux at the base of the mixed layer, and entrainment of waters into the mixed layer due to temporal or spatial variations in mixed-layer depth. These processes are often assumed to account for a smaller proportion of mixed-layer temperature changes associated with MHWs, and so are often neglected or considered part of a residual term (Oliver et al., 2021).

Therefore, to generate MHWs the physical processes described must contribute a sufficiently large net positive temperature tendency to increase the surface ocean temperature over a threshold (Hobday et al., 2016). While the equation explicitly describes temperature variations that extend throughout the mixed layer, MHWs may extend deeper. The expression of surface intensified MHWs may also depend on the state of the subsurface ocean, such as shoaling of the mixed layer base (Benthuysen et al., 2018; Kataoka et al., 2017).

1.3 Measurement of marine heatwaves

Hobday et al. (2016) propose both a general and specific definition for MHWs, based on hierarchical set of metrics that allow for different data sets to be used in identifying MHWs. A hierarchy is useful as different temperature datasets,

based on their spatial and temporal resolution, have different abilities to provide different metrics. Also, it allows some flexibility in the reporting of MHWs, particularly for non-scientific audiences. Once a standard MHW definition is provided, a set of metrics can be derived (Figure 2).

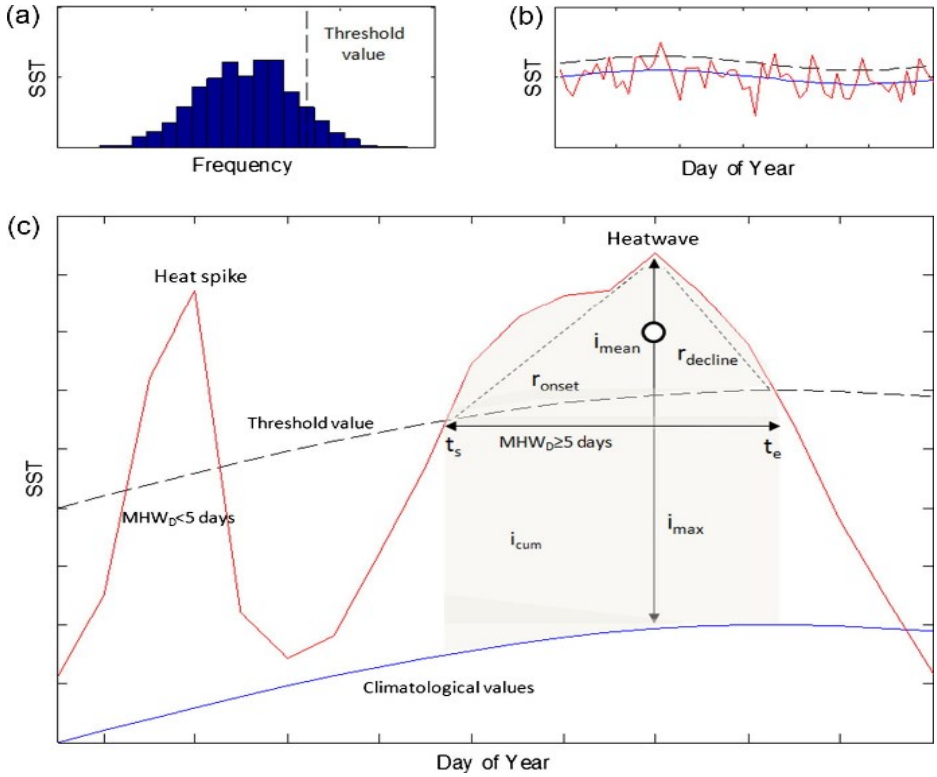

Figure 2. *(a) Threshold values for each location for each day of the year are defined based on the 90th percentile value. (b) These percentile values vary through the year (dashed line), as does the climatological mean (solid blue line). (c) Short duration heat spikes less than five days are not MHWs. A temperature event that is at least five days or longer than this minimum duration is defined according to duration (MHW_D) above the threshold value, intensity (i_{max}, temperature above the climatological mean) and the rate of temperature increase (r_{onset}) and decrease ($r_{decline}$) during the event. The mean event intensity (open circle, i_{mean}) is the mean intensity during the MHW, while i_{cum} (shading) is the sum of daily intensities during the MHW. The start and end days of the MHW are represented by t_s and t_e respectively (Hobday et al., 2016).*

Primary metrics allow for the most general comparison between duration and magnitude (intensity). For a MHW, duration is defined as the period over which the temperature is greater than the seasonally varying threshold value, while the maximum, mean and variance intensity represent the highest temperature and the mean temperature anomaly, and the variation in intensity of the MHW over the duration, respectively. Secondary metrics distinguish the temporal trend (i.e. the rate of event onset and decline), the cumulative intensity, that is the integral of intensity over the duration of the event and the spatial extent of the MHW (i.e the area and the length of the coast where MHW is detected). Tertiary metrics are very specific to the system under investigation, and include preconditioning environmental conditions, that are specific to habitats, regions and species via potential local adaptation to extremes (Table 1; Palumbi et al., 2014).

	Name	Definition		Units
Primary	Climatology	T_m: The climatological mean, calculated over a reference period, to which all values are relative	$T_m(j) = \sum_{y=y_s}^{y_e} \sum_{d=j-5}^{j+5} \frac{T(y,d)}{11(y_e-y_s+1)}$ where j is day of year, y_s and y_e are the start and end of the climatological base period respectively, and T is the daily SST on day d of year y	°C
	Threshold	T_s: The seasonally varying temperature value that defines a MHW (e.g. T_{90} is the 90th percentile value based on the baseline periods)	$T_{90}(j) = P_{90}(X)$ where P_{90} is the 90th percentile and $P_{90}(X)$ where $X = \{T(y,d) \mid y_s \leqslant y \leqslant y_e, j-5 \leqslant d \leqslant j+5\}$	°C
	Start and end of MHW	t_s, t_e: dates on which a MHW begins and ends	t_s is the time, t, where $T(t) > T_{90}(j)$ and $T(t-1) < T_{90}(j)$ t_e is the time, t, where $t_e > t_s$ and $T(t) < T_{90}(j)$ and $T(t-1) > T_{90}(j)$ For MHWs, $t_e - t_s \geqslant 5$, and where gap ⩽2 days (see text)	days
	Duration	D: Consecutive period of time that temperature exceeds the threshold	$D = t_e - t_s$	days
	Intensity (max/ mean/variance)	i_{max}: highest temperature anomaly value during the MHW i_{mean}: mean temperature anomaly during the MHW i_{var}: variation in intensity of the MHW over the duration	$i_{max} = \max(T(t) - T_m(j))$ $i_{mean} = \overline{T(t) - T_m(j)}$ $i_{var} = \sigma_{T(t)}$ where $t_s \leqslant t \leqslant t_e, j(t_s) \leqslant j \leqslant j(t_e)$, σ is the standard deviation, and the overbar indicates the time mean	°C
Secondary	Rate measures	r_{onset}: rate of temperature change from the onset of the MHW to the maximum intensity $r_{decline}$: rate of temperature change from the maximum intensity to the end of the MHW	$r_{onset} = \frac{i_{max} - (T(t_s-1) - T_m(j-1))}{t_{max} - (t_s - 1)}$ $r_{decline} = \frac{i_{max} - (T(t_e) - T_m(j))}{t_e - t_{max}}$ where t_{max} is the time of MHW_{max}	°C/day
	Cumulative measure	i_{cum}: sum of daily intensity anomalies. Note that the integral omits t_e which is below the T_{90} threshold	$i_{cum} = \int_{t_s}^{t_e-1} (T(t) - T_m(j))dt$	°C days
	Spatial extent	A: Area of ocean meeting the MHW definition L: Length of coastline for the MHW	A = area over which MHW detected L = length of coast where MHW detected	km^2 km
Tertiary	Preconditioning factors	Factors such as time of year relative to the onset of the MHW, or periods of above mean temperature preceding the MHW may lead to greater impacts	n/a	Various – specific to study system

Table 1. *Hierarchical classification of metrics proposed by Hobday et al. (2016) used to characterise marine heatwaves. All definitions assume that daily SST data,* T*, and that a MHW has a discrete start day and end day.* T *is both written as a function of time* t*,* T*(t), and as a function of year* y *and day of the year* d*,* T(y, d)*.*

Thus, these consistent set of metrics allows different MHW events to be uniquely described and compared, and comparative analyses, including linking ecological impacts to specific MWH characteristics, can be undertaken.

1.4 Categories of marine heatwaves

As more regional studies have been completed regarding MHWs, scientists have recognized that their impacts can vary dramatically and appear to be context dependent. These differences in the apparent biological and socioeconomic impacts of MHWs suggest that the metrics proposed by Hobday et al. (2016) may be extended to further understand the apparent differences.

Hobday et al. (2018a) provided a refined definition that categorizes the severity of an MHW and allows for the identification of the more extreme events. The categorization scheme is based on intensity (I), which is the sea surface temperature anomaly (SSTA) based on the long-term climatology for a location (Hobday et al., 2016). After an event has concluded, the maximum intensity can be used to categorize the overall event. Categories are delineated by the number of times the maximum observed temperature anomaly is greater than the local difference between the climatological mean and the 90th-percentile threshold, which is the threshold used to identify MHW. Multiples of the 90th

percentile difference (2× twice, 3× three times, etc.) from the mean climatology value define each of the categories: moderate (1–2×, Category I), strong (2–3×, Category II), severe (3–4×, Category III), and extreme (>4×, Category IV; Figure 3).

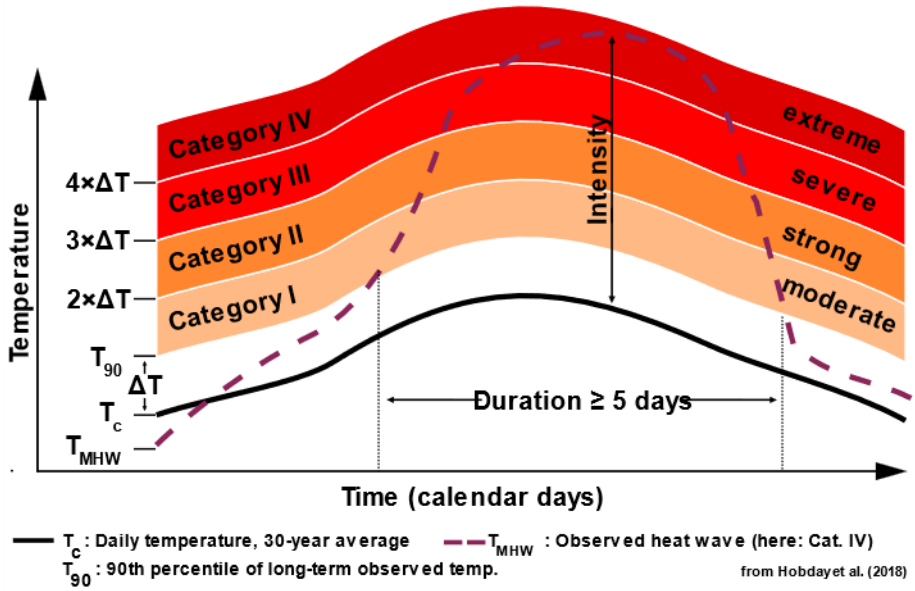

Figure 3. *Categorization schematic for marine heatwaves (Hobday et al., 2018) showing the observed temperature time series (dashed line), the long-term regional climatology (bold line), and the 90th percentile climatology (thin line). Multiples of the local difference between the climatological mean and the climatological 90th percentile describe each of the categories I–IV, with corresponding descriptors from moderate to extreme. This example peaked as a Category IV (extreme) MHW.*

This approach results in a simple numbered system that categorizes the severity of an MHW and can be used to monitor an ongoing event or applied retrospectively given the maximum value reached (Oliver et al., 2021).

1.5 Available datasets

Different datasets may provide substantially different heatwave information despite the use of the same metrics (Hobday et al., 2016). This is generally due

to the resolution of the data, but can also relate to other issues of quality, consistency and instrumentation. Datasets with a high spatial and temporal resolution have more variability than those aggregating across larger areas or based on (smoother) longer time means (Smale & Wernberg, 2009). Not only can different datasets generate different values for the same metric, but certain indices may also simply not be appropriate or derivable from some data sources (Hobday et al., 2016).

Temperature data with daily resolution are ideal to identify and characterize MHWs in a consistent way (Oliver et al., 2021). In addition, the data period needs to be sufficiently long for estimating a climatology (ideally a minimum of 30 years; WMO, 2018). However, Schlegel et al. (2019) showed that as few as 10 years of data may be sufficient for constraining the climatology, and recent studies have used fewer data, from short records or those with temporal gaps, to identify MHWs (Oliver et al., 2017).

Most studies have characterized MHWs using available SST products. Satellite-based SST data sets provide global, continuous, multidecadal, and near-real-time products for the study of MHWs. On local to regional scales, high-frequency subsurface ocean temperatures can be used to construct

climatologies and analyse MHW characteristics (Schaeffer & Roughan, 2017; Benthuysen et al., 2018; Elzahaby & Schaeffer, 2019). However, subsurface measurements are generally available only in select locations (i.e., long-term moorings) or at a lower temporal resolution from depth-profiling drifting floats (e.g., Argo) or gliders. In fact, little is known about the characteristics of MHWs below the ocean surface due to sparsely collected data (Oliver et al. 2021). Therefore, despite the importance of these events for benthic ecosystems, systematic studies of subsurface MHWs are difficult to undertake robustly.

When daily temperature data are not available (some seasonal forecasts and climate models save only monthly data), the ability to apply the formal MHW definitions is limited, given the necessity for daily measurements (Hobday et al., 2016). However, such data have been used to examine longer-lasting MHWs in order to monitor coral bleaching risk (Donner et al., 2005) and perform seasonal forecasting of major events (Doi et al., 2013; Spillman et al., 2013; Jacox et al., 2019). In addition, the monthly temperature variations offer statistical insight into the frequency of extremes, a property that has been used to develop centennial-scale proxies of MHW properties globally (Oliver et al., 2018a).

In global ocean and climate models, SSTs and MHW estimates may have biases if subgrid-scale processes are not represented (Pilo et al., 2019) or do not include feedback from air–sea heat coupling (Frankignoul, 1985). While data sets derived from observations, even coarsely resolved ones, inherently represent the physical processes of the natural world, coarse-resolution ocean models are challenged in representing ocean temperatures at the local scale. In global climate models, issues in representing boundary currents, eddies, teleconnections, coastal processes, and interannual-to-decadal variability will affect SST patterns (Taschetto et al., 2014; Sen Gupta et al., 2016; Power et al., 2017). These shortcomings may be mitigated by bias correction of the SST time series (Oliver et al., 2017; Pilo et al., 2019), but such an approach corrects only for the statistical aspects of the bias and not the underlying issues of poorly captured or unrepresented physical processes. Increases in model resolution and process parameterization may provide some improvements in this regard (Coupled Model Intercomparison Project Phase 6 (CMIP6); Eyring et al., 2016).

Many of the MHW metrics can be calculated from gridded products, such as SST datasets, reconstructed observational data, and model/reanalysis data (Hobday et al., 2016). These provide generally similar quality metrics (Table 2). Where possible, a comparison with in situ data is recommended (Smale & Wernberg, 2009), because they provide high frequency information for the more accurate calculation of intensity and duration. However, these local data would not provide an estimate of the spatial extent of a MHW, while gridded products allow greater spatial inferences.

Data source	Metrics						Other considerations			
	Primary			Secondary		Tertiary				
	Duration (D) [days]	i_{max} [°C]	i_{mean}, i_{cum} [°C days]	Rate of event onset/decay [°C/day]	Spatial area (A) [km^2]	Preconditioning	Length of records	Temporal resolution	Quality control	Data consistency
In situ temperatures (e.g. loggers)	4	4	4	4	1 (if multiple loggers), else N/A	2	High	High	Low	Low/Med
Satellite SST	3	3	3	4	3	3	Med	High	High	Low/Med
Argo floats (NB: gridded products do not provide SST)	N/A	N/A	1	1	2	2	Low	Low	High	Med/High
Reconstructed monthly data (e.g. ERSST, HadISST)	2	2	N/A	2	2	2	High	Low	High	Med
Palaeo-proxy SST (seasonal to annual records, e.g. coral cores)	N/A	N/A	N/A	N/A	N/A	N/A	High	Low	Low	Low/Med
Global Climate Models (e.g. daily SST fields)	2	2	2	3	2	2	High	Low	N/A	High
Re-analysis SST products (e.g. BRAN)	3	3	3	3	3	3	Med	High	Low/ Med	Med/High
Regional Ocean Models (e.g. OFAM)	3	3	3	3	2	2	Low	High	N/A	High
Traditional Ecological Knowledge, citizen science, and anecdotal information	N/A	1	N/A	N/A	N/A	1	Med/ High	Low	Low	Low

Table 2. *Qualitative comparison of different data sources and their suitability to provide primary, secondary and tertiary MHW metrics for sea surface temperature (Hobday et al., 2016). For each option a score is assigned: 1 indicates that only low resolution metrics can be derived and 4 indicates that high resolution metrics can be derived. N/A indicates no utility.*

While coarser resolution datasets may provide information about larger areas and/or longer time periods, this information may not be particularly relevant for marine managers who require accurate local scale information, particularly on magnitude, to assess likely impacts. For other research applications, such as studies of large-scale climate variability, MHW metrics may require further modification based on the resolution of datasets being used (Scannell et al., 2016).

1.6 Marine heatwaves drivers

Most of the available studies on drivers of MHWs focused on specific individual MHW events and predominantly on atmospheric processes, partly due to the greater availability of such data from satellite records and reanalysis data compared to the sparser coverage of oceanic (sub-)surface measurements. Essentially MHWs can be triggered by both large scale and regional atmospheric or oceanic processes, or by a combination of them, acting across a large range of spatial and temporal scales (Holbrook et al., 2019).

However, the drivers of the onset and decline of individual MHW events are diverse and can differ across regions, seasons and may depend on the persistence of the MHW event (Vogt et al., 2022). These processes can range from anomalous air-sea heat fluxes or ocean heat advection through changes in atmospheric circulation associated with large-scale teleconnections to small-scale local mesoscale processes in the ocean (Holbrook et al., 2019; Sen Gupta et al., 2020). The strength of many of these local processes, including surface heat fluxes and vertical mixing, are a function of the overlying atmospheric synoptic conditions (wind stress, cloud cover, humidity, and surface air temperature; Oliver et al., 2021). It has been shown that the prevalent weather patterns of different seasons may lead to different kinds of driving forces

depending on season (Amaya et al., 2020). Sen Gupta et al. (2020) show that the most intense MHWs tend to occur in summer, due to factors such as shallow mixed layer depths and weaker wind speeds, among others.

Key mechanisms that drive temperature changes in the mixed layer include large-scale modes of climate variability that act to modulate the local conditions, either from local sources, for example, extreme ocean-atmosphere coupled feedbacks in the eastern equatorial Pacific during extreme El Niño-Southern Oscillation (ENSO) events, or remote sources via teleconnection mechanisms, for example, the propagation of planetary waves in the atmosphere, that give rise to distant changes in the surface winds and cloud cover, or ocean that can change the depth of the thermocline and drive remote circulation changes (Holbrook et al., 2019, 2020b). The relationship between MHW occurrences and large-scale climate modes are complex as different phases of known climate modes are associated with enhanced or suppressed likelihoods of MHWs (Scannell et al., 2016), and often, multiple climate modes have a significant relationship with increased MHW occurrences at a given location (Holbrook et al., 2019).

ENSO (El Niño-Southern Oscillation) is the dominant mode of interannual climate variability across the globe (McPhaden et al., 2006). It is also a leading cause of MHW occurrences globally (Oliver et al., 2018a), with key influences and impacts in the Indo-Pacific and more distant links to the Atlantic and Southern Oceans (Holbrook et al., 2019, 2020a). Indeed, in the tropical Pacific, two-thirds of documented MHWs have been associated with El Niño events. The onset of El Niño coincides with trade wind weakening and reduced equatorial upwelling with the eastward propagation of warm water anomalies that deepen the thermocline along the equator (McPhaden, 1999). The large increase in SST during El Niño in the eastern tropical Pacific can result in long duration MHW events in this region (Podestá et al., 2021).

MHWs in the middle and high ocean regions have been associated with shifts in warm ocean currents (Caputi et al., 2014; Feng et al., 2013), mesoscale eddy activity, and atmosphere-ocean interactions (Black et al., 2004; Napp & Hunt, 2001). MHWs have also been attributed to anomalous reductions in wind speed and wintertime surface cooling (Chen et al., 2014), shifts in the jet stream position and the weakening of cold-water currents and Ekman pumping (Bond et al., 2015). Furthermore, ENSO teleconnections favour the seasonal persistence of large-scale weather patterns, such as atmospheric high-pressure

ridge systems that cause clear skies, warm air, and reduced wind speeds. These conditions make rapid ocean warming, coupled with increase thermal stratification due to reduced vertical mixing (Overland et al., 2001).

In the North Atlantic and European regions, the North Atlantic Oscillation (NAO) is the most influential large-scale mode of SST and atmospheric variability (Scannell et al., 2016). During its strong positive phases, westerly winds are anomalously strong (Chafik et al., 2017), resulting in more intense storms and higher-than-average air temperatures in northern Europe, increasing the possibility of MHWs in this region. Schlegel et al. (2021) found that MHWs in the Northwest Atlantic tend to be primarily driven by anomalous air-sea heat fluxes during the onset phase, but by oceanic processes during the decline phase. In addition, during cold seasons anomalous air-sea heat fluxes are more important than anomalous horizontal advection for MHW onset and decline in the Northwest Atlantic, while this may be reversed during warm seasons.

In summary, MHWs can result from atmospheric forcing, oceanic processes, or a combination of both, and the contribution of these factors can vary from event to event depending on the season and geographic location. Air-sea interactions, particularly heat and wind fluxes, are the most common causes of recorded

MHWs (Mavrakis and Tsiros, 2019; Smale et al., 2019; Benthuysen et al., 2020; Ibrahim et al., 2021).

1.7 MHW long term-trends and the role of anthropogenic climate change

While anomalously warm seawater events are not a new phenomenon, they have occurred with increasing frequency and duration over the past century (Oliver et al., 2018a) and have had significant impacts on marine ecosystems. Upper ocean temperatures have warmed significantly in most regions of the world over recent decades, with anthropogenic greenhouse gas forcing very likely being the main contributor (Hansen et al., 2010; Stocker et al., 2013; Rey et al., 2020).

Using a multi-data set approach and a unified MHW framework, Oliver et al. (2018a) characterised MHW trends and variability globally. They find that from 1925 to 2016, global average marine heatwave frequency and duration increased by 34% and 17%, respectively, resulting in a 54% increase in the total number of annual MHW days. Given the dependence of MHW characteristics on the underlying SST properties, along with a warming ocean, significant changes in MHW characteristics have been identified over the historical record.

Notably, increases in both the mean SST and the variability of SST can lead to increases in warm temperature extremes (Field et al., 2012).

Remotely sensed SSTs indicate that MHW frequencies range from approximately one to three events per year on average (Oliver et al., 2018a; Figure 4a). The most notable exception is in the eastern tropical Pacific, where El Niño-Southern Oscillation events manifest as individual long-duration MHWs and result in less than one MHW per year on average (Holbrook et al., 2020a). As a global average, MHW frequency increased over 82% of the global ocean (Oliver et al., 2018a). The largest increase occurred in the high-latitude North Atlantic Ocean (north of 50° N; an increase of 2–6 annual events). More moderate increases occurred in the subtropical portions of the North and South Atlantic Ocean, central and western portions of the North and South Pacific Ocean, and parts of the Indian Ocean (1–4 annual events).

Hotspots of high intensity occur in regions of large SST variability (Figure 4b) including the five western boundary current extension regions (+2-5 °C; Chen et al., 2014, Oliver et al., 2017), the central and eastern equatorial Pacific Ocean (+1-4 °C; Echevin et al., 2018) and eastern boundary current regions (+1-3 °C; Rouault et al., 2007). MHW intensity increased in over 65% of the global

ocean, most notably in all five western boundary current regions, areas noted to be warming considerably faster than the global mean rate (Wu et al., 2012, Hu et al., 2015).

The typical duration of MHWs vary considerably across the global ocean (Figure 4c). Typical MHW durations are longest in the eastern tropical Pacific, a region dominated by ENSO SST variability with an average duration of up to 60 days (Holbrook et al., 2020a), and shortest over other tropical regions, typically 5–10 days. Across extra-tropical regions, MHW durations are more uniformly 10–15 days, except for the northeast and southeast Pacific Ocean with up to 30-day mean durations (Di Lorenzo & Mantua, 2016). The global-average duration of MHWs has nearly doubled over the satellite record, particularly over the mid- and high-latitude regions of all ocean basins (Oliver et al., 2018a).

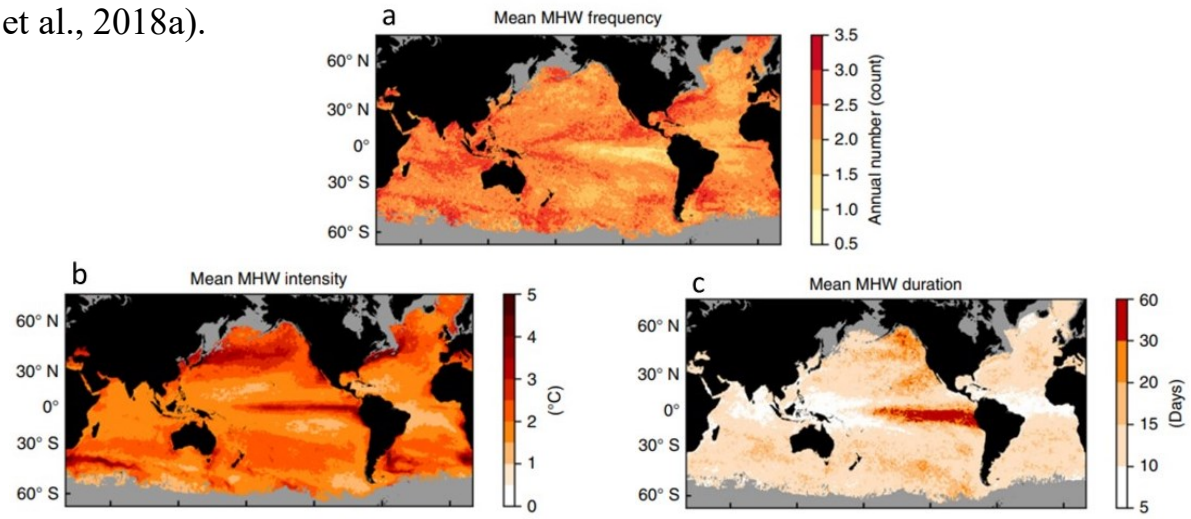

Figure 4. *Mean of (a) MHW frequency (count), (b) MHW intensity (°C) and (d) MHW duration (days) over the 1982–2016 period. MHW properties are computed from NOAA OI SST data (Oliver et al. 2018a).*

The spatial influence of ENSO on the mean and variability of MHW properties is strongest in the eastern tropical Pacific. El Niño events tend to drive long duration, high intensity MHW events there and with a higher frequency. However, ENSO also increases the mean and variability of MHW duration in the northeast Pacific Ocean, the variability of intensity off Western Australia and California and the variability of frequency over much of the Tropics in all ocean basins as well as the mid- and high latitudes in the Pacific Ocean.

In global climate model simulations, substantial increases in global MHW frequency, intensity, duration, and spatial extent were consistent with anthropogenic forcing (Frölicher et al., 2018). These increases are expected to continue under projected future emissions scenarios, and it is possible that much of the global ocean will reach a permanent MHW state by the late twenty-first century (Oliver et al., 2019).

1.8 Marine heatwaves impacts

Marine heatwaves can cause devastating impacts to marine life. In most of the research conducted to date MHWs have been identified and characterized based on sea surface temperature. This focus reflects the relative scarcity of subsurface ocean data, and the reported ecological impacts that are prevalent in

the upper ocean where biological productivity is greatest (Holbrook et al., 2019). However, MHWs are not restricted to the surface and can propagate deeper in the water column (Elzahaby and Schaeffer, 2019). The depth penetration of such warm events also has negative ecological consequences (Schaeffer and Roughan, 2017) and could also impact the mesopelagic habitats (Santora et al., 2020).

Several prominent marine heatwaves have had severe impacts on marine ecosystems in recent years. Notable events occurred in the northern Mediterranean Sea in 2003 (Sparnocchia et al., 2006; Olita et al., 2007), along the Western Australian coast in 2011 (Pearce & Feng, 2013), the northwest Atlantic in 2012 (Chen et al., 2014), the northeast Pacific over 2013–2015 (Di Lorenzo & Mantua, 2016), off southeastern Australia in 2015/16 (Oliver et al., 2018) and across northern Australia in 2016 (Benthuysen et al., 2018). These events resulted in substantial ecological and economic impacts, including sustained loss of kelp forests (Wernberg et al., 2016), coral bleaching (Hughes et al., 2017), reduced surface chlorophyll levels due to increased surface layer stratification (Bond et al., 2015), mass mortality of marine invertebrates due to heat stress (Garrabou et al., 2009), rapid long-distance species' range shifts and associated reshaping of community structure (Cavole et al., 2016), fishery

closures or quota changes (Caputi et al., 2016) and even intensified economic tensions between nations (Mills et al., 2012).

Responses to warming have been observed across biological scales, from genes to ecosystems, in many regions around the world (Doney et al., 2012), with major consequences for human societies (Smith et al., 2021). It is increasingly apparent that biological responses to short-term thermal extremes are wide-ranging and pervasive, and the combination of gradual warming trends and extreme events can drive unprecedented ecosystem change (Harris et al., 2018).

Negative responses of individuals to MHWs vary from sublethal effects on core physiological processes to mortality. Elevated temperatures increase basal metabolic rates, and the energy demand can exceed the metabolic capacity of the species (Lemoine & Burkepile, 2012). Where these debts are not matched by increased energy acquisition, other aspects of performance will be negatively impacted (Begon & Townsend, 2020). In such cases, individuals may modify their behaviour, relocate, and/or adjust their physiology (Smith et al., 2023).

Species with a narrow thermal niche (stenotherms) are more likely to be negatively affected by MHWs than those with broader thermal tolerances (eurytherms), but populations may also respond differently to one another depending on disturbance history (Hughes et al., 2021). Moreover, selection pressure can lead to local adaptation either over many generations in response to gradual warming or much more rapidly through exposure to acute thermal stress (King et al., 2018; Coleman & Wernberg, 2020). Responses include mass mortality events (Pearce et al., 2011; Garrabou et al., 2019; Genin et al., 2020), reproductive failure (Caputi et al., 2016; Shanks et al., 2020), range shifts (Cavole et al., 2016; Lenanton et al., 2017), and establishment of nonnative species (Thomsen & South, 2019; Verdura et al., 2019).

Community- and ecosystem-level impacts of MHWs have been reported across many regions when shifts in foundation species occur (Smale et al., 2019). Specific responses include range shifts that lead to restructuring of entire habitats (Johnson et al., 2003; Wernberg et al., 2016; Eakin et al., 2019), altered community composition (Stella et al., 2011; Vergés et al., 2014; Gómez-Gras et al., 2021a; Serrano et al., 2021), biodiversity loss (Grilo et al., 2011; Verdura et al., 2019), and declines in abundance or shifts in behaviour of large, iconic top consumers (Kendrick et al., 2019). The impacts, however, depend on MHW

characteristics and are not uniform across all species, times, or regions, but can reverberate throughout the food web, directly or indirectly affecting species across multiple trophic levels (Smith et al., 2023).

Extreme temperature events can drive abrupt changes in the structure and functioning of entire ecosystems, with major consequences for marine resource users that depend on the ocean for ecological goods and services (Arias-Ortiz et al., 2018; Ruthrof et al., 2018). Given the expected intensification in ocean temperature extremes due to anthropogenic climate change and the potential for profound ecological and socioeconomic impacts, marine conservation and management approaches must consider MHWs to maintain and conserve the integrity of highly valuable marine ecosystems over the coming decades (Smale et al., 2019).

1.9 Marine heatwaves in the Mediterranean Sea

As a semi-enclosed and relatively small basin, including many coastal areas and islands, the Mediterranean Sea is one of the most vulnerable regions to climate change and responds rapidly to global warming (Giorgi, 2006; Lionello and Scarascia, 2018). The Mediterranean SST has also experienced significant warming as established in recent studies from satellite data (Pastor et al., 2017,

2020; Mohamed et al., 2019), estimated 3.7 times higher than the global ocean trend with basin-averaged trend estimations of sea surface temperature around 0.041 ± 0.006°C/year over 1982–2018 (Pisano et al., 2020), 0.037 ± 0.003°C/year over 1982– 2019 (Von Schuckmann et al., 2020) and 0.038 ± 0.002°C/year over 1982–2020 (Juza and Tintoré, 2021). The authors also highlighted the strong spatial variability in SST trend estimations. Trend values over 1982–2020 have been estimated at 0.032 and 0.044 ± 0.002°C/year as averages in the western and eastern Mediterranean, respectively (Juza and Tintoré, 2021), and at 0.033 ± 0.004°C/year in the Ionian and Levantine Seas (Ibrahim et al., 2021). The rapid sea surface warming trend in this ocean basin has been linked to the increasing occurrence of MHWs in the last decades (Ciappa, 2022).

Regarding the characterization of MHWs in the Mediterranean basin, a growing trend has been found in terms of frequency, duration, and intensity that accelerated since 2000 and especially in the last decade (Pastor & Khodayar, 2023), pointing not just to a steady intensification and higher frequency of MHWs but to the emergence of a new set of more intense, long-lasting and spatially extensive MHWs in the recent years (Darmaraki et al., 2019a). Ibrahim et al. (2021) examined the spatial variability and trends of MHWs in

the Eastern Mediterranean basin from 1982 to 2020 and found that the mean frequency and duration of MHW have increased by 40% and 15%, respectively, over the past two decades. Recently, Juza et al. (2022) studied subregional MHWs in the Mediterranean Sea between 2012 and 2020. They found that subregional trend estimates for mean and maximum MHW intensity, mean duration, and number of events varied by 0.06-013 °C/decade, 0.26-0.55 °C/decade, 1.23-3.82 days/decade, and 1.1-1.8 events/decade, respectively. In addition, the study concluded that the most intense and near-surface events preferentially occur in summer and fall when the water column is most stratified, and that MHWs propagate deeper in the water column in winter when wind-driven vertical mixing weakens the stratification.

MHWs in the Mediterranean have been related to large-scale atmospheric anomalies (e.g., persistent high-pressure system) inducing hot and dry weather as the extreme event occurred in the summer of 2003 (Holbrook et al., 2019), where surface anomalies of 2-3 ◦C above climatological mean lasted over a month due to significant increases in air temperature and a reduction of wind stress and air-sea exchanges (Sparnocchia et al., 2006; Olita et al., 2007). These factors seem to have also triggered an anomalous SST warming in the eastern

Mediterranean area during the heatwave of 2007, at the order of + 5 °C above climatology (Mavrakis and Tsiros, 2019).

Besides, for the Mediterranean basin extreme warming episodes were reported in the summers of 1999 (Perez et al., 2000; Cerrano et al., 2000; Garrabou et al., 2001), 2003 (Garrabou et al., 2009; Schiaparelli et al., 2007), 2006 (Kersting et al., 2013) and 2008 (Huete-Stauffer et al., 2011) affecting a wide variety of species and taxa up to 50 m deep (e.g., gorgonians, sponges, and seagrass *Posidonia oceanica* meadows; Rivetti et al., 2014). According to Coma et al. (2009), most of the mass mortalities documented in the basin were related to positive thermal anomalies in the water column that occurred regionally during the summer. MHWs can be especially lethal for organisms with reduced mobility that are usually limited to the upper water column. Their severity is determined by both temperature and duration (Galli et al., 2017).

1.10 Baseline periods for marine heatwave analyses

Given that MHWs are identified by ocean temperatures much higher than typical conditions, generally defined upon a reference climatology, the definition of the latter is crucial, as they will strictly affect the detection's derived results (Oliver et al., 2021). This consideration becomes even more

compelling under the effect of climate change that produces sustained ocean warming, introducing a positive trend in the temperature time series or, in other words, a shift of typical conditions (Martínez et al., 2023). The problem is quite general and has been recently shown to affect any percentile-based indices of extreme values (Dunn and Morice, 2022).

Indeed, various studies indicate that most of the changes in the variability of MHWs, if defined relative to a fixed temperature climatology, are associated with, and driven by, a slow warming term (Frölicher and Laufkötter, 2018; Frölicher et al., 2018; Oliver et al., 2018; Jacox, 2019; Oliver, 2019; Schlegel et al., 2019; Ciappa, 2022). Similarly, recent research evidenced that the intensification in the main MHW properties, i.e., intensity, duration, and frequency, is mainly due to the historical trend that, accelerating over the past decades, has shifted the mean SST to become increasingly warmer in most ocean regions (Xu et al., 2022). Thus, the temperature records will move further away from the climatological values as time goes by, even in the absence of extreme events (Chiswell, 2022).

Recently, Amaya et al., (2023) discuss how the MHW definition based on a fixed climatology - extreme conditions compared with historical temperatures

- and the MHW definition based on a shifting baseline - extreme conditions compared with an evolving ‘new normal’ of rising temperatures owing to climate change - lead to different interpretations and estimates of the properties and trends of present and future MHWs. The fixed baseline approach doesn’t consider that oceans are getting warmer over time because of climate change. Ocean surface waters have warmed at an average rate of 0.06 °C per decade since pre-industrial times (IPCC, 2021), and over the coming decades, more frequent and more intense marine heatwaves are projected (Oliver et al., 2021), until the oceans warm so much that they reach a ‘perpetual heatwave’ state. Instead, shifting baseline conditions accounts for long-term ocean warming separately and effectively subtracts that from the total. From this perspective, in the future, ocean temperature anomalies would have to be much warmer than those derived from a fixed historic baseline to qualify as a marine heatwave. This definition retains the idea that a heatwave should be an exceptional event in time and space, a central tenet of the original, qualitative definition of marine heatwaves proposed by Hobday et al. (2016).

Thus, according to their recommendations, the phrase ‘long-term temperature trends’ should be used to describe the slow changes in ocean temperature occurring over decades or longer, while the term ‘marine heatwave’ should be

reserved for ocean temperature changes that are transient and extremely warm relative to the expected conditions for a given place and time, as defined by an evolving, recent climatological reference period. Finally, use the term ‘total heat exposure’ to describe the combination of long-term warming and marine heatwave.

2. AIM OF THE STUDY

Marine heat waves (MHWs) are local, prolonged, anomalously warm sea temperature extreme events. Depending on their intensity and duration, these events can have moderate to extreme impacts on living organisms, marine ecosystems, and the related services they provide (Smith et al., 2023). Since the first formal statistical definition that allowed a systematic study of these extreme warm water events was put into use (Hobday et al., 2016), there has been increasing interest among the scientific community to advance the understanding of their mechanisms, also considering that concurrent global ocean warming seems to strengthen the occurrence and severity of these events (Holbrook et al., 2019; Oliver et al., 2021). The influence of a warming trend becomes remarkable in regions particularly sensitive to climate variability and global warming, as is the case of the Mediterranean Sea (Pisano et al., 2020). The aim of this work is to evaluate the trend-induced effects on Adriatic MHW properties and change points in annual MHW metrics. To this purpose, the MHW detection technique is applied to both original and detrended SST data, the latter obtaining by removing the trend. Both detections are based on fixed climatology baselines over the same period. The purpose of detrending is to separate the effect of continuous warming from abrupt variations (Amaya et al., 2023; Martínez et al., 2023).

3. DATA AND METHODOLOGY

3.1. Satellite SST data

Satellite observations are the main data source for SST and MHW global or regional analysis that offer long time series with enough spatial coverage at high spatial resolution (Pastor & Khodayar, 2023). In this work, marine heatwaves were detected from a stable and consistent long-term, namely, multi-year, sea surface temperature (SST) dataset over the Mediterranean Sea (SST_MED_SST_L4_REP_OBSERVATIONS_010_0211), specifically designed for climate applications and distributed within the Copernicus Marine Environment Monitoring Service (CMEMS; Le Traon et al., 2019). It consists of daily optimally interpolated (level 4, L4) satellite-based estimates of the foundation SST (namely, the temperature free, or nearly free, of any diurnal cycle) at a 0.05° resolution grid covering the period from 1 January 1982 to the present (currently up to 6 months before real time; Merchant et al., 2019). For our analysis we consider SST time series over the Adriatic Sea (12-20E, 40-46N) for the period 1982-2022.

Furthermore, the product is built from a consistent reprocessing of the collated level 3 (merged single-sensor, L3C) climate data record provided by the ESA Climate Change Initiative (CCI) and the Copernicus Climate Change Service

(C3S) initiatives (Buongiorno Nardelli et al., 2013; Pisano et al., 2016), but also includes in input an adjusted version of the AVHRR Pathfinder dataset version 5.3 to increase the input observation coverage (Korak et al., 2018). This product is freely available through the Copernicus Marine Service catalogue (doi.org/10.48670/moi-00173).

3.2. Study area

The Adriatic Sea is an elongated basin, with its major axis in the Northwest–Southeast direction, located in the central Mediterranean, between the Italian peninsula and the Balkans. The basin shows clear morphological differences, along its longitudinal axis and the transversal one as well, and it is divided into three sub-basins (Artegiani et al., 1997a). The northern sub-basin spans from the northernmost part to the 100 m bathymetric line (in front of Giulianova, Italy) and it is very shallow and gently sloping, with an average bottom depth of about 35 m. The middle Adriatic spans from the 100 m contour to the Pelagosa sill, is 140 m deep on average with the two Pomo depressions reaching 260 m. The southern sub-basin extends from Pelagosa sill to Otranto sill and it is characterized by a wide depression more than 1200 m deep. Water exchange with the Mediterranean Sea takes place through the Otranto Channel, having an 800-m deep sill (Russo & Artegiani, 1996).

The Adriatic Sea is a dilution basin (precipitation plus river runoff is greater than evaporation, with a fresh water gain of 1.14 ± 0.20 m per year). At the same time the Adriatic Sea imports heat (it has been computed that there is a surface heat loss of 19-22 W/m^2 per year); hence salt and heat balances are maintained through the water exchanges across the Otranto Straits, where relatively fresh and cold waters leave the Adriatic basin and warmer, saltier waters enter from the Ionian Sea in the Adriatic Sea (Artegiani et al., 1997a). Due to the geographical position, its orography and bathymetry, the Adriatic Sea hydrography is strongly influenced by meteorological conditions, particularly in the north. Climatologically, temperature variations greater than 20°C are observed between winter and summer, and about 8°C from north to south in winter, as well as a salinity gradient of about 3 psu between the western coastal water and the offshore water (Artegiani et al., 1997a).

The Adriatic Sea general circulation is cyclonic with a flow towards the northwest along the eastern side (Eastern Adriatic Current) and a return flow towards the southeast along the western side (Western Adriatic Current; Artegiani et al., 1997b). The circulation regime is strongly influenced by winds, with significant differences between winter, mainly Sirocco (SE) and Bora (NE), and summer, mainly Mistral (NW) (Russo and Artegiani, 1996). In

particular, the cold Bora wind, occurring frequently in fall and winter seasons, plays a significant role in determining the cooling and mixing of the water column and in the formation of Northern Adriatic Dense Water (NAdDW), flowing then southward (Bergamasco et al., 1999; Marini et al., 2006; Vilibic and Supic, 2005).

In the present study, we consider the northern Adriatic Sea (NAS), a shallow and semi enclosed continental shelf delimited by the 100 m isobath, characterized by a high freshwater input and by a prevalent cyclonic circulation of the water masses (Artegiani et at., 1997a). The hydrodynamic behaviour of this area is rather complex, and a number of important physical and biogeochemical processes occur there. River discharges, in particular by the Po River (mean daily flow rate of 1500 m3/s; Cozzi & Giani, 2011), drive the stratification of the water column and affect both the thermoaline circulation and the trophic state, by introducing a large amount of nutrients (Brush et al., 2021; Degobbis et al., 2000; Marini et al., 2008). They cause the outflowing of fresher and nutrient-rich waters southward by the Western Adriatic Current (Artegiani et al., 1997b; Campanelli et al., 2011) and the Eastern Adriatic Current flows northwards along the eastern coast, bringing Ionian saltier, warmer and more oligotrophic waters (Poulain & Cushman-Roisin, 2001).

For MHWs analyses, we divided the NAS in six sub-areas, based on depth and/or trophic conditions: (i) the Po River area (PR) strongly affected by the Po river outflow and by the Western Adriatic Current (therefore, more eutrophic), (ii) the Venice Lagoon (VL), (iii) the Gulf of Trieste (GoT), (iv) the Eastern Coast (EC) affected by the Eastern Adriatic Current (therefore, more oligotrophic than the PR area), (v) the remaining sub-area with depth <40 m (L40) and (vi) that > 40 m (H40) (Figure 5).

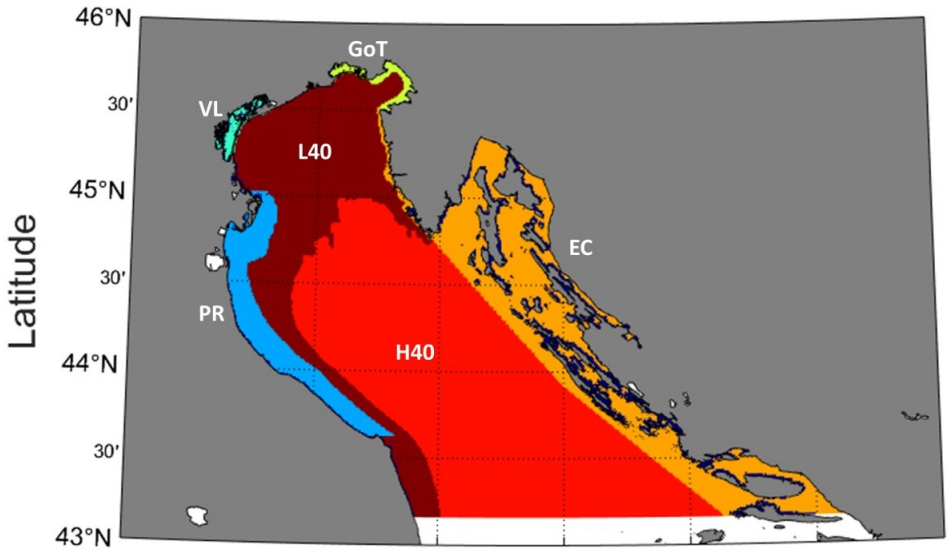

Figure 5. *Division of northern Adriatic Sea (NAS) in six sub-areas: (i) Po River area (PR, blue), (ii) Venice Lagoon (VL, green), (iii) the Gulf of Trieste (GoT, yellow), (iv) the Eastern Coast (EC, orange), (v) the remaining sub-area with depth <40 m (L40, brown) and (vi) that > 40 m (H40, red).*

3.3. Separating long-term trend and extreme variability

To separate the warming trend contribution in the MHW analysis, we apply a detrending pre-processing step before computing the baseline climatology. This consists in computing the pixel-wise trend component over the whole period of

study, removing it from the SST time series, obtaining what we call detrended data, and pursuing MHWs detection on such series (Martínez et al., 2023).

The trend component has been computed using Singular Spectrum Analysis (SSA), a non-parametric multivariate statistical method (Golyandina and Nekrutkin, 2001; Hassani, 2007; Golyandina and Zhigljavsky, 2013). SSA is a consolidated technique used to identify the main patterns of variability in a given set of observations and has been successfully applied in many contexts including climate series (Ghil and Vautard, 1991; Schoellhamer, 2001; Macias et al., 2014; Beşel and Tanir Kayikçi, 2020; Yi and Sneeuw, 2021). SSA extracts the minimum independent information by which the entire original dataset can be reconstructed. The trend component is identified through the first singular value.

In MATLAB we applied the function ‘trenddecomp’ to decompose the daily SST time series. This function finds trends in data using Singular Spectrum Analysis (SSA), which assumes an additive decomposition of the data such that:

$$SST = LT+ST+R \quad (2)$$

In this decomposition model (2), SST is given by the sum of three different factors: LT is the long-term trend in the data, ST is the seasonal or oscillatory trend, and R is the remainder (Figure 6).

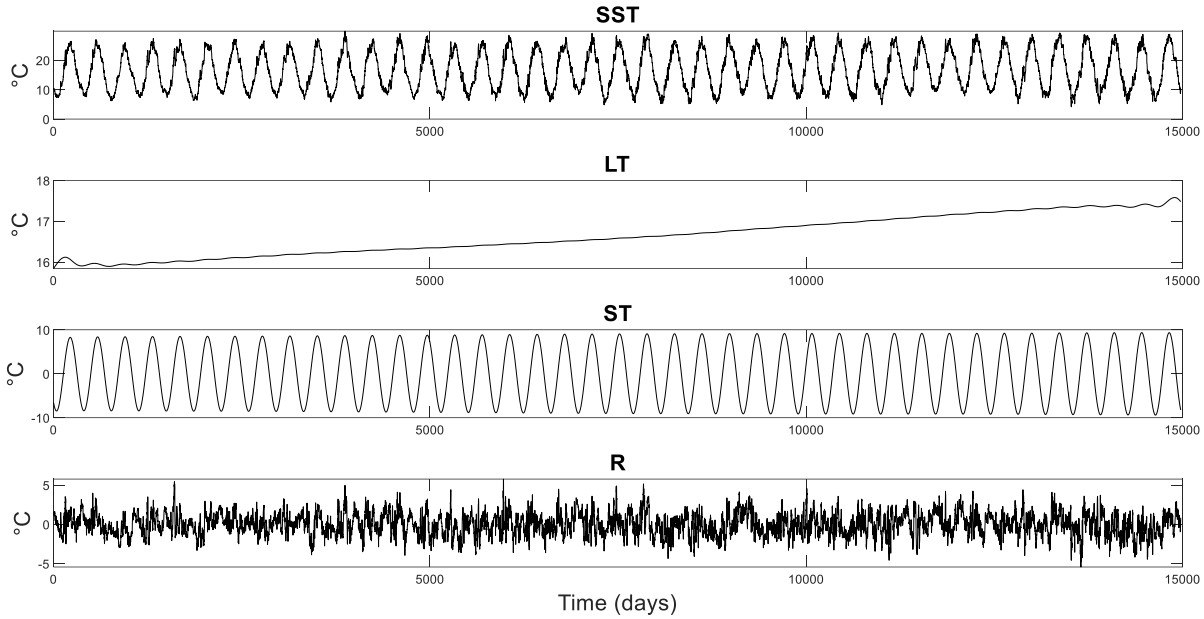

Figure 6. *Additive decomposition of daily sea surface temperature (SST) from 1° January 1982 to 31st December 2022 using Singular Spectrum Analysis method in long-term trend (LT), seasonal trend (ST) and the remainder term (R). All variables are expressed in degrees Celsius (°C).*

The pixel-wise detrended SST time series is computed by subtracting the pixel-wise trend component (LT), which is a continuous interannual trend signal, whose slope gives the trend estimate (Martínez et al., 2023), from the original pixel-wise SST time series (3).

$$SST_{detrended} = SST_{original} - LT \quad (3)$$

3.4. Marine heatwaves identification

In the present study, we use the MATLAB toolbox M_MHW (Zhao and Marin, 2019) designed to detect and analyse MHWs, which includes functions for detecting, visualizing and calculating mean states and annual trends for MHW metrics. It is designed to determine spatial MHWs, i.e. events in each grid of the dataset, according to the standard MHW definition proposed by Hobday et al. (2016), which is "an abnormally warm water event that lasts at least 5 days with SST above the seasonally varying 90th percentile threshold for that time of year." According to Hobday et al. (2016), the baseline SST climatology should be based on at least 30-year of data.

In our work we compute, for both time series (original and detrended), the fixed climatology baseline and the 90th percentile threshold at each grid cell for each calendar day of the year using daily SST data over a 40-year historical baseline period. The fixed climatology baseline is computed as the daily average over the whole period 1982–2022. In practice, the average of each calendar day is calculated across all years and the climatology then coincides with the annual cycle. Given the baseline climatology as the reference at each grid point (i.e. pixel), an MHW is detected whenever an SST value (original or detrended) at each grid point exceeds the 90th percentile threshold for at least 5 days (Hobday

et al., 2016). If this occurs, a set of metrics characterizing an MHW event can be computed. In the present study, the following are considered:

- duration of the event, defined as the pixel-wise number of days for which SST exceeds the 90th percentile for each event;
- frequency, defined as the pixel-wise count of events over the whole period;
- maximum and mean intensity, defined as the pixel-wise maximum and average SST anomalies during each event and expressed in °C;
- cumulative intensity, the pixel-wise integral of the intensity over the duration of the event and expressed in °C day.

In addition, mean states and annual linear trends of MHW metrics are computed over the last four decades from 1982 to 2022 to estimate long-term changes in MHW characteristics. For duration and the intensity metrics this was the average of these properties across all events in each year. Two additional annual metrics were also calculated: “frequency”, the count of events in each year, and “total MHW days”, the sum of the durations of all events in each year. The annual mean and linear trend, estimated by Ordinary Least Squares including a 95% confidence interval, were calculated for each annual time series for the whole Adriatic Sea.

Then, the annual MHW metrics were spatially averaged over each of the sub-areas defined in section 3.2 to generate a set of 6 regional annual MHW metrics (i.e frequency, duration, total days, maximum and mean intensity, and cumulative intensity) covering 1982–2022 period. The same procedure was applied to the annual MHW metrics calculated from the SST detrended data.

3.5. Trend detection and break point analysis method

To assess whether a monotonic upward or downward trend in the annual MHW metrics over each sub-area, computed over SST original and detrended data, exists against the null hypothesis of no trend two different statistical tests were applied.

Simple linear regression is a statistical method used to model the relationship between a dependent variable and a single independent variable (DuMouchel & O'Brien, 1989). When applied to a time series to estimate the trend magnitude, the independent variable typically represents time. The goal is to quantify and understand the linear trend in the time series over time (Holland & Welsch, 1977). Trends magnitude was estimated by Least Squares method and the statistical significance of the slope coefficient was assessed by a t-test with a 95% confidence level ($p < 0.05$). Moreover, the coefficient of

determination, commonly denoted as R-squared (R^2), measure in a regression model the proportion of variance in the dependent variable that can be explained by the independent variable. Essentially, it shows how well the data fit the regression model.

Another test used to discover trends in the annual time series is the Mann–Kendall rank-based test (Mann, 1945; Kendall, 1975). Among advantages of this test is that it does not require a normal distribution of the data, the presence of outliers does not significantly affect the test results and its power is comparable to that of other similar statistical tests. Trends magnitude was estimated by the Sen's slope method (Sen, 1968) based on Kendall's tau. It can be significantly more accurate than simple linear regression for skewed and heteroskedastic data and competes well against simple least squares even for normally distributed data. The significance level for the trend estimate has been fixed at 95% ($p < 0.05$).

Finally, the Pettitt's test (Pettitt, 1979) consists of a non-parametric approach to detect the likely location of a single change point in time series data. The test is a rank-based and distribution-free method used when the exact time of the

change is unknown. A change point can be defined as a point in time when the variable under study undergoes an abrupt change.

Single mass curve is a graphical representation of the accumulate values of a variable against the time period. It consists of plotting the accumulate values of the annual MHW metrics on y-axis and time on x-axis. The slope of the cumulative curve represents the rate of change of the variable with respect to time at that time. It helps in understanding trends, identifying periods of rapid change or stability, and assessing the overall behaviour of the variable over time. In this study, single mass curve has been used as a further confirmation of the change points detected by the Pettitt's test.

4. RESULTS

4.1. Mean states and long-term trends in the Adriatic Sea

The 2D maps of the annual MHW metrics averaged over the whole period 1982–2022, computed on SST original and detrended data, show a spatial variability in the Adriatic Sea, highlighting longitudinal and latitudinal differences in MHW characteristics. The MHW properties showed a similar pattern of spatial distribution and magnitude for both temperature dataset (Figure 7, 8).

Considering the MHW metrics calculated on SST original data (Figure 7 A-F), we see that the mean annual MHW frequency varies between 1.3 and 2.3 annual events with maximum values recorded in the northern sub-basin as well as along the Adriatic western coast. The mean MHW duration over 1982–2022 range between 9.8 and 15.4 days, and the mean annual MHW total days oscillates between 17 and 27 days, with maxima detected in the northern basin, in the eastern and western coast and minima in the southern Adriatic Sea. The mean and maximum annual MHW intensities show the same pattern of spatial distribution with slightly different magnitudes, 1.75-2.93°C and 2.19-3.73°C respectively. The most intense MHWs are observed in the northern part of the Adriatic Sea. The mean annual cumulative MHW intensity varies considerably

across the region, with values between 19 and 38°C days, since it is influenced by both MHW intensity and duration, and it exhibits the same spatial pattern. However, duration appears to play a dominant role and so the middle and southern part of the basin with shortest duration events also appear to have the smallest mean values of cumulative intensity.

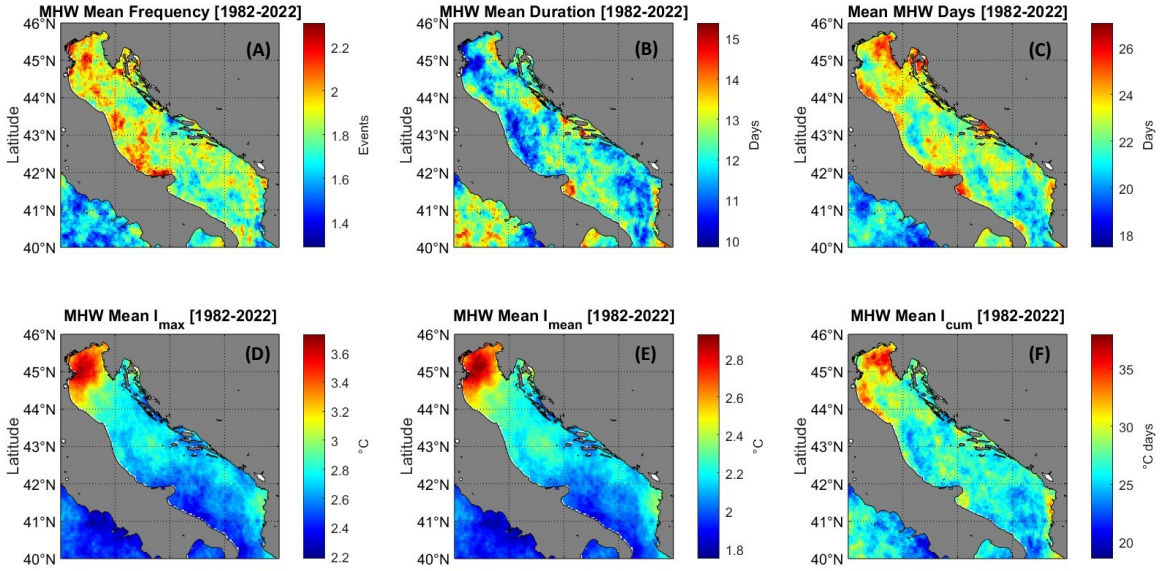

Figure 7. *The Adriatic MHW metrics, computed on original SST data, over the 1982-2022 period, averaged time series of (A) mean MHW frequency (events), (B) mean MHW duration (days), (C) mean MHW total days (days), (D) mean maximum MHW intensity Imax (°C), (E) mean MHW intensity Imean (°C) and (F) mean MHW cumulative intensity Icum (°C days).*

The detrended annual MHW metrics (Figure 8 A-F) show similar values to the original ones. The frequency of events is between 1.3 and 2.6 annual events with the coastal areas the most affected, the mean MHW duration also varies from 9.5 and 15.3 days and the total number of MHW days per year oscillates between 17 in the southern basin and 26 days in the northern part and along the western Adriatic coast. MHW mean and maximum intensities exhibits the same

pattern of spatial distribution with slightly different magnitudes, 1.61-2.75°C and 2.03-3.52°C respectively. The most intense MHWs are observed in the northern part of the Adriatic Sea. Cumulative intensity varies between 16 and 36°C days with the highest values found in the northern Adriatic Sea.

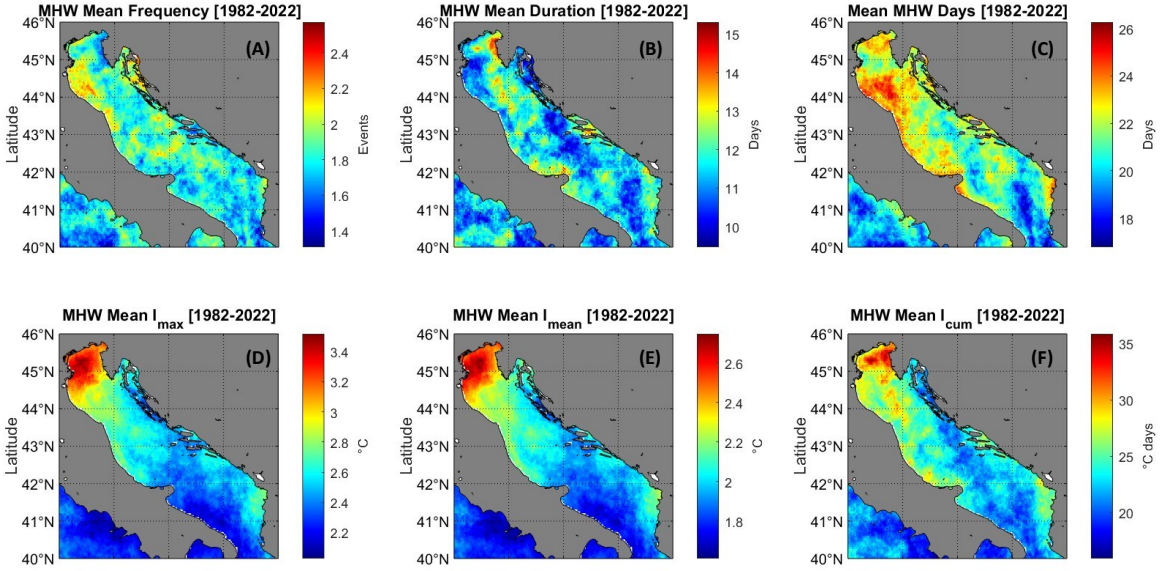

Figure 8. *The Adriatic MHW metrics, computed on detrended SST data, over the 1982-2022 period, averaged time series of (A) mean MHW frequency (events), (B) mean MHW duration (days), (C) mean MHW total days (days), (D) mean maximum MHW intensity Imax (°C), (E) mean MHW intensity Imean (°C) and (F) mean MHW cumulative intensity Icum (°C days).*

The linear trend of MHW metrics, calculated for the entire Adriatic Sea from 1982 to 2022, and their significance was tested with a 95% confidence interval ($p < 0.05$). Figure 9 A-F and Figure 10 A-F depicts the spatial distribution of trends per decade of the Adriatic MHW metrics, which are overlaid with no significant values ($p > 0.05$) for the entire study period. Long-term trends in MHW properties, calculated on SST original data (Figure 9 A-F), are clearest in frequency and total MHW days. Indeed, MHW frequency exhibits a

statistically significant positive trend across all the basin as well as total annual MHW days, ranging over 0.6-1.5 events/decade and 11-21 days/decade, respectively. The spatial pattens of duration and cumulative intensity are nearly identical, with significant trends oscillating between -0.9 and 6.3 days/decade and -3 and 10°C days/decade, while there is no clear trend for mean and maximum intensity (-0.26 and 0.23°C/decade and -0.30 and 0.33°C/decade, respectively) with extensive areas without significant changes, except in near-shore areas, such as Venice Lagoon.

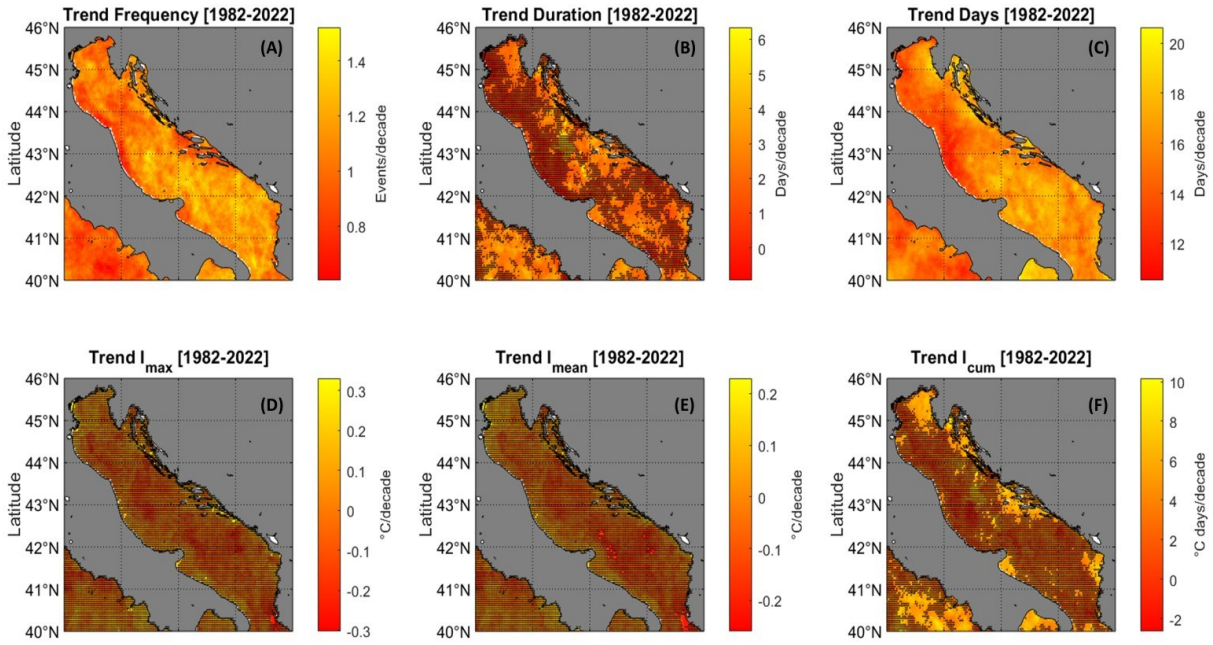

Figure 9. *MHW trends, calculated on SST original data, over the 1982-2022 period of (A) frequency (events/decade), (B) duration (days/decade), (C) total days (days/decade), (D) maximum intensity Imax (°C/decade), (E) mean intensity Imean (°C/decade) and (F) cumulative intensity Icum (°C days/decade). The black dots indicate the trend is not significant (p>0.05).*

Conversely, the detrended MHW metrics (Figure 10 A-F) exhibit greater temporal stability and more consistent values over time indicating that the influence of long-term trend in SST has been removed from the analysis. No

significant positive changes are detected for MHW frequency and total days, which remain stable over time or even statistically decrease (-0.6 and 0.4 events/decade and -6 and 1.8 days/decade, respectively). MHW duration and cumulative intensity exhibits almost the same trend spatial pattern ranging over -5.4 and 2.2 days/decade and -10 and 8°C days/decade, with significant negative trends in the northern Adriatic Sea. MHW mean and maximum intensity show significant trends over the study period in most the Adriatic basin (-0.05 and 0.33°C/decade and -0.16 and 0.42°C/decade).

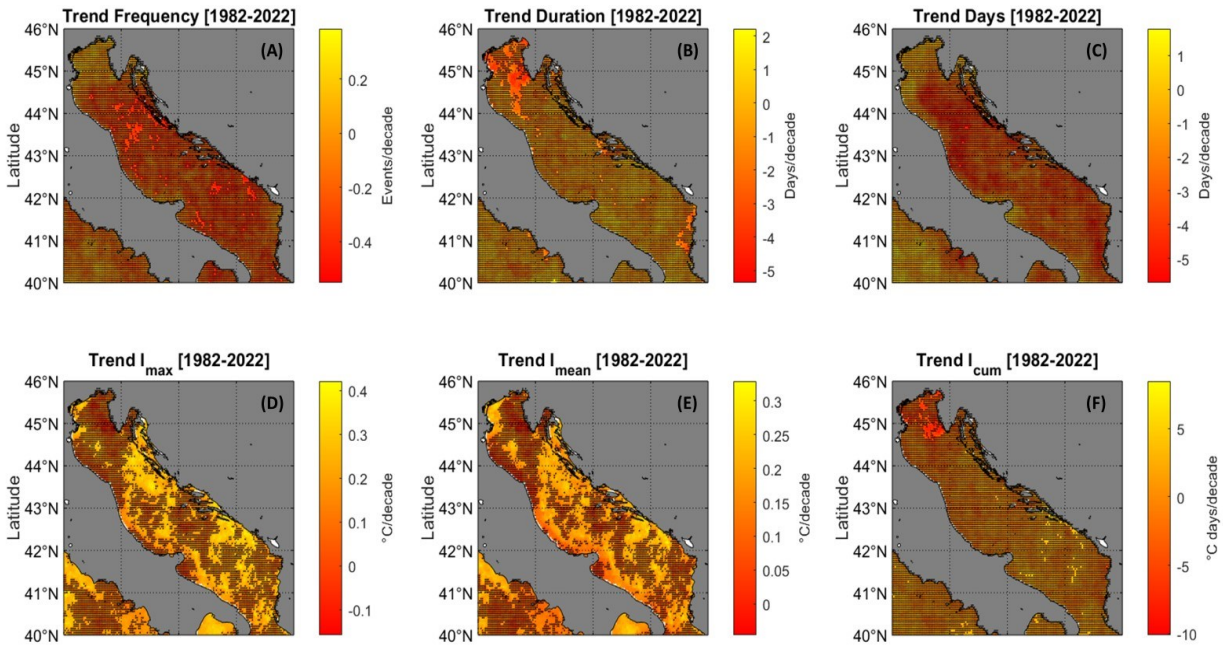

Figure 10. *MHW trends, calculated on SST detrended data, over the 1982-2022 period of (A) frequency (events/decade), (B) duration (days/decade), (C) total days (days/decade), (D) maximum intensity Imax (°C/decade), (E) mean intensity Imean (°C/decade) and (F) cumulative intensity Icum (°C days/decade). The black dots indicate the trend is not significant (p>0.05).*

4.2. Change in MHW statistics over northern Adriatic sub-areas

The spatially averaged annual time series of the MHW metrics, obtained from the original and detrended detections, clearly evidence the different impact of the two approaches for all the northern Adriatic sub-areas. When the original detection is applied, a clear positive and statistically significant trend is found for nearly all MHWs statistics (Figure 11-16; Table 3). The situation is very different for the detrended case, where almost all MHW metrics do not any significant trends (Figure 11-16; Table 4), thus appearing more stable over the whole period. In Figure 11-16, the spatial average of annual MHW metrics and change points for each sub-area are represented.

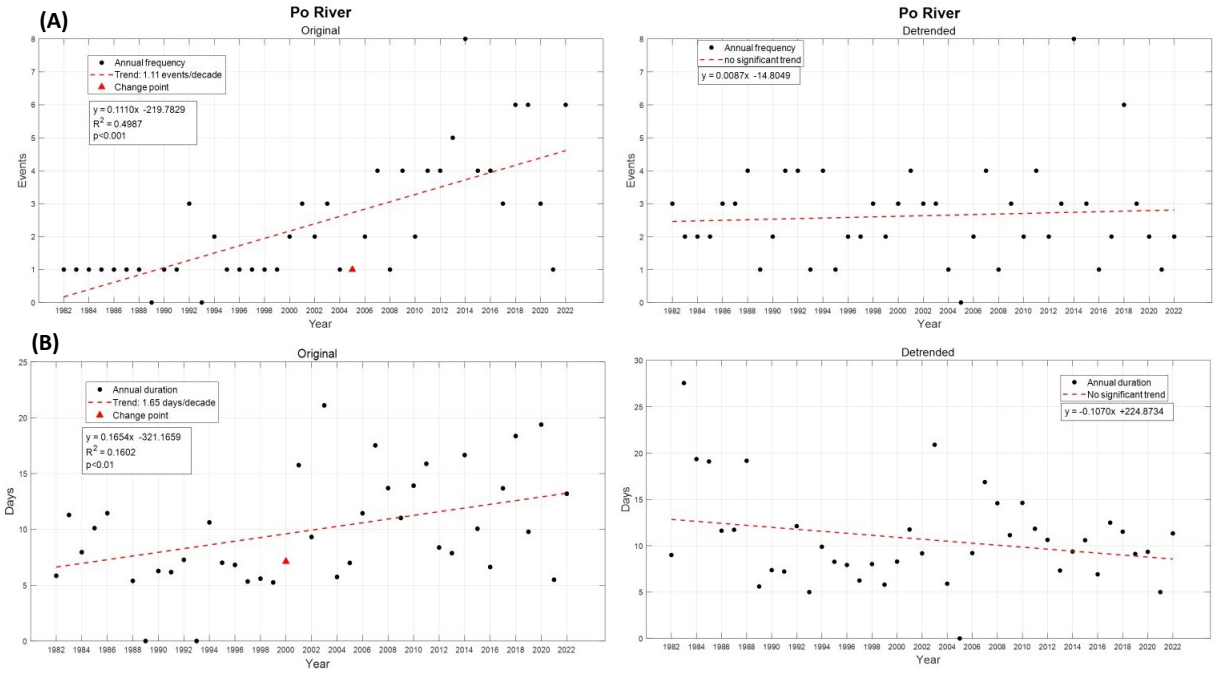

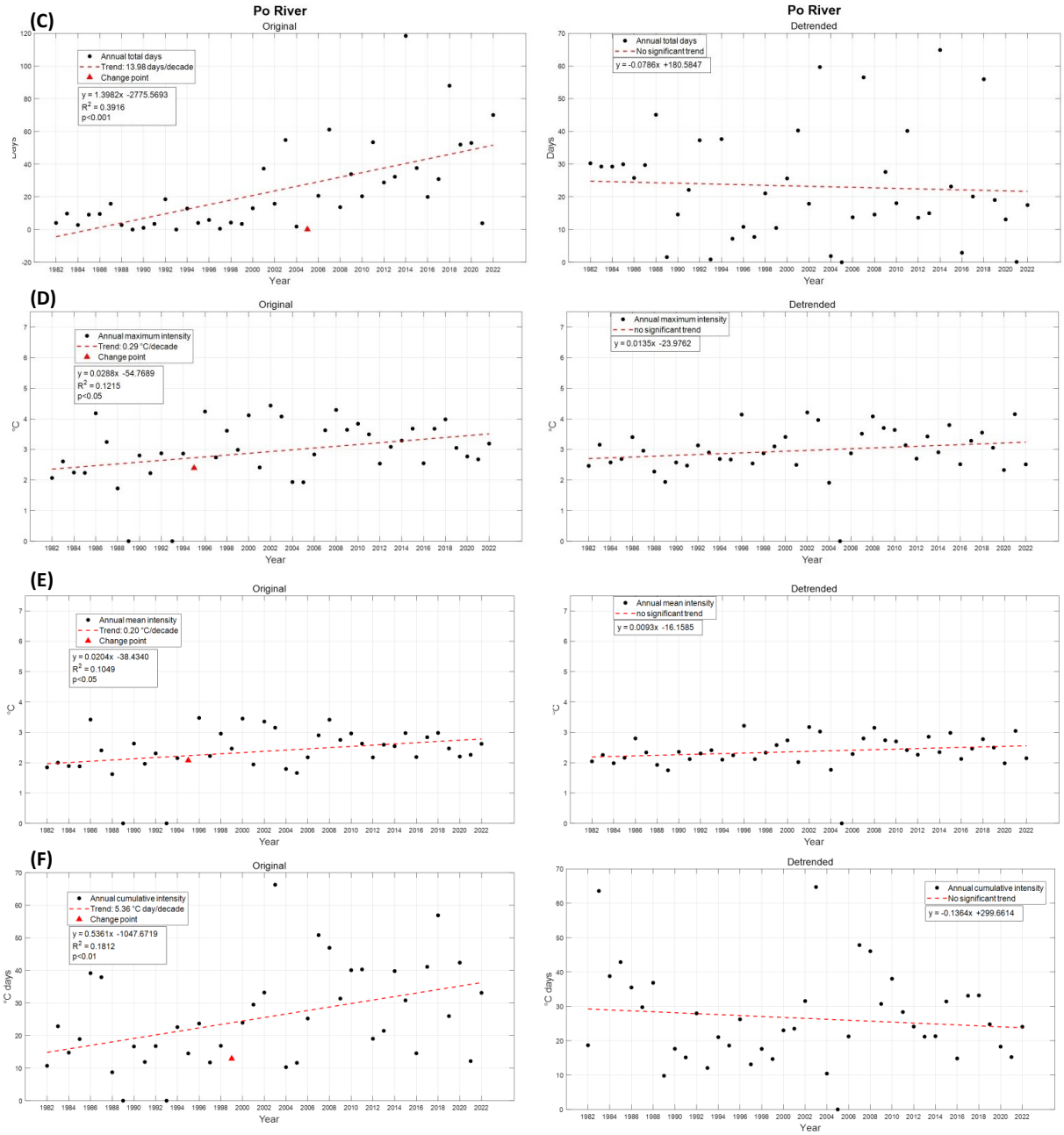

Figure 11. *Spatially averaged annual time series of the MHW metrics of the original (left panels) and detrended approaches (right panels) for the Po River area. Red dashed lines indicate the linear trend computed using the linear regression model, whose value is reported in the legends with R-squared coefficient. Red triangle represents the significant change point of the time series. (A) MHW frequency, (B) MHW duration, (C) MHW total days, (D) MHW maximum intensity, (E) MHW mean intensity, (F) MHW cumulative intensity.*

The results obtained with the Hobday et al. (2016) method applied to original SST time series for Po River region (Figure 11) show a statistical increase of

all MHW metrics, such as the frequency of events (+1.11 events/decade), the MHW duration (+1.65 days/decade), the total MHW days (+13.98 days/decade), the maximum (+0.29°C/decade) and mean intensity (+0.20°C/decade) and the cumulative intensity (+5.36°C days/decade). Instead with the detrended approach, none of the metrics show statistically significant trends.

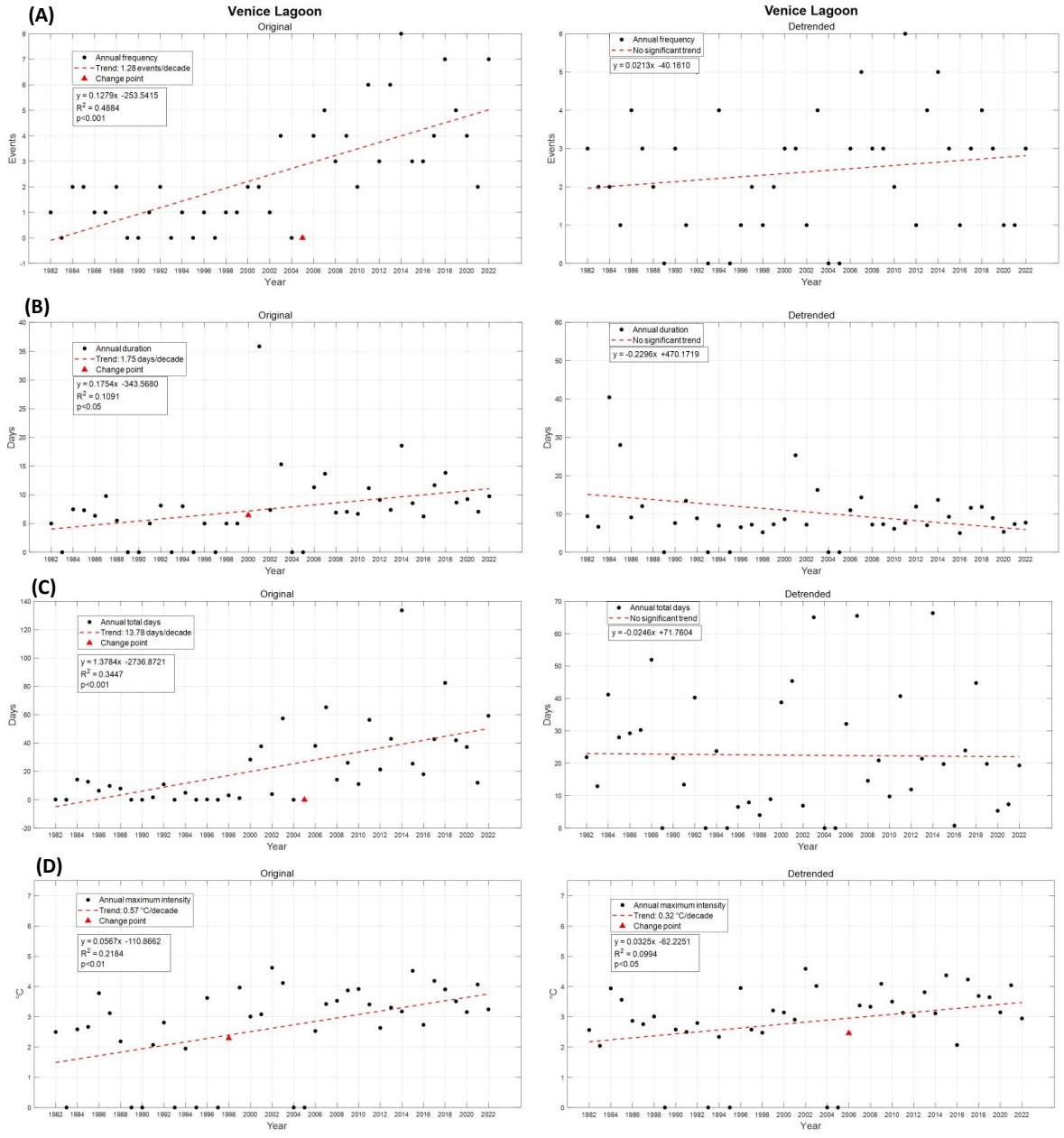

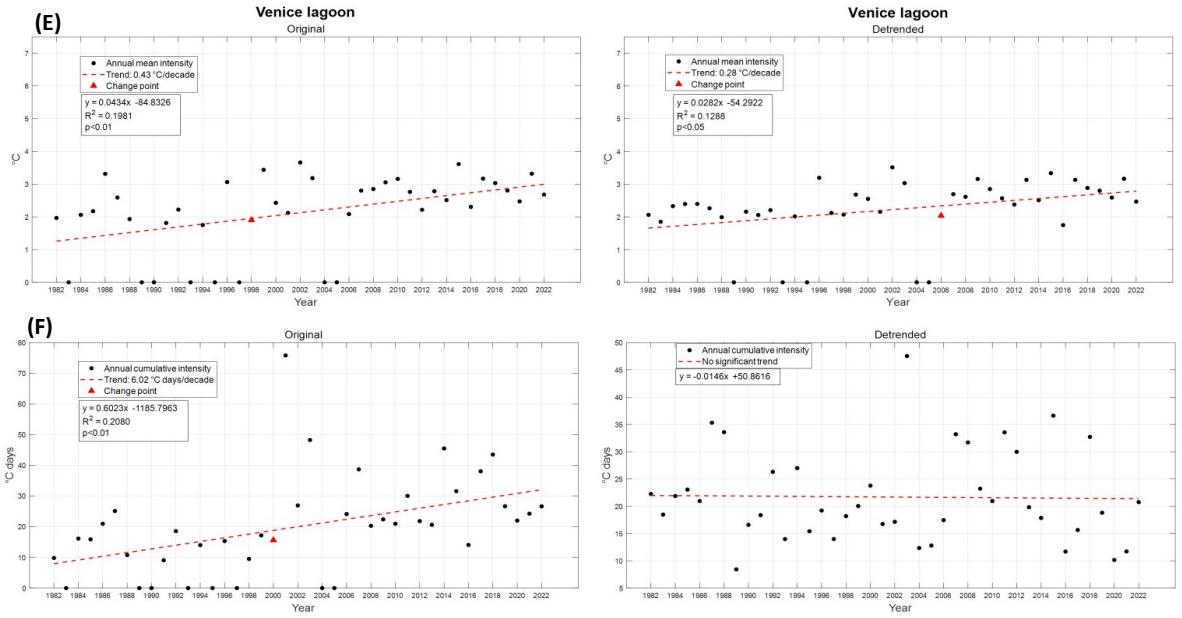

Figure 12. *Spatially averaged annual time series of the MHW metrics of the original (left panels) and detrended approaches (right panels) for the Venice Lagoon. Red dashed lines indicate the linear trend computed using the linear regression model, whose value is reported in the legends with R-squared coefficient. Red triangle represents the significant change point of the time series. (A) MHW frequency, (B) MHW duration, (C) MHW total days, (D) MHW maximum intensity, (E) MHW mean intensity, (F) MHW cumulative intensity.*

With the original approach, all MHW metrics for the Venice Lagoon (Figure 12) increase significantly: frequency (+1.28 events/decade), duration (+1.75 days/decade), total days (+13.78 days/decade), maximum (+0.57°C/decade) and mean intensity (+0.43°C/decade) and cumulative intensity (+6.02°C days/decade). The MHW metrics computed from the detrended SST time series do not show statistically significant trends, except for maximum (+0.32°C/decade) and mean (+0.28°C/decade) intensity.

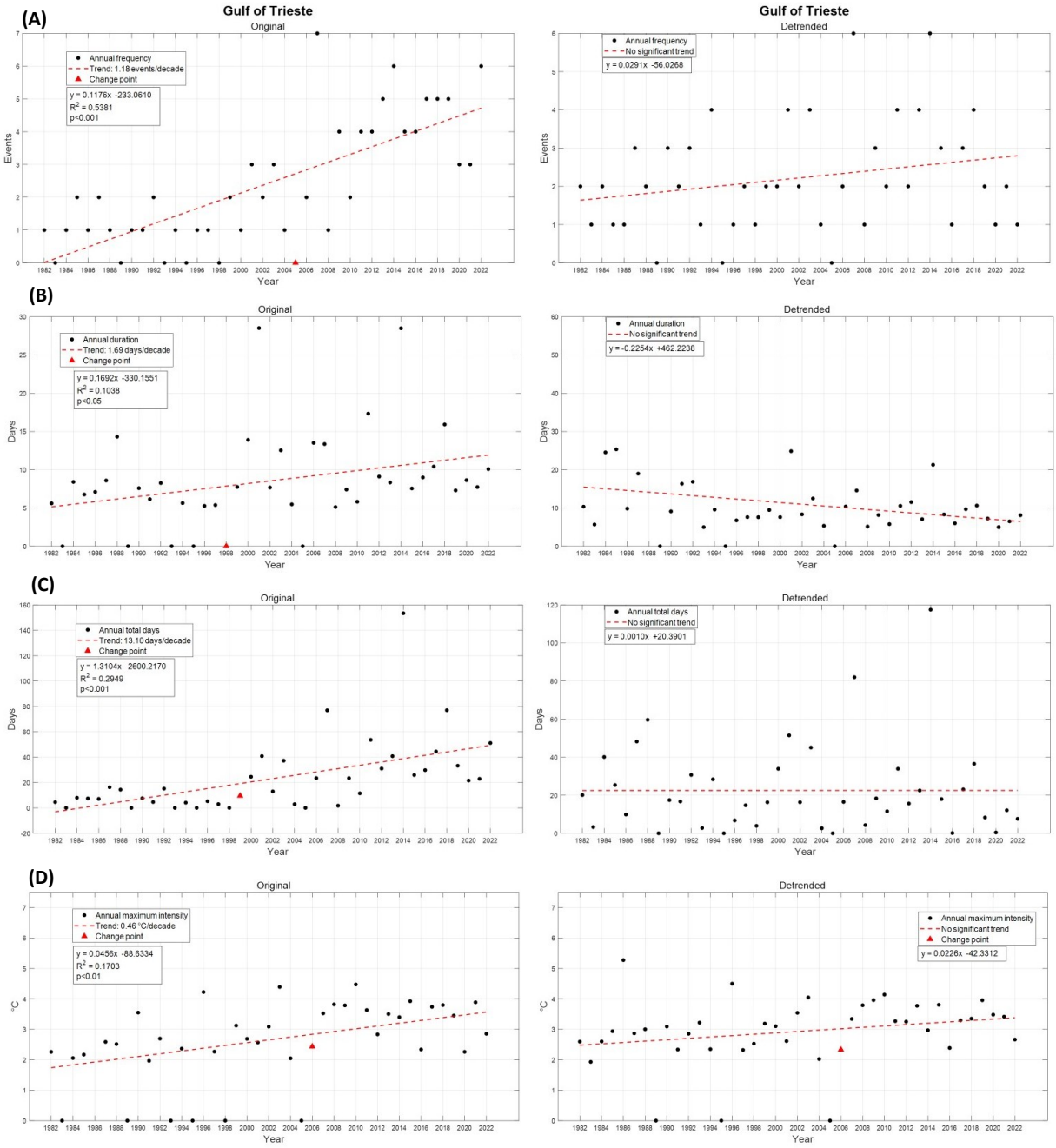
(A)
Gulf of Trieste
Original
Annual frequency
Trend: 1.18 events/decade
Change point
y = 0.1176x -233.0610
R² = 0.5381
p<0.001
Events
Year
Gulf of Trieste
Detrended
Annual frequency
No significant trend
y = 0.0291x -56.0268
Events
Year
(B)
Original
Annual duration
Trend: 1.69 days/decade
Change point
y = 0.1692x -330.1551
R² = 0.1038
p<0.05
Days
Year
Detrended
Annual duration
No significant trend
y = -0.2254x +462.2238
Days
Year
(C)
Original
Annual total days
Trend: 13.10 days/decade
Change point
y = 1.3104x -2600.2170
R² = 0.2949
p<0.001
Days
Year
Detrended
Annual total days
No significant trend
y = 0.0010x +20.3901
Days
Year
(D)
Original
Annual maximum intensity
Trend: 0.46 °C/decade
Change point
y = 0.0456x -88.6334
R² = 0.1703
p<0.01
°C
Year
Detrended
Annual maximum intensity
No significant trend
Change point
y = 0.0226x -42.3312
°C
Year

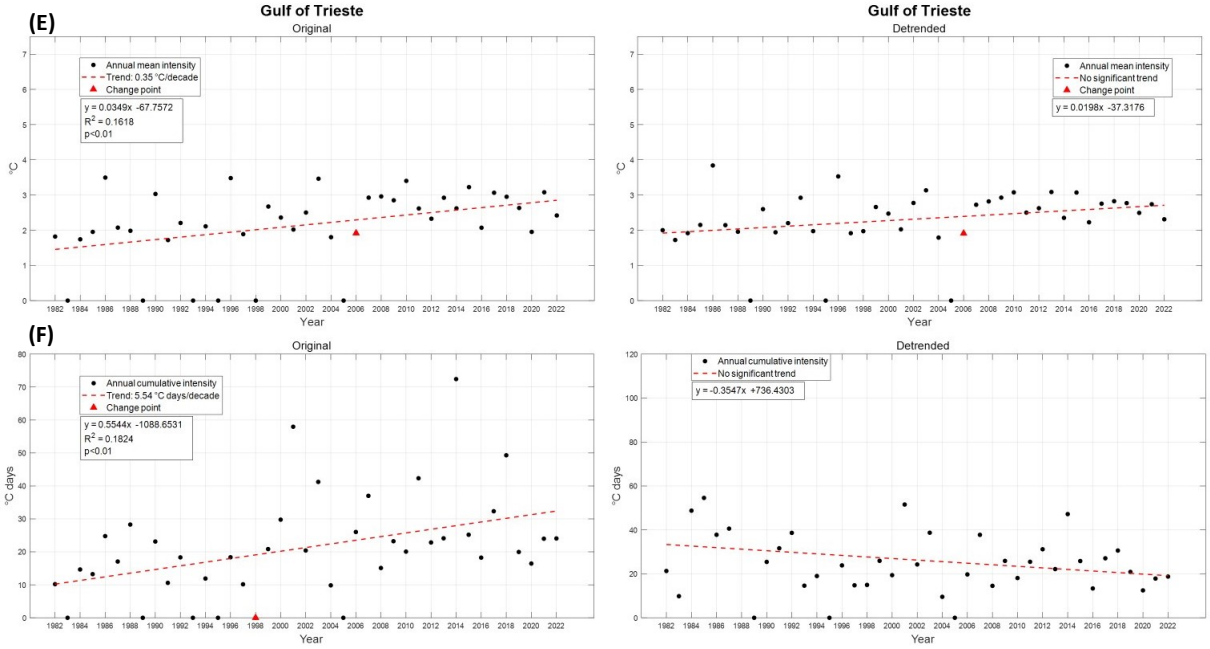

Figure 13. *Spatially averaged annual time series of the MHW metrics of the original (left panels) and detrended approaches (right panels) for the Gulf of Trieste. Red dashed lines indicate the linear trend computed using the linear regression model, whose value is reported in the legends with R-squared coefficient. Red triangle represents the significant change point of the time series. (A) MHW frequency, (B) MHW duration, (C) MHW total days, (D) MHW maximum intensity, (E) MHW mean intensity, (F) MHW cumulative intensity.*

The results obtained for the Gulf of Trieste (Figure 13) with the Hobday et al. (2016) method applied to original SST time series show a statistical increase of all MHW metrics, such as the MHW frequency (+1.18 events/decade), the MHW duration (+1.69 days/decade), the total MHW days (+13.10 days/decade), the maximum (+0.46°C/decade) and mean intensity (+0.35°C/decade) and the cumulative intensity (+5.54°C days/decade). Conversely, none of the metrics show statistically significant trends with the detrended detection.

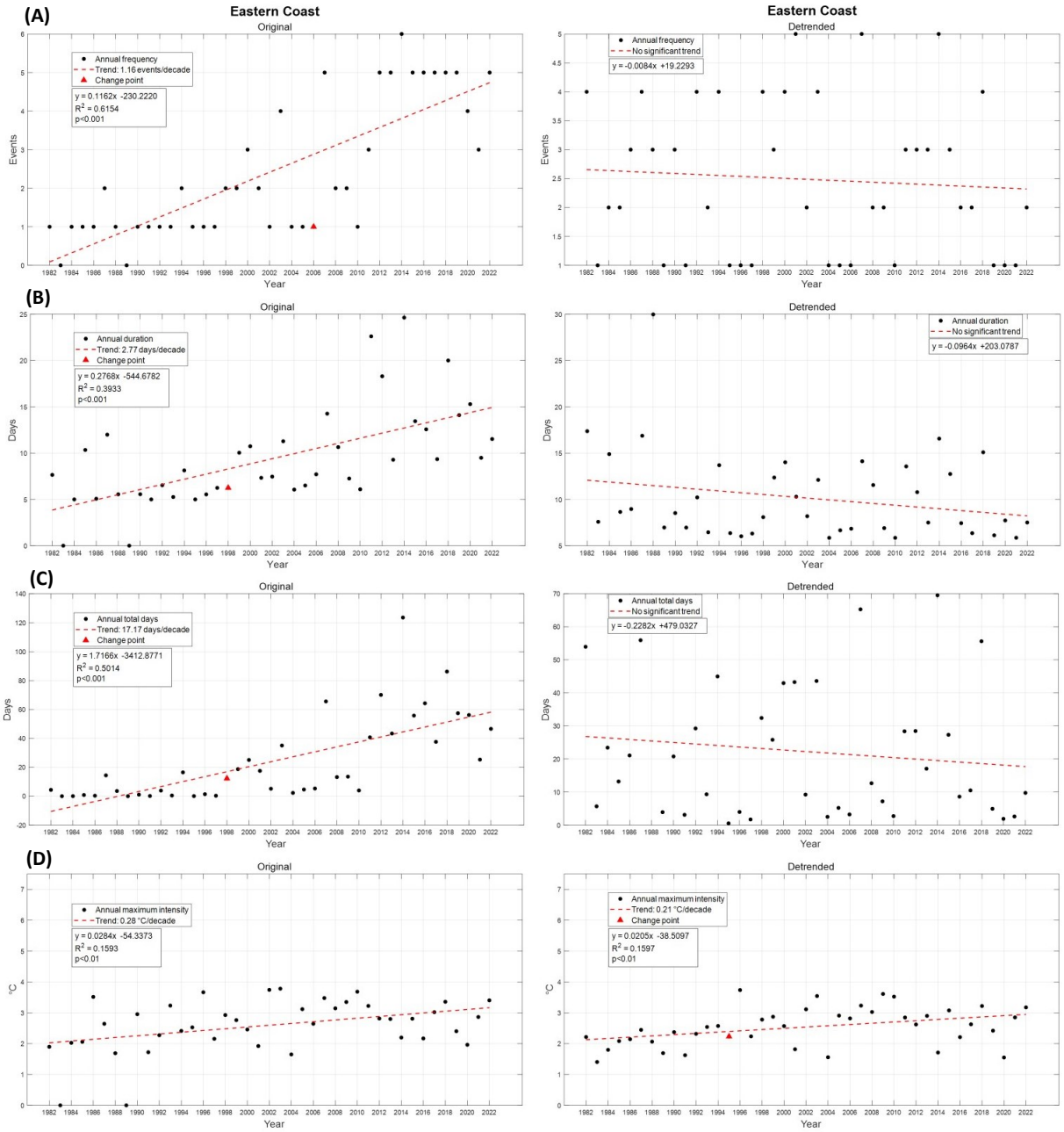
(A)
Eastern Coast
Original
Annual frequency
Trend: 1.16 events/decade
Change point
y = 0.1162x -230.2220
R² = 0.6154
p<0.001
Events
Year
Eastern Coast
Detrended
Annual frequency
No significant trend
y = -0.0084x +19.2293
Events
Year
(B)
Original
Annual duration
Trend: 2.77 days/decade
Change point
y = 0.2768x -544.6782
R² = 0.3933
p<0.001
Days
Year
Detrended
Annual duration
No significant trend
y = -0.0964x +203.0787
Days
Year
(C)
Original
Annual total days
Trend: 17.17 days/decade
Change point
y = 1.7166x -3412.8771
R² = 0.5014
p<0.001
Days
Year
Detrended
Annual total days
No significant trend
y = -0.2282x +479.0327
Days
Year
(D)
Original
Annual maximum intensity
Trend: 0.28 °C/decade
y = 0.0284x -54.3373
R² = 0.1593
p<0.01
°C
Year
Detrended
Annual maximum intensity
Trend: 0.21 °C/decade
Change point
y = 0.0205x -38.5097
R² = 0.1597
p<0.01
°C
Year

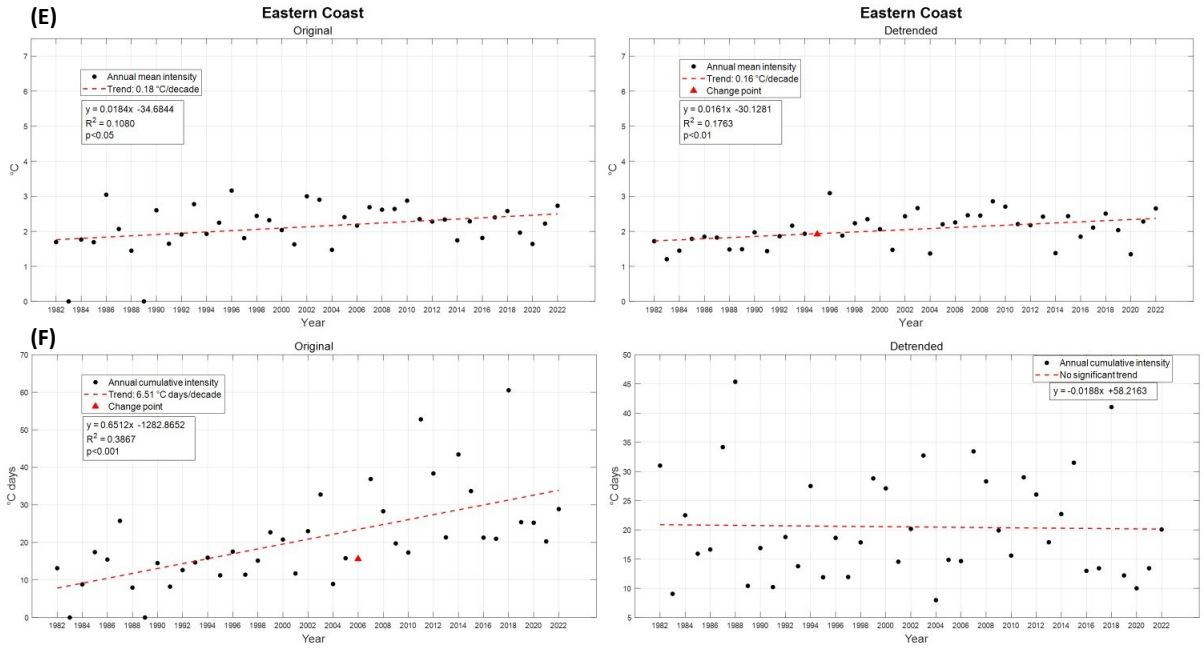

Figure 14. *Spatially averaged annual time series of the MHW metrics of the original (left panels) and detrended approaches (right panels) for the Eastern Coast. Red dashed lines indicate the linear trend computed using the linear regression model, whose value is reported in the legends with R-squared coefficient. Red triangle represents the significant change point of the time series. (A) MHW frequency, (B) MHW duration, (C) MHW total days, (D) MHW maximum intensity, (E) MHW mean intensity, (F) MHW cumulative intensity.*

The MHW metrics computed from the original SST time series for the Eastern Coast (Figure 14) increase significantly: frequency (+1.16 events/decade), duration (+2.77 days/decade), total days (+17.17 days/decade), maximum (+0.28°C/decade) and mean intensity (+0.18°C/decade) and cumulative intensity (+6.51°C days/decade). With the detrended approach, MHW metrics do not show statistically significant trends, except for maximum (+0.21°C/decade) and mean (+0.16°C/decade) intensity.

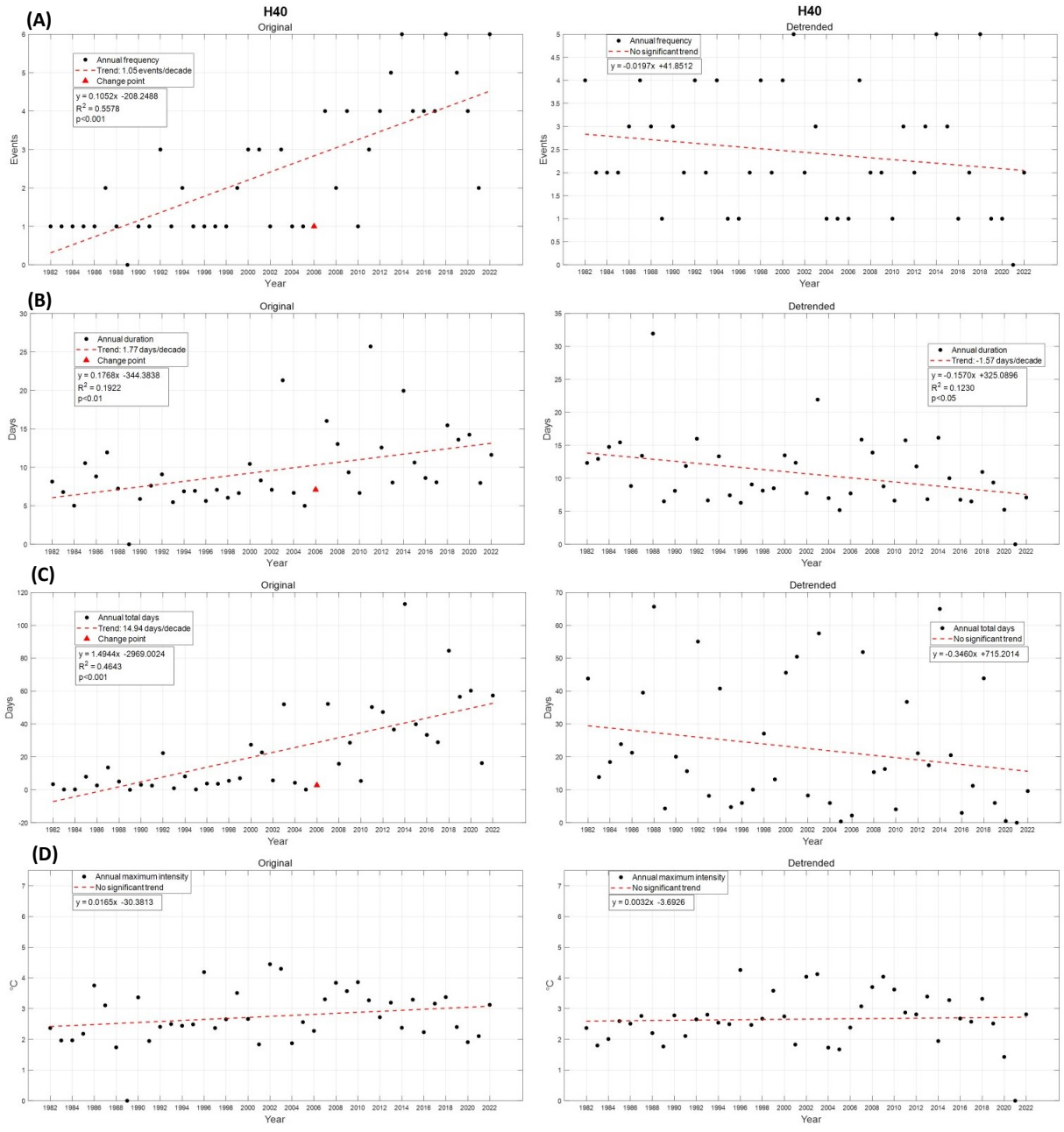
(A)
H40
Original
Annual frequency
Trend: 1.05 events/decade
Change point
y = 0.1052x -208.2488
R2 = 0.5578
p<0.001
Events
Year
H40
Detrended
Annual frequency
No significant trend
y = -0.0197x +41.8512
Events
Year
(B)
Original
Annual duration
Trend: 1.77 days/decade
Change point
y = 0.1768x -344.3838
R2 = 0.1922
p<0.01
Days
Year
Detrended
Annual duration
Trend: -1.57 days/decade
y = -0.1570x +325.0896
R2 = 0.1230
p<0.05
Days
Year
(C)
Original
Annual total days
Trend: 14.94 days/decade
Change point
y = 1.4944x -2969.0024
R2 = 0.4643
p<0.001
Days
Year
Detrended
Annual total days
No significant trend
y = -0.3460x +715.2014
Days
Year
(D)
Original
Annual maximum intensity
No significant trend
y = 0.0165x -30.3813
°C
Year
Detrended
Annual maximum intensity
No significant trend
y = 0.0032x -3.6926
°C
Year

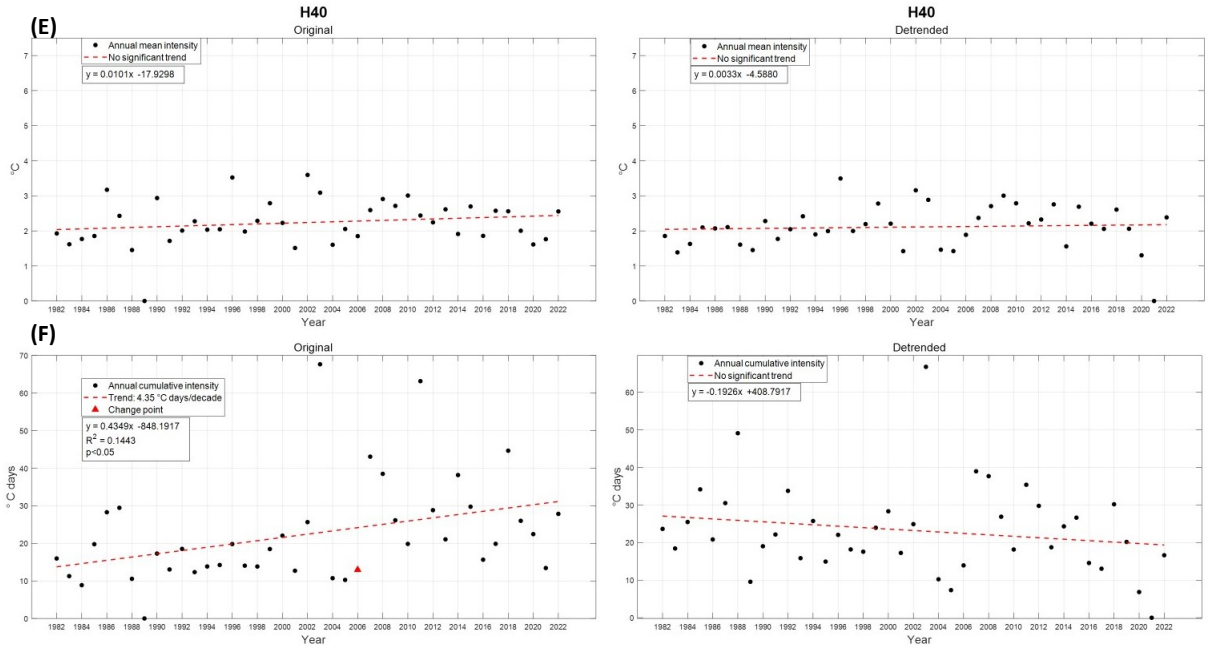

Figure 15. *Spatially averaged annual time series of the MHW metrics of the original (left panels) and detrended approaches (right panels) for the area with depth > 40m (H40). Red dashed lines indicate the linear trend computed using the linear regression model, whose value is reported in the legends with R-squared coefficient. Red triangle represents the significant change point of the time series. (A) MHW frequency, (B) MHW duration, (C) MHW total days, (D) MHW maximum intensity, (E) MHW mean intensity, (F) MHW cumulative intensity.*

The MHW metrics computed from the original SST time series for the sub-area with depth > 40m (Figure 15) show statistically significant trends, such as frequency (+1.05 events/decade), duration (+1.77 days/decade), total days (+14.94 days/decade), and cumulative intensity (+4.35°C days/decade). Maximum and mean intensity do not increase significantly. With the detrended approach, MHW metrics do not show statistically significant trends, except for MHW duration (-1.57 days/decade) which shows a significantly negative trend.

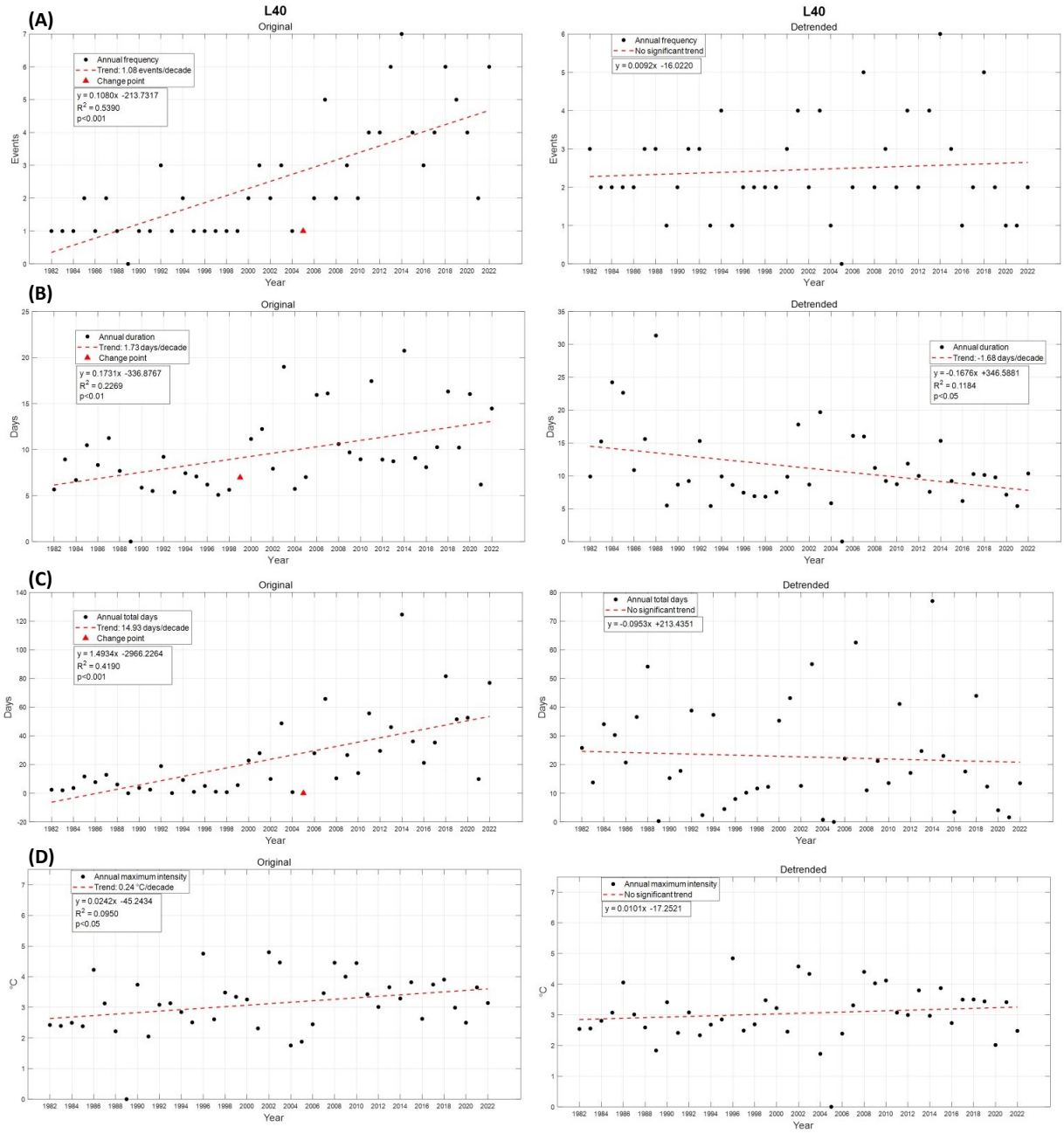
(A)
L40
Original
Annual frequency
Trend: 1.08 events/decade
Change point
y = 0.1080x -213.7317
R² = 0.5390
p<0.001
Events
Year
L40
Detrended
Annual frequency
No significant trend
y = 0.0092x -16.0220
Events
Year
(B)
Original
Annual duration
Trend: 1.73 days/decade
Change point
y = 0.1731x -336.8767
R² = 0.2269
p<0.01
Days
Year
Detrended
Annual duration
Trend: -1.68 days/decade
y = -0.1676x +346.5881
R² = 0.1184
p<0.05
Days
Year
(C)
Original
Annual total days
Trend: 14.93 days/decade
Change point
y = 1.4934x -2966.2264
R² = 0.4190
p<0.001
Days
Year
Detrended
Annual total days
No significant trend
y = -0.0953x +213.4351
Days
Year
(D)
Original
Annual maximum intensity
Trend: 0.24 °C/decade
y = 0.0242x -45.2434
R² = 0.0950
p<0.05
°C
Year
Detrended
Annual maximum intensity
No significant trend
y = 0.0101x -17.2521
°C
Year

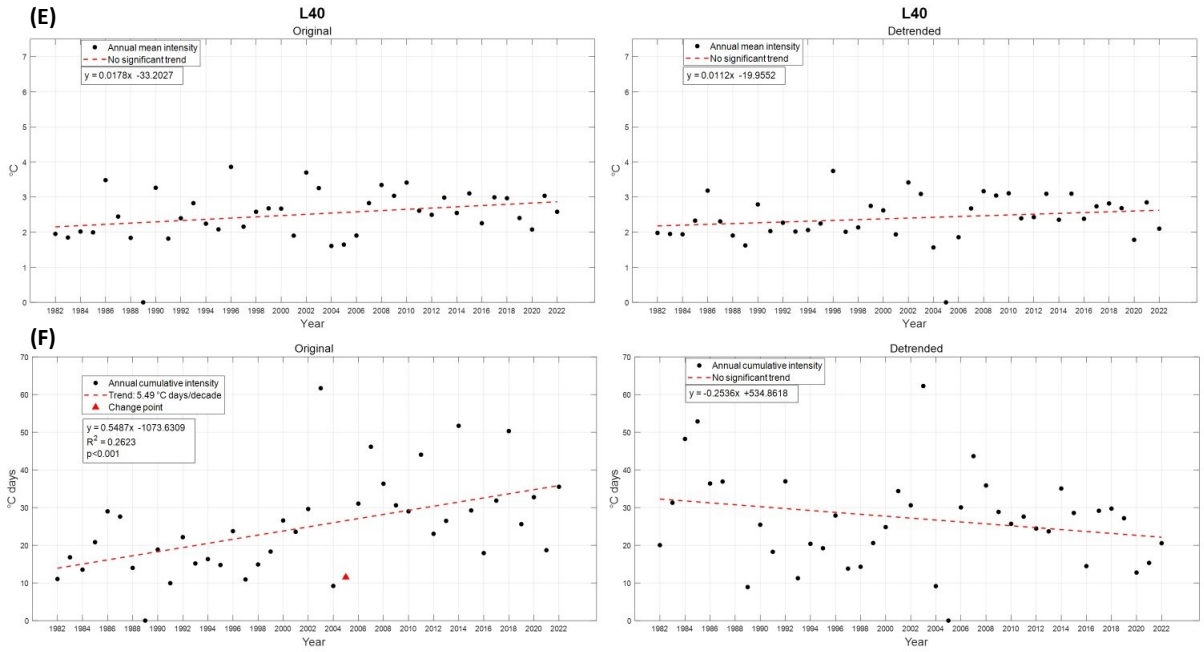

Figure 16. *Spatially averaged annual time series of the MHW metrics of the original (left panels) and detrended approaches (right panels) for the area with depth < 40m (L40). Red dashed lines indicate the linear trend computed using the linear regression model, whose value is reported in the legends with R-squared coefficient. Red triangle represents the significant change point of the time series. (A) MHW frequency, (B) MHW duration, (C) MHW total days, (D) MHW maximum intensity, (E) MHW mean intensity, (F) MHW cumulative intensity.*

The MHW metrics computed from the original SST time series for the sub-area with depth < 40m (Figure 16) show statistically significant trends: frequency (+1.08 events/decade), duration (+1.73 days/decade), total days (+14.93 days/decade), maximum (+0.24°C/decade) and cumulative intensity (+5.49°C days/decade). Only mean intensity does not increase significantly. With the detrended detection, MHW metrics do not show statistically significant trends, except for MHW duration (-1.68 days/decade) which decreases significantly.

Additionally, looking at the mean states of annual MHW metrics of the six sub-areas of the northern Adriatic, there is no significant difference if these are obtained with the original or detrended approach (Table 3, 4). Indeed, for both cases, the mean frequency is estimated in ∼2 events per year, with a mean duration around ∼10 days, a total number of annual days of ∼23 days, a maximum and mean intensity of ∼3°C. The cumulative intensity is the sole metric that evidences a difference up to ∼ 5°C days between the original and detrended detection.

	Original											
	Frequency (events/decade)		Duration (days/decade)		Total days (days/decade)		Maximum intensity (°C/decade)		Mean intensity (°C/decade)		Cumulative intensity (°C days/decade)	
	Mean	Trend	Mean	Trend	Mean	Trend	Mean	Trend	Mean	Trend	Mean	Trend
Po River	2.39	**1.11**	9.93	**1.65**	23.62	**13.98**	2.93	**0.29**	2.37	**0.20**	25.56	**5.36**
Venice lagoon	2.46	**1.28**	7.54	**1.75**	22.64	**13.78**	2.62	**0.57**	2.13	**0.43**	20.01	**6.02**
Gulf of Trieste	2.37	**1.18**	8.54	**1.69**	23.11	**13.10**	2.65	**0.46**	2.15	**0.35**	21.30	**5.54**
Eastern coast	2.41	**1.16**	9.39	**2.77**	23.81	**17.17**	2.60	**0.28**	2.13	**0.18**	20.87	**6.51**
Depth > 40m	2.41	**1.05**	9.59	**1.77**	22.73	**14.94**	2.75	0.17	2.24	0.10	22.43	**4.35**
Depth < 40m	2.51	**1.08**	9.61	**1.73**	23.66	**14.93**	3.12	**0.24**	2.51	0.18	24.88	**5.49**

Table 3. *Mean states and linear trend of MHW metrics of each region, computed on original SST data. Bold values indicate a statistically significant trend.*

	Detrended											
	Frequency (events/decade)		Duration (days/decade)		Total days (days/decade)		Maximum intensity (°C/decade)		Mean intensity (°C/decade)		Cumulative intensity (°C days/decade)	
	Mean	Trend	Mean	Trend	Mean	Trend	Mean	Trend	Mean	Trend	Mean	Trend
Po River	2.63	0.09	10.71	-1.07	23.22	-0.79	2.97	0.13	2.37	0.09	26.50	-1.36
Venice lagoon	2.39	0.21	10.52	-2.30	22.50	-0.25	2.82	**0.32**	2.22	**0.28**	21.69	-0.15
Gulf of Trieste	2.22	0.29	10.98	-2.25	22.48	0.01	2.93	0.23	2.31	0.20	26.26	-3.55
Eastern coast	2.49	-0.08	10.14	-0.96	22.26	-2.28	2.54	**0.21**	2.05	**0.16**	20.52	-0.19
Depth > 40m	2.44	-0.20	10.70	**-1.57**	22.56	-3.46	2.66	0.03	2.11	0.03	23.20	-1.93
Depth < 40m	2.46	0.09	11.15	**-1.68**	22.68	-0.95	3.05	0.10	2.40	0.11	27.20	-2.54

Table 4. *Mean states and linear trend of MHW metrics of each region, computed on detrended SST data. Bold values indicate a statistically significant trend.*

In practice, the removal of the trend redistributes more uniformly to the 90th percentile, thus avoiding assigning to the MHW metrics lower values during the first years and higher during the last ones. This concept is further

investigated by analysing three years (1982, 2003, and 2022) corresponding to the beginning, middle, and end of the study period (Figure 17). When the original detection is applied, MHW metrics drastic increase from the beginning to the end of the period. When detrending is applied, the MHW properties are respectively higher in 1982 and lower in 2022 with respect to the original detection. In the middle (2003), the behaviour is similar for both procedures.

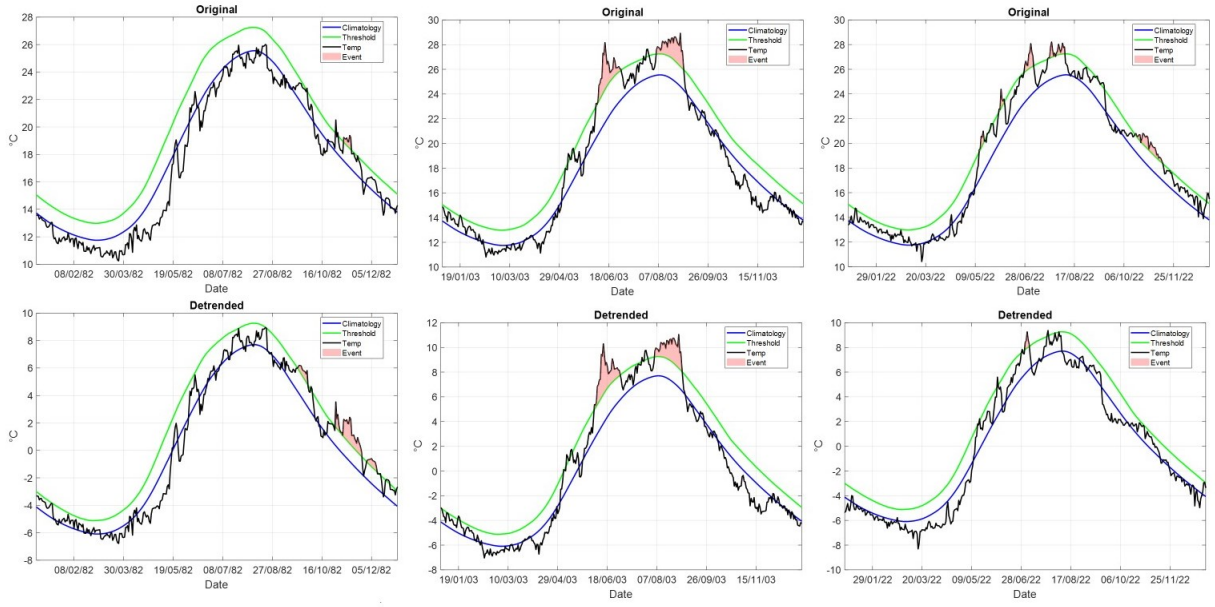

Figure 17. *The MHW events detected at the beginning (1982), in the middle (2003) and in the end (2022) of the study period with the original approach (above) and the detrended one (below). The SST climatology from Copernicus Marine Service Mediterranean multi-year SST dataset for the detection of MHWs (blue), 90th percentile MHW threshold (green), and SST time series (black) for each MHW. The pink filled area indicates the period associated with the identified MHW.*

The results obtained with change points analyses are statistically significant when the original approach is applied (Table 5). Change point detection method shows statistical abrupt changes in nearly all spatially averaged annual MHW statistics computed on original SST data. Significant change points in the years

2005-2006 are common for MHW frequency and total days at most of the sub-areas considered, while at Gulf of Trieste and Eastern Coast change points are detected in 1999 and 1998, respectively. MHW maximum and mean intensity have the same significant change points at Po River area (1995), Venice Lagoon (1998) and Gulf of Trieste (2006). For MHW duration significant change points are detected in 2000 at Po River area and Venice Lagoon, in 1998 at Gulf of Trieste and Eastern Coast, in 2006 at the sub-area with depth > 40m and in 1999 at that < 40m. Finally, MHW cumulative intensity show significant change point in 1999 at Po River area, in 2000 at Venice Lagoon, in 1998 at Gulf of Trieste, in 2006 at Eastern Coast and sub-area with depth > 40m, in 2005 at sub-area with depth < 40m. Cumulative intensity by definition depends on MHW duration and intensity; thus the change point is defined by the variation of both metrics.

	Original											
	Frequency		Duration		Total days		Maximum intensity		Mean intensity		Cumulative intensity	
	Year	Significance	Year	Significance	Year	Significance	Year	Significance	Year	Significance	Year	Significance
Po River	2005	**	2000	**	2005	**	1995	**	1995	**	1999	**
Venice lagoon	2005	**	2000	**	2005	**	1998	**	1998	**	2000	**
Gulf of Trieste	2005	**	1998	*	1999	**	2006	*	2006	*	1998	**
Eastern coast	2006	**	1998	**	1998	**	2001	ns	1992	ns	2006	**
Depth > 40m	2006	**	2006	**	2006	**	1995	ns	1995	ns	2006	**
Depth < 40m	2005	**	1999	**	2005	**	2006	ns	2006	ns	2005	**

Table 5. *Change point from Pettit's test. *** and ** indicate confidence level of 99% and 95% respectively; ns indicates confidence level under 95%.*

The situation is very different for the spatially averaged annual MHW metrics calculated from detrended SST time series (Table 6), which do not show any statistically significant change point, except for MHW maximum and mean intensity at Venice Lagoon (2006), Gulf of Trieste (2006) and Eastern Coast (1995).

	Detrended											
	Frequency		Duration		Total days		Maximum intensity		Mean intensity		Cumulative intensity	
	Year	Significance	Year	Significance	Year	Significance	Year	Significance	Year	Significance	Year	Significance
Po River	2019	ns	1988	ns	1988	ns	2006	ns	1995	ns	1988	ns
Venice lagoon	2005	ns	1988	ns	1988	ns	2006	*	2006	**	1988	ns
Gulf of Trieste	2005	ns	1992	ns	1988	ns	2006	*	2006	*	1992	ns
Eastern coast	2018	ns	1988	ns	1988	ns	1995	**	1995	**	2015	ns
Depth > 40m	2003	ns	1992	ns	2003	ns	1995	ns	1995	ns	2015	ns
Depth < 40m	2015	ns	1988	ns	1988	ns	2006	ns	2006	ns	1988	ns

Table 6. *Change point from Pettit's test. *** and ** indicate confidence level of 99% and 95% respectively; ns indicates confidence level under 95%.*

To further study change points of spatially averaged annual MHW time series single mass curve method was applied. Figure 18-23 (A-F) show the annual MHW metrics, computed on original and detrended SST data, for each sub-area under study. Black line represents the original annual MHW properties, the red line the detrended ones. Significant change points are displayed with a blue star for the original MHW time series and with a green star for the detrended ones.

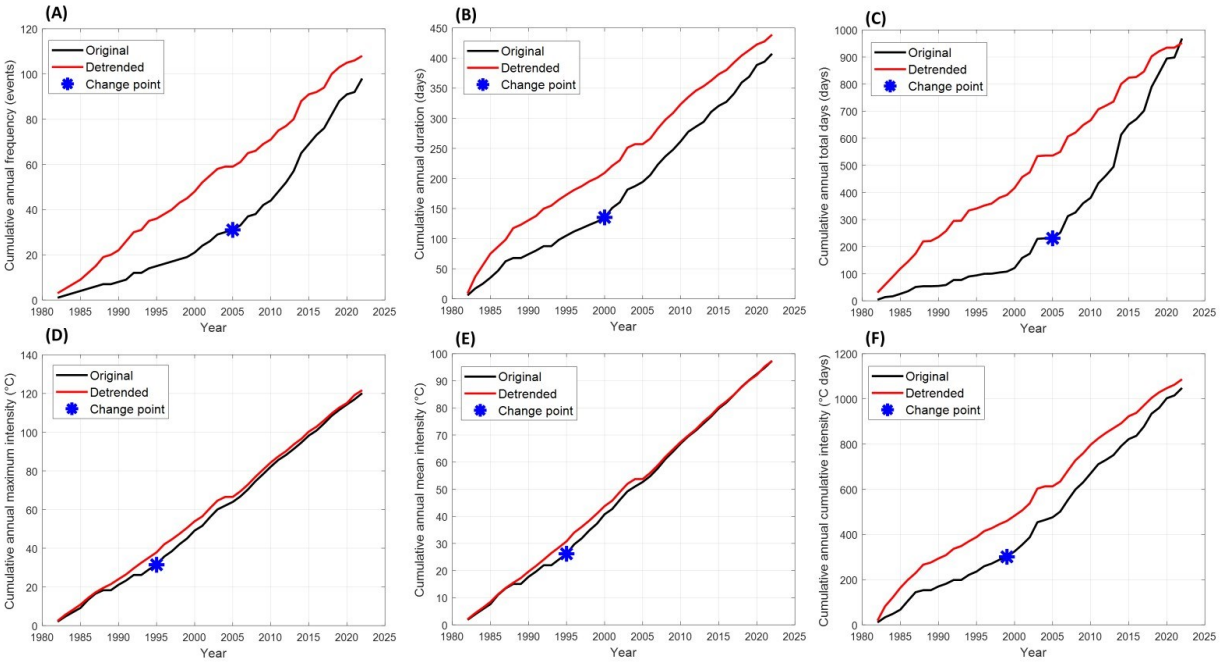

Figure 18. *Single mass curve of spatially averaged MHW time series calculated from original (black line) and detrended (red line) SST data for the Po River area. Blue star represents the significant change point of the original MHW time series. (A) MHW frequency, (B) MHW duration, (C) MHW total days, (D) MHW maximum intensity, (E) MHW mean intensity, (F) MHW cumulative intensity.*

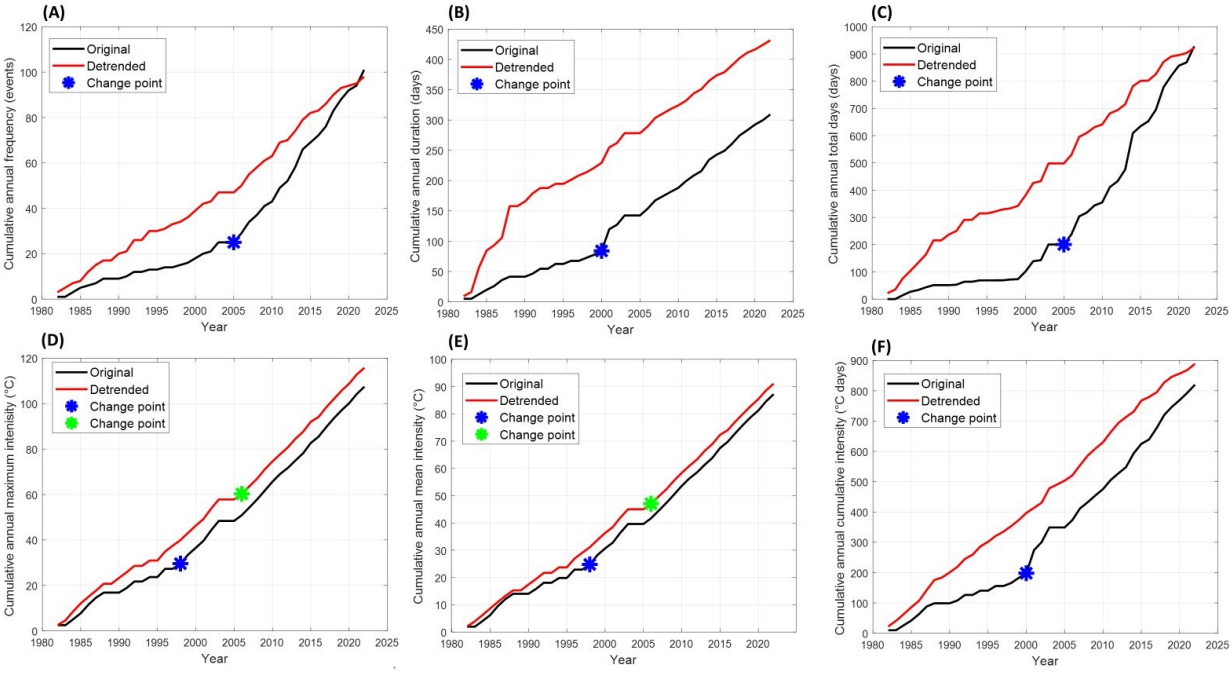

Figure 19. *Single mass curve of spatially averaged MHW time series calculated from original (black line) and detrended (red line) SST data for the Venice Lagoon. Blue and green stars represent the significant change point of the original and detrended MHW time series, respectively. (A) MHW frequency, (B) MHW duration, (C) MHW total days, (D) MHW maximum intensity, (E) MHW mean intensity, (F) MHW cumulative intensity.*

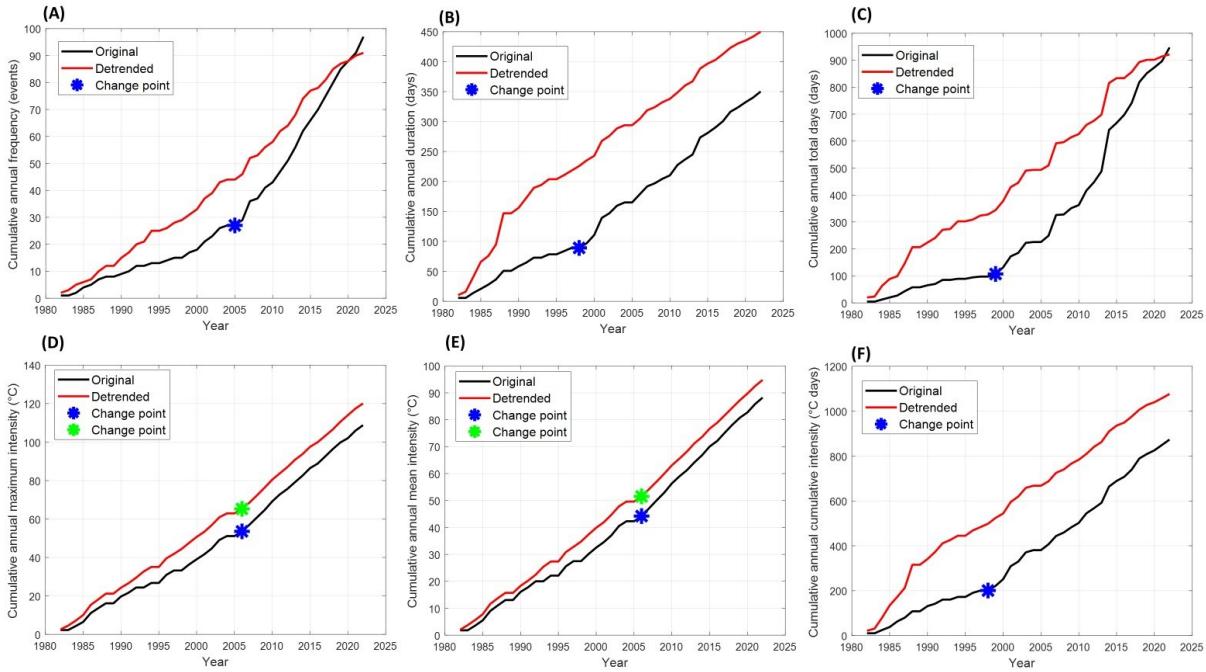

Figure 20. *Single mass curve of spatially averaged MHW time series calculated from original (black line) and detrended (red line) SST data for the Gulf of Trieste. Blue and green stars represent the significant change point of the original and detrended MHW time series, respectively. (A) MHW frequency, (B) MHW duration, (C) MHW total days, (D) MHW maximum intensity, (E) MHW mean intensity, (F) MHW cumulative intensity.*

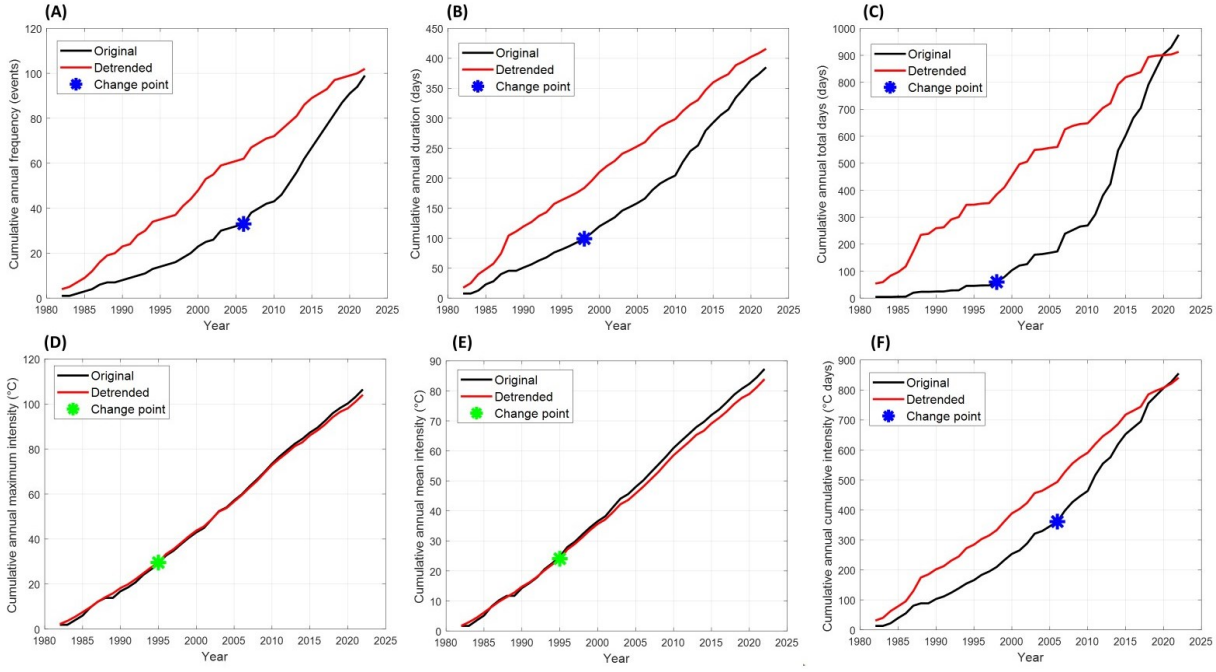

Figure 21. *Single mass curve of spatially averaged MHW time series calculated from original (black line) and detrended (red line) SST data for the Eastern Coast. Green stars represent the significant change point of the detrended MHW time series. (A) MHW frequency, (B) MHW duration, (C) MHW total days, (D) MHW maximum intensity, (E) MHW mean intensity, (F) MHW cumulative intensity.*

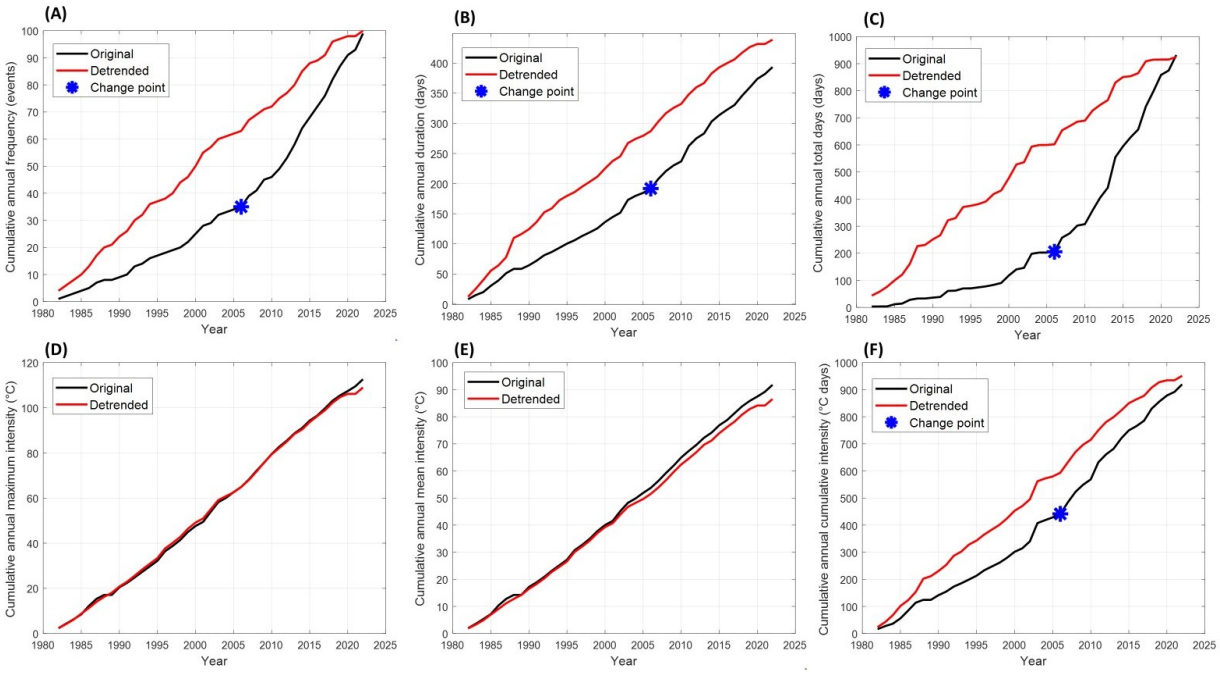

Figure 22. *Single mass curve of spatially averaged MHW time series calculated from original (black line) and detrended (red line) SST data the area with depth > 40m (H40). Blue star represents the significant change point of the original MHW time series. (A) MHW frequency, (B) MHW duration, (C) MHW total days, (D) MHW maximum intensity, (E) MHW mean intensity, (F) MHW cumulative intensity.*

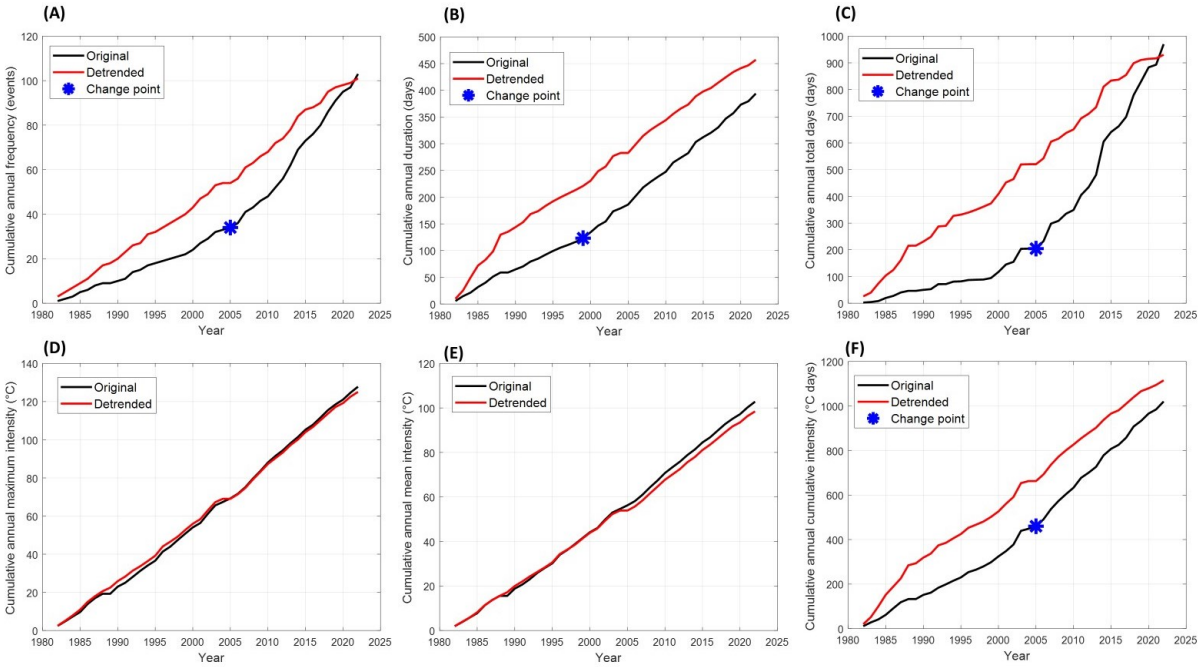

Figure 23. *Single mass curve of spatially averaged MHW time series calculated from original (black line) and detrended (red line) SST data the area with depth < 40m (L40). Blue star represents the significant change point of the original MHW time series. (A) MHW frequency, (B) MHW duration, (C) MHW total days, (D) MHW maximum intensity, (E) MHW mean intensity, (F) MHW cumulative intensity.*

Results from single mass curve are in agreement with the change points detected by the Pettitt's test, as annual MHW frequency and total days cumulative curves indicate rapid change over the last two decades for all areas considered. MHW duration and cumulative intensity of each sub-region show a similar increasing rate of change with time as they are closely related. Finally, MHW maximum and mean intensity appear more stable over time with slower changes resulting in a gentle slope of the cumulative curves of each sub-area. Being the cumulative curves mostly visual and qualitative, in case of uncertainty, we decided to use the change point from the Pettitt's test which instead provides quantitative results more reliable from a statistical point of view.

5. DISCUSSION

The Mediterranean Sea, which is a hotspot for climate change (Giorgi, 2006; Pisano et al., 2020), has been subject to several intense MHWs, especially over the last decades (Darmaraki et al., 2019a; Pastor & Khodayar, 2023). Model projections (Darmaraki et al., 2019b) indicate that Mediterranean MHWs will be longer lasting and more intense in the future due to global warming. MHWs in the Mediterranean Sea have caused substantial economic and ecological damages, such as loss of biodiversity and mass mortality events (Garrabou et al., 2009, 2022), and therefore this marginal sea provides opportunities for testing mitigation strategies. Impacts are generally not limited to the uppermost water layers. Indeed, it has been shown that MHWs can alter conditions below the surface as well (Hu et al., 2021; Dayan et al., 2023), potentially amplifying circulation changes and affecting deep convection in the basin (Margirier et al., 2020; Josey and Schroeder, 2023).

In the present work, the spatial variability and long-term trends of Adriatic MHW metrics computed from the SST data over the study period (1982-2022) are reported in section 4.1. They are in good agreement with what was found by the recent literature (Juza et al., 2022; Hamdeno & Alvera-Azcaràte, 2023). In fact, our results show a clear significant increase in MHW frequency (0.6-

1.5 events/decade) and total days (11-21 days/decade) across all the Adriatic basin. A significant trend is detected for MHW duration (-0.9 and 6.3 days/decade), and cumulative intensity (-3 and 10 °C days/decade), which presents similarities with the duration pattern as they are closely related. Finally, for MHW mean and maximum intensity the north Adriatic suffered very intense extreme events with maxima exceeding 2.9°C and 3.7°C, respectively. However, no clear trend is appreciated regarding both temperature indices over the whole study period except for some coastal areas (such as Venice Lagoon), suggesting that further studies from seasonal to interannual and decadal temporal scales are required for a better and comprehensive understanding of MHW intensity temporal variability.

Nowadays, it is widely recognized that some of the properties and trends of MHWs over time can be strongly affected by global warming (Oliver et al., 2021; Xu et al., 2022; He et al., 2023). Recent literature (Amaya et al., 2023) suggests a definition of MHWs relative to an evolving climatology or, in other words, based on the separation of the long-term warming trend from the total temperature signal, either with a shifting baseline or by detrending. The purpose of detrending is thus analogous to the shifting baseline approach (Oliver et al., 2021; Amaya et al., 2023). However, the shifting approach must incorporate

the shift of the reference period in its definition and to do so it would require a large temporal window around the year under analysis (Oliver et al., 2021), which may be suitable for model data but non for the relatively short time series of observations. When using observation data, the detrending approach could be a more affordable solution, since it does not require having years beyond the year under analysis (Martínez et al., 2023).

The objective of this work is to quantify the impact of the observed trend on the MHW properties in some key sub-areas in the northern Adriatic basin. The impact of the trend in MHW detection has been investigated by applying the Hobday method (Hobday et al., 2016) to original and detrended SST data, covering the whole period (1982–2022). Considering the original detection method, MHW frequency and total number of annual days show a strong and positive increase over time for all regions considered. Also, MHW duration and intensity significantly increase, except for maximum and mean intensity in the last two regions studied. Conversely, when using the detrended approach no significant trend are found for MHW frequency and total annual days, which are mainly steady or even decrease over time, as well as MHW duration and cumulative intensity. Moreover, MHW duration show a statistically negative trend in the last two regions investigated. Finally, MHW maximum and mean

intensity are not significant except for the Venice Lagoon and the Eastern Coast. Thus, the presence of a warming trend effectively seems to lead to an increase in the occurrence, intensity, and a larger duration of marine heatwaves.

These results are consistent with recent works indicating that the observed increase in MHWs and their metrics results from regional trends that alone increase the probability of SSTs exceeding the percentile threshold (Ciappa, 2022; Xu et al., 2022). The use of original data underestimates the number of events at the beginning of the period under analysis. Likewise, not detrending the data overestimates the number of events at the end of the period. In practice, detrending the data allows a more uniform redistribution of the MHW percentile threshold.

An analogous conclusion is reported by Martínez et al. (2023) that evaluate the trend-induced effects on Mediterranean MHW properties by applying the Hobday method (Hobday et al., 2016) to original and detrended SST data over the last 41 years (1982-2022). Their results show that the intensification in frequency, intensity, and duration of Mediterranean MHWs in recent years is mainly due to a shift in SST mean that occurred in the last two decades and largely reduced when analysing detrended SST data. Moreover, they assess the

importance of detrending also for short temporal series by analysing 13 years (2007–2020) of in situ data collected at different depths (5 to 40 m) at Columbretes Islands (Spain).

Additionally, in the same study they underpin an exceptionally long-lasting and intense MHW in the Mediterranean Sea, started in May 2022 and persisting until spring 2023 (Marullo et al., 2023), resulting in the event with the highest cumulative intensity just after the well-known 2003 MHW event. The onset and growth of 2022/23 MHW is found to be related to the prevalence of anticyclonic conditions in the atmosphere (Faranda et al., 2023) and to the wind-driven vertical mixing, which led to the penetration of the warm anomalies below the sea surface. In any case, the anomalous low wind speeds and high insolation conditions, together with the relatively weak mixing of the Mediterranean Sea, are key driving factors for the development of MHW conditions (Guinaldo et al., 2023). Interestingly, major MHWs in the recent decades occurred during a positive phase of the Atlantic Multidecadal Oscillation (Marullo et al., 2011; Macias et al., 2013), but more studies are needed to understand if and how global modes of variability influence Mediterranean MHWs, in analogy with their atmospheric counterparts (Liu et al., 2022).

Change point analyses and single mass curve method indicate that considering the MHW properties significant and rapid changes occurred in terms of annual frequency and annual total days and in MHW duration and cumulative intensity as well. For all sub-areas in the northern Adriatic basin the acceleration of these MHW metrics is evident over the last two decades, where significant change points are detected. MHW maximum and mean intensity show regional differences and appear more stable in the sub-area with depth <40 m (L40) and that > 40 m (H40) without significant change point than in the other sub-areas, where significant changes are detected over the last two decades.

Our change points results agree with what was found in recent studies. Indeed, MHWs properties have experienced increasing trends in the last 40 years across the Mediterranean basin but with regional differences (Pastor & Khodayar, 2023). Additionally, an acceleration in the increase of duration and number of events in the last decade (2012–2021) leads to an accelerated increasing of MHW total days in all Mediterranean sub-regions with higher acceleration in the Adriatic Sea (Juza et al., 2022). According to Bensoussan et al. (2019) since the late nineties Mediterranean MHWs are more frequent and last longer, while variability for mean intensity tends to decrease, which indicates that MHW

events have become longer, more frequent, and more uniform regarding mean intensity. Furthermore, Juza et al. (2022) evidence that the increase of temperature characteristics of MHWs has accelerated in recent years with mean and maximum intensity much higher during the two last decades (2002– 2011 and 2012–2020).

In defining MHWs, the choice of whether to use a fixed or moving climatological baseline influences metrics, trends, and forecasts and should be tailored to the research question (Oliver et al., 2021). From the point of view of the impact of MHWs on marine ecosystems, the total heat stress and other metrics (Jacox et al., 2020; Li and Donner, 2022; Amaya et al., 2023) are essential to assess their potential severity in ecological terms. Detrending should thus not exclude such analysis mainly for marine organisms and ecosystems impacted by a total temperature change, since the response to a slow variation (changes in mean conditions) or abrupt changes (changes in variance or distribution's shape) differs (Smale and Wernberg, 2013; Garrabou et al., 2022; Smith et al., 2023). Therefore, both fixed and moving baselines can be employed separately or in conjunction to highlight the long timescale impacts (fixed baseline) and short timescale impacts (moving baseline) of extreme SST events.

In a warming ocean, a range of tools and approaches will be needed to document MWHs and their ecological impacts. As with other extreme events, naming and categorizing MHWs allows for straightforward communication (Hobday et al., 2018a). Real-time tracking and monitoring of MHWs also offer a communication opportunity. The advances in remote sensing and greater spatio-temporal coverage by *in situ* instruments are expected to be of considerable interest and potential value to marine managers and the tourism, fishing, and aquaculture industries (Oliver et al., 2021). Improved forecasting will inform short-term management actions to reduce the risk to ecosystems or related services on timescales of days to seasons (Spillman et al., 2021). On longer timescales, societal or biological adaptation measures can help alleviate negative impacts in the future. Additionally, combining predictive forecasting with experimental approaches that identify species-level physiological tipping points may increase our ability to predict responses to future MHWs (Smith et al., 2023). Developing such an understanding will enable identification of both high-risk areas and potential climatic refugia, which will be fundamental for conservation actions such as building climate-resilient marine protected areas and protecting range-shift corridors (Burrows et al. 2014; Verdura et al. 2021). Recent developments are enhancing understanding of the physical mechanisms

that give rise to MHWs, which underpin prediction systems of MHWs (Jacox et al., 2020).

MHWs, as extreme events with dramatic effects, can help scientists, policy makers, and the public build understanding about the urgency of response to long-term environmental change (Oliver et al., 2021). A key challenge will thus be to elucidate drivers of MHW events in a changing climate, allowing a tailored detection for biological, physical or environmental impact studies. Ultimately, to mitigate future impacts of MHWs, which will intensify because of anthropogenic climate change (Frölicher et al. 2018; Oliver et al. 2018a; Guo et al., 2022), rapid measures to reduce greenhouse gas emissions or increase rates of carbon capture and storage are needed.

CONCLUSION

In conclusion, this study shows that the presence of a trend in Adriatic Sea surface temperatures can drive MHW detection toward more frequent and long-lasting marine heatwaves events. Conversely, the detrended procedure allows separating the effect of a continuous warming from extreme variations without overestimating MHW metrics over time. We highlight that the characterization of MHWs is sensitive to the presence of underlying trends and the definition of reference conditions upon which MHWs are identified is crucial. In line with the recent literature, we suggest that detrending is conceived to define more properly a fixed climatology baseline in an evolving ocean with rising temperatures. However, detrending should not substitute or exclude the analysis based on the total heat stress (a combination of the warming trend and marine heatwave), which is necessary to assess the impacts on marine organisms and ecosystems.

References

Alexander, M.A., Scott, J.D., Deser, C., (2000). Processes that influence sea surface temperature and ocean mixed layer depth variability in a coupled model. Journal of Geophysical Research: Oceans, 105:16823–42.

Amaya, D.J., Miller, A.J., Xie, S.-P., Kosaka, Y., (2020). Physical drivers of the summer 2019 North Pacific marine heatwave. Nature Communications, 11:1903.

Amaya, D.J., Jacox, MG.., Fewings, M.R., Saba, V.S., Malte, M.F., Rykaczewski, R.R., Ross, A.C., Stock, C.A., Capotondi, A., Petrik, C.M., Bograd, S.J., Alexander, M.A., Cheng, W., Hermann, A.J., Kearney, K.A., Powell, B.S., (2023). Marine heatwaves need clear definitions so coastal communities can adapt. Nature 616:29–32.

Arias-Ortiz, A., Serrano, O., Masqué, P., Lavery, P.S., Mueller, U., Kendrick, G.A., Rozaimi, M., Esteban, A., Fourqurean, J.W., Marbà, N., Mateo, M.A., Murray, K., Rule, M.J., Duarte, C.M., (2018). A marine heatwave drives massive losses from the world's largest seagrass carbon stocks. Nature Climate Change, 8:338–344.

Artegiani, A., Bregant, D., Paschini, E., Pinardi, N., Raicich, F., Russo, A., (1997a). The Adriatic Sea general circulation. Part I: air-sea interactions and water mass structure. Journal of Physical Oceanography, 27:1492–1514.

Artegiani, A., Bregant, D., Paschini, E., Pinardi, N., Raicich, F., Russo, A., (1997b). The Adriatic Sea general circulation. Part II: baroclinic circulation structure. Journal of Physical Oceanography, 27:1515–1532.

Begon, M., Townsend, C.R., (2020). Ecology: From Individuals to Ecosystems. Oxford, UK: Wiley & Sons. 5th ed.

Bensoussan, N., Chiggiat, J., Buongiorno Nardelli, B., Pisano, A., Garrabou, J., (2019). Insights on 2017 marine heat waves in the Mediterranean Sea. Copernicus Marine Service Ocean State Report, Issue 3. Journal of Operational Oceanography, 12:26–30.

Benthuysen, J.A., Feng, M., Zhong, L., (2014). Spatial patterns of warming off Western Australia during the 2011 Ningaloo Niño: quantifying impacts of remote and local forcing. Continental Shelf Research, 91:232–46.

Benthuysen, J.A., Oliver, E.C.J., Feng, M., Marshall, A.G., (2018). Extreme marine warming across tropical Australia during austral summer 2015–2016. Journal of Geophysical Research: Oceans, 123:1301–26.

Benthuysen, J.A., Oliver, E.C.J., Chen, K., Wernberg, T., (2020). Editorial: advances in understanding marine heatwaves and their impacts. Frontiers in Marine Science, 7:1.

Bergamasco, A., Oguz, T., Malanotte-Rizzoli, P., (1999). Modelling dense water mass formation and winter circulation in the northern and central Adriatic Sea. Journal of Marine Systems, 20:279–300.

Beşel, C., Tanir Kayikçi, E., (2020). Investigation of black sea mean sea level variability by singular spectrum analysis. International Journal of Engineering and Geosciences, 5:33–41.

Black, E., Blackburn, M., Harrison, R.G., Hoskins, B.J., Methven, J., (2004). Factors contributing to the summer 2003 European heatwave. Royal Meteorological Society, 59:217–223.

Bond, N.A., Cronin, M.F., Freeland, H., Mantua, N., (2015). Causes and impacts of the 2014 warm anomaly in the NE Pacific. Geophysical Research Letters, 42:3414–3420.

Brush, M.J., Giani, M., Totti, C., Testa, J.M., Faganeli, J., Ogrinc, N., Kemp, W.M., Fonda Umani, S., (2021). Eutrophication, harmful algae, oxygen depletion, and acidification. In: Malone, T.C., Malej, A., Faganeli, J. (Eds.), Coastal Ecosystems in Transition: A Comparative Analysis of the Northern Adriatic and Chesapeake Bay. Geophysical Monograph, 256:75–104.

Burrows, M.T., Schoeman, D.S., Richardson, A.J., Molinos, J.G., Hoffmann, A., (2014). Geographical limits to species-range shifts are suggested by climate velocity. Nature, 507:492–95.

Campanelli, A., Grilli, F., Paschini, E., Marini, M., (2011). The influence of an exceptional Po River flood on the physical and chemical oceanographic properties of the Adriatic Sea. Dynamics of Atmosphere and Oceans, 52:284–297.

Caputi, N., Kangas, M.I., Denham, A., Feng, M., Pearce, A., Hetzel, Y., Chandrapavan, A., (2016). Management adaptation of invertebrate fisheries to an extreme marine heat wave event at a global warming hot spot. Ecology and Evolution, 6:3583–93.

Cavole, L.M., Demko, A.M., Diner, R.E., Giddings, A., Koester, I., Pagniello M.L.S., Paulsen M.L., Ramirez-Valdez A., Schwenck S.M., Yen, N.K., Zill, M.E., Franks P.J.S., (2016). Biological impacts of the 2013–2015 warm-water anomaly in the northeast Pacific: winners, losers, and the future. Oceanography, 29:273–85.

Cerrano, C., Bavestrello, G., Bianchi, C.N., Cattaneo-Vietti, R., Bava, S., Morganti, C., Morri, C., Picco, P., Sara, G., Schiaparelli, S., Siccardi, A., Sponga, F., (2000). Catastrophic mass-mortality episode of gorgonians and other organisms in the Ligurian Sea (North-Western Mediterranean), summer 1999. Ecology Letters, 3:284–293.

Chafik, L., Nilsen, J.E.Ø., Dangendorf, S., (2017). Impact of North Atlantic teleconnection patterns on Northern European sea level. Journal of Marine Science and Engineering, 5:43.

Chen, K., Gawarkiewicz, G.G., Lentz, S.J., Bane, J.M., (2014). Diagnosing the warming of the northeastern U.S. coastal ocean in 2012: a linkage between the atmospheric jet stream variability and ocean response. Journal of Geophysical Research: Oceans, 119:218–27.

Chen, K., Gawarkiewicz, G., Kwon, Y.O., and Zhang, W.G., (2015). The role of atmospheric forcing versus ocean advection during the extreme warming of the Northeast U.S. continental shelf in 2012. Journal of Geophysical Research: Oceans, 120:4324–4339.

Chiswell, S.M., (2022). Global trends in marine heatwaves and cold spells: the impacts of fixed versus changing baselines. Journal of Geophysical Research: Oceans, 127:e2022JC018757.

Ciappa, A.C., (2022). Effects of marine heatwaves (MHW) and cold spells (MCS) on the surface warming of the Mediterranean Sea from 1989 to 2018. Progress in Oceanography, 205:102828.

Coleman, M.A., Wernberg, T., (2020). The silver lining of extreme events. Trends in Ecology & Evolution, 35:1065–67.

Coma, R., Ribes, M., Serrano, E., Jiménez, E., Salat, J., Pascual, J., (2009). Global warming-enhanced stratification and mass mortality events in the Mediterranean. Proceedings of the National Academy Science, USA, 106:6176–6181.

Cozzi, S., Giani, M., (2011). River water and nutrient discharges in the Northern Adriatic Sea: current importance and long-term changes. Continental Shelf Research, 31:1881–1893.

Cronin, M.F., Gentemann, C.L., Edson, J.B., Ueki, I., Bourassa, M., Brown, S., Clayson, C.A., Fairall, C.W., (2019). Air-sea fluxes with a focus on heat and momentum. Frontiers in Marine Science, 6:430.

Darmaraki, S., Somot, S., Sevault, F., Nabat, P., (2019a). Past variability of Mediterranean Sea marine heatwaves. Geophysical Research Letters, 46:9813–9823.

Darmaraki, S., Somot, S., Sevault, F., Nabat, P., Cabos Narvaez, W.D., Cavicchia, L., Djurdjevic, V., Li, L., Sannino, G., Sein, D.V., (2019b). Future evolution of marine heatwaves in the Mediterranean Sea. Climate Dynamics, 53:1371–1392.

Dayan, H., McAdam, R., Juza, M., Masina, S., Speich, S., (2023). Marine heat waves in the Mediterranean Sea: an assessment from the surface to the subsurface to meet national needs. Frontiers of Marine Science, 10:1045138.

DeCastro, M., Gómez-Gesteira, M., Costoya, X., Santos, F., (2014). Upwelling influence on the number of extreme hot SST days along the Canary upwelling ecosystem. Journal of Geophysical Research: Oceans, 119:3029–40.

Degobbis, D., Precali, R., Ivancic, I., Smodlaka, N., Fuks, D., Kveder, S., (2000). Long-term changes in the northern Adriatic ecosystem related to anthropogenic eutrophication. International Journal of Environment and Pollution, 13:495–533.

Deser, C., Alexander, M.A., Xie, S.P., Phillips, A.S., (2010). Sea surface temperature variability: patterns and mechanisms. Annual Review of Marine Science, 2:115–43.

Di Lorenzo, E., Mantua, N., (2016). Multi-year persistence of the 2014/15 North Pacific marine heatwave. Nature Climate Change, 6:1042–47.

Doi, T., Behera, S., Yamagata, T., (2013). Predictability of the Ningaloo Niño/Niña. Scientific Reports, 3:2892.

Doney, S.C., Ruckelshaus, M., Emmett Duffy, J., Barry, J.P., Chan, F., English, C.A., Galindo, H.M., Grebmeier, J.M., Hollowed, A.B., Knowlton, N., Polovina, J., Rabalais, N.N., Sydeman, W.J., Talley, L.D., (2012). Climate change impacts on marine ecosystems. Annual Review of Marine Science, 4:11–37.

Donner, S.D., Skriving, W.J., Little, C.M., Oppenheimer, M., Hoegh-Guldberg, O., (2005). Global assessment of coral bleaching and required rates of adaptation under climate change. Global Change Biology, 11:2251–2265.

DuMouchel, W.H., F.L. O'Brien., (1989). “Integrating a Robust Option into a Multiple Regression Computing Environment.” Computer Science and Statistics: Proceedings of the 21st Symposium on the Interface. Alexandria, VA: American Statistical Association.

Dunn, R.J., and Morice, C.P., (2022). On the effect of reference periods on trends in percentile-based extreme temperature indices. Environmental Research Letters, 17:034026.

Eakin, C.M., Morgan, J.A., Heron, S.F., Smith, T.B., Liu, G., (2010). Caribbean corals in crisis: record thermal stress, bleaching, and mortality in 2005. PLOS ONE, 5:e13969.

Eakin, C.M., Sweatman, H.P.A., Brainard, R.E., (2019). The 2014–2017 global-scale coral bleaching event: insights and impacts. Coral Reefs, 38:539–45.

Echevin, V., Colas, F., Espinoza-Morriberon, D., Vasquez, L., Anculle, T., Gutierrez, D., (2018). Forcings and evolution of the 2017 coastal El Niño off Northern Peru and Ecuador. Frontiers in Marine Science, 5:3.

Elzahaby, Y., Schaeffer, A., (2019). Observational insight into the subsurface anomalies of marine heatwaves. Frontiers in Marine Science, 6:745.

Eyring, V., Bony, S., Meehl, G.A., Senior, C.A., Stouffer, R.J., Taylor, K.E., (2016). Overview of the Coupled Model Intercomparison Project Phase 6 (CMIP6) experimental design and organization. Geoscientific Model Development, 9:1937– 58.

Faranda, D., Pascale, S., Bulut, B., (2023). Persistent anticyclonic conditions and climate change exacerbated the exceptional 2022 European-Mediterranean drought. Environmental Research Letters, 18:034030.

Feng, M., McPhaden, M. J., Xie, S. P., Hafner, J., (2013). La Niña forces unprecedented Leeuwin Current warming in 2011. Scientific Reports, 3:1277.

Fewings, M.R., Brown, K.S., (2019). Regional structure in the marine heat wave of summer 2015 off the western United States. Frontiers in Marine Science, 6:564.

Field, C.B., Barros, V., Stocker, T.F., Dahe, Q., Dokken, D.J., (2012). Managing the Risks of Extreme Events and Disasters to Advance Climate Change Adaptation: Special Report of the Intergovernmental Panel on Climate Change. Cambridge, UK: Cambridge Univ. Press.

Fordyce, A.J., Ainsworth, T.D., Heron, S.F., Leggat, W., (2019). Marine heatwave hotspots in coral reef environments: physical drivers, ecophysiological outcomes and impact upon structural complexity. Frontiers in Marine Science, 6:498.

Frankignoul, C., (1985). Sea surface temperature anomalies, planetary waves, and air-sea feedback in the middle latitudes. Review of Geophysics, 23:357–90.

Frölicher, T.L., Fischer, E.M., Gruber, N., (2018). Marine heatwaves under global warming. Nature, 560:360–64.

Frölicher, T.L., Laufkötter, C., (2018). Emerging risks from marine heat waves. Nature Communications, 9:650.

Galli, G., Solidoro, C., Lovato, T., (2017). Marine heat waves hazard 3D maps, and the risk for low motility organisms in a warming Mediterranean Sea. Frontiers in Marine Science, 4:136.

Garrabou, J., Perez, T., Sartoretto, S., & Harmelin, J., (2001). Mass mortality event in red coral *Corallium rubrum* populations in the provence region (France, NW Mediterranean). Marine Ecology Progress Series, 217:263–272.

Garrabou, J., Coma, R., Bensoussan, N., Bally, M., Chevaldonné, P., Cigliano, M., (2009). Mass mortality in Northwestern Mediterranean rocky benthic communities: effects of the 2003 heat wave. Global Change Biology, 15:1090–1103.

Garrabou, J., Gómez-Gras, D., Ledoux, J.B., Linares, C., Bensoussan, N., (2019). Collaborative database to track mass mortality events in the Mediterranean Sea. Frontiers in Marine Science, 6:707.

Garrabou, J., Gómez-Gras, D., Medrano, A., Cerrano, C., Ponti, M., Schlegel, R., (2022). Marine heatwaves drive recurrent mass mortalities in the mediterranean sea. Global Change Biology, 28:5708–5725.

Genin, A., Levy, L., Sharon, G., Raitsos, D.E., Diamant, A., (2020). Rapid onsets of warming events trigger mass mortality of coral reef fish. PNAS, 117:25378–85.

Gentemann, C.L., Fewings, M.R., García-Reyes, M., (2017). Satellite sea surface temperatures along the West Coast of the United States during the 2014–2016 northeast Pacific marine heat wave. Geophysical Research Letters, 44:312–319.

Ghil, M., Vautard, R., (1991). Interdecadal oscillations and the warming trend in global temperature time series. Nature, 350:324–327.

Giorgi, F., (2006). Climate change hot-spots. Geophysical Research Letters, 33:L08707.

Gómez-Gras, D., Linares, C., Dornelas, M., Madin, J.S., Brambilla, V., Ledoux, J.B., Sendino P.L., Bensoussan N., Garrabou, J., (2021a). Climate change transforms the functional identity of Mediterranean coralligenous assemblages. Ecology Letters, 24:1038–51.

Golyandina, N., Nekrutkin, V., (2001). Analysis of time series Structure: SSA and related techniques (Andover, England, UK: Taylor & Francis).

Golyandina, N., Zhigljavsky, A., (2013). Singular spectrum analysis for time series. (Heilderberg New York Dordrecht London: Springer).

Grilo, T.F., Cardoso, P.G., Dolbeth, M., Bordalo, M.D., Pardal, M.A., (2011). Effects of extreme climate events on the macrobenthic communities' structure and functioning of a temperate estuary. Marine Pollution Bulletin, 62:303–11.

Guinaldo, T., Voldoire, A., Waldman, R., Saux Picart, S., Roquet, H., (2023). Response of the sea surface temperature to heatwaves during the France 2022 meteorological summer. Ocean Science, 19:629–47.

Guo, X., Gao, Y., Zhang, S., Wu, L., Chang, P., Cai, W., Zscheischler, J., Leung, L.R., Small, J., Danabasoglu, G., Thompson, L., Gao, H., (2022). Threat by marine heatwaves to adaptive large marine ecosystems in an eddy-resolving model. Nature Climate Change, 12:179–186.

Hamdeno, M., Alvera-Azcaràte, A., (2023). Marine heatwaves characteristics in the Mediterranean Sea: Case study the 2019 heatwave events. Frontiers of Marine Science, 10:1093760.

Hansen, J., Ruedy, R., Sato, M., and Lo, K., (2010). Global surface temperature change. Reviews of Geophysics, 48:1–3.

Harris, R.M., Beaumont, L.J., Vance, T.R., Tozer, C.R., Remenyi, T.A., (2018). Biological responses to the press and pulse of climate trends and extreme events. Nature Climate Change, 8:579–87.

Hassani, H., (2007). Singular spectrum analysis: methodology and comparison. Journal of Data Science.

He, Y., Zhang, B., Xia, Z., Wang, S., Guan, X., (2023). Global warming has increased the distance traveled by marine heatwaves. Geophysical Research Letters, 50:e2022GL102032.

Helmuth, B., Mieszkowska, N., Moore, P.J., Hawkins, S.J., (2006). Living on the edge of two changing worlds: forecasting the responses of intertidal ecosystems to climate change. Annual Review of Ecology, Evolution, and Systematics, 37:373– 404.

Hobday, A.J., Alexander, L.V., Perkins, S.E., Smale, D.A., Straub, S.C., Oliver E.C.J., Benthuysen, J.A., Burrows, M.T., Donat, M.G., Feng, M., Holbrook, N.J., Moore, P.J., Scannell, H.A., Sen Gupta, A., Wernberg, T., (2016). A hierarchical approach to defining marine heatwaves. Progress in Oceanography, 141:227–38.

Hobday, A.J., Oliver, E.C.J., Sen Gupta, A., Benthuysen, J.A., Burrows, M.T., Donat, M.G., Holbrook, N.J., Moore, P.J., Thomsen, M.S., Wernberg, T., Smale, D.A., (2018a). Categorizing and naming marine heatwaves. Oceanography, 31:162–73.

Holbrook, N.J., Scannell, H.A., Sen Gupta, A., Benthuysen, J.A., Feng, M., Oliver, E.C.J, Alexander, L.V., Burrows, M.T., Donat, M.G., Hobday, A.J., Moore, P.J., Perkins-Kirkpatrick, S.E., Smale, D.A., Straub, S.C., Wernberg, T., (2019). A global assessment of marine heatwaves and their drivers. Nature Communications, 10:2624.

Holbrook, N.J., Sen Gupta, A., Oliver, E.C., Hobday, A.J., Benthuysen, J.A., Scannell, H.A., Smale, D.A., Wernberg, T., (2020). Keeping pace with marine heatwaves. Nature Reviews Earth & Environment, 1:482–493.

Holland, P.W., R.E. Welsch., (1977). “Robust Regression Using Iteratively Reweighted Least-Squares.” Communications in Statistics: Theory and Methods, A6:813–827.

Hu, D., Wu, L., Cai, W., Sen Gupta, A., Ganachaud, A., Qiu, B., (2015). Pacific western boundary currents and their roles in climate. Nature 522:299–308.

Hu, S., Li, S., Zhang, Y., Guan, C., Du, Y., Feng, M., Ando, K., Wang, F., Schiller, A., Hu, D., (2021). Observed strong subsurface marine heatwaves in the tropical western Pacific Ocean. Environmental Research Letters, 16:104024.

Huete-Stauffer, C., Vielmini, I., Palma, M., Navone, A., Panzalis, P., Vezzulli, L., Misic, C., Cerrano, C., (2011). *Paramuricea clavata* (anthozoa, octocorallia) loss in the marine protected area of tavolara (sardinia, italy) due to a mass mortality event. Marine Ecology, 32:107–11.

Hughes, T.P., Kerry, J., Álvarez-Noriega, M., (2017). Global warming and recurrent mass bleaching of corals. Nature, 543:373–377.

Hughes, T.P., Kerry, J.T., Connolly, S.R., Álvarez-Romero, J.G., Eakin, C., (2021). Emergent properties in the responses of tropical corals to recurrent climate extremes. Current Biology, 31:5393–99.

Ibrahim, O., Mohamed, B., and Nagy, H., (2021). Spatial variability and trends of marine heat waves in the Eastern Mediterranean sea over 39 years. Journal of Marine Science and Engineering, 9:643.

IPCC. Summary for Policymakers. In: Climate Change 2021: The Physical Science Basis 3−32 (Cambridge Univ. Press, 2021).

Jacox, M.G., (2019). Marine heatwaves in a changing climate. Nature, 571:485-87.

Jacox, M.G., Alexander, M., Bograd, S., Scott, J., (2020). Thermal displacement by marine heatwaves. Nature, 584:82–86.

Johnson, M.R., Williams, S.L., Lieberman, C.H., Solbak, A., (2003). Changes in the abundance of the seagrasses *Zostera marina* L. (eelgrass) and *Ruppia maritima* L. (widgeongrass) in San Diego, California, following an El Niño event. Estuaries, 26:106–15.

Josey, S.A., Schroeder, K., (2023). Declining winter heat loss threatens continuing ocean convection at a Mediterranean dense water formation site Environmental Research Letters, 18:024005.

Juza, M., Tintoré, J., (2021). Multivariate sub-regional ocean indicators in the Mediterranean sea: from event detection to climate change estimations. Frontiers in Marine Science, 8:610589.

Juza, M., Fernández-Mora, À., Tintoré, J., (2022) Sub-Regional marine heat waves in the Mediterranean Sea from observations: Long-term surface changes, Sub-surface and coastal responses. Frontiers in Marine Science, 9:785771.

Kataoka, T., Tozuka, T., Yamagata, T., (2017). Generation and decay mechanisms of Ningaloo Niño/Niña. Journal of Geophysical Research: Oceans, 122:8913–32.

Kendall, M. (1948). Rank correlation methods (London: Charles Griffin).

Kendrick, G.A., Nowicki, R., Olsen, Y.S., Strydom, S., Fraser, M.W., (2019). A systematic review of how multiple stressors from an extreme event drove ecosystem-wide loss of resilience in an iconic seagrass community. Frontiers of Marine Science, 6:455.

Kersting, D.K., Bensoussan, N., Linares, C., (2013). Long-term responses of the endemic reef-builder *Cladocora caespitosa* to Mediterranean warming. PLOS ONE, 8:1–12.

King, N.G., McKeown, N.J., Smale, D.A., Moore, P.J., (2018). The importance of phenotypic plasticity and local adaptation in driving intraspecific variability in thermal niches of marine macrophytes. Ecography, 41:1469–84.

Korak, S., Xuepeng, Z., Huai-min, Z., Kenneth, S.C., Dexin, Z., Sheekela, B.Y., Kilpatrick, K.A., Evans, R.H., Ryan, T., Relph, J.M., (2018). AVHRR Pathfinder version 5.3 level 3 collated (L3C) global 4km sea surface temperature for 1981-Present. NOAA National Centers for Environmental Information: Asheville, NC, USA.

Le Grix, N., Zscheischler, J., Laufkötter, C., Rousseaux, C. S., and Frölicher, T. L., (2021). Compound high-temperature and low-chlorophyll extremes in the ocean over the satellite period. Biogeosciences, 18:2119–2137.

Le Traon, P. Y., Reppucci, A., Alvarez Fanjul, E., Aouf, L., Behrens, A., Belmonte, M., (2019). From observation to information and users: the Copernicus marine service perspective. Frontiers of Marine Science, 6.

Lemoine, N.P., Burkepile, D.E., (2012). Temperature-induced mismatches between consumption and metabolism reduce consumer fitness. Ecology, 93:2483–89.

Lenanton, R.C.J., Dowling, C.E., Smith, K.A., Fairclough, D.V., Jackson, G., (2017). Potential influence of a marine heatwave on range extensions of tropical fishes in the eastern Indian Ocean-Invaluable contributions from amateur observers. Regional Studies in Marine Science, 13:19–31.

Li, X., Donner, S.D., (2022). Lengthening of warm periods increased the intensity of warm-season marine heatwaves over the past 4 decades. Climate Dynamics, 59:2643–2654.

Ling, S., Johnson, C., Ridgway, K., Hobday, A., Haddon, M., (2009). Climate-driven range extension of a sea urchin: inferring future trends by analysis of recent population dynamics. Global Change Biology, 15:719–31.

Lionello, P., Scarascia, L., (2018). The relation between climate change in the Mediterranean region and global warming. Regional Environmental Change, 18:1481– 1493.

Liu, G., Heron, S.F., Eakin, C.M., Muller-Karger, F.E., Vega-Rodriguez, M., (2014). Reef-scale thermal stress monitoring of coral ecosystems: new 5-km global products from NOAA Coral Reef Watch. Remote Sensing, 6:11579–606.

Liu, Y., Sun, C., Li, J., (2022). The boreal summer zonal wavenumber-3 trend pattern and its connection with surface enhanced warming. Journal of Climate, 35:833–50.

Macias, D., Garcia-Gorriz, E., Stips, A., (2013). Understanding the causes of recent warming of Mediterranean waters. How much could be attributed to climate change? PLoS One, 8:e81591.

Macias, D., Stips, A., Garcia-Gorriz, E., (2014). Application of the singular spectrum analysis technique to study the recent hiatus on the global surface temperature record. PLoS One, 9:1–7.

Mann, H., (1945). Non-parametric tests against trend. Econometrica, 13:163–171.

Margirier, F., Testor, P., Heslop, E., (2020). Abrupt warming and salinification of intermediate waters interplays with decline of deep convection in the Northwestern Mediterranean Sea. Scientific Reports, 10:20923.

Marini, M., Russo, A., Paschini, E., Grilli, F., Campanelli, A., (2006). Short-term physical and chemical variations in the bottom water of middle Adriatic depressions. Climate Research, 31:227–237.

Marini, M., Jones, B.H., Campanelli, A., Grilli, F., Lee, C.M., (2008). Seasonal variability and Po River plume influence on biochemical properties along western Adriatic coast. Journal of Geophysical Research: Oceans, 113:1–18.

Martínez, J., Leonelli, F.E., García-Ladona, E., Garrabou, J., Kersting, D.K., Bensoussan, N., Pisano, A., (2023). Evolution of marine heatwaves in warming seas: the Mediterranean Sea case study. Frontiers of Marine Science, 10:1193164.

Marullo, S., Artale, V., Santoleri, R., (2011). The SST multidecadal variability in the Atlantic–Mediterranean region and its relation to AMO. Journal of Climate, 24:4385–401.

Marullo, S., Serva, F., Iacono, R., Napolitano, E., Di Sarra, A., Meloni, D., Monteleone, F., Sferlazzo, D., De Silvestri, L., De Toma, V., Pisano, A., Bellacicco, M., Landolfi, A., Organelli, E., Yang, C., Santoleri, R., (2023). Record-breaking persistence of the 2022/23 marine heatwave in the Mediterranean Sea. Environmental Research Letters, 18:114041.

Marx, W., Haunschild, R., and Bornmann, L., (2021). Heat waves: a hot topic in climate change research. Theor. Applied Climatology, 146:781–800.

Mavrakis, A.F., Tsiros, I.X., (2019). The abrupt increase in the Aegean sea surface temperature during June 2007 – a marine heatwave event? Weather 74:201–207.

Maynard, J.A., Turner, P.J., Anthony, K.R.N., Baird, A.H., Berkelmans, R., Eakin, C.M., Johnson, J., Marshall, P.A., Packer, G.R., Rea, A., Willis, B.L., (2008). ReefTemp: an interactive monitoring system for coral bleaching using high-resolution SST and improved stress predictors. Geophysical Research Letters, 35:L05603.

McPhaden, M.J., (1999). Genesis and evolution of the 1997–98 El Niño. Science 283:950–954.

McPhaden, M.J., Zebiak, S.E., Glantz, M.H., (2006). ENSO as an integrating concept in earth science. Science, 314:1740–45.

Merchant, C.J., Embury, O., Bulgin, C.E., Block, T., Corlett, G.K., Fiedler, E., Eastwood, S. (2019). Satellite-based time-series of sea-surface temperature since 1981 for climate applications. Scientific data, 6:1-18.

Mills, K.E., Pershing, A.J., Brown, C.J., Chen, Y., Chiang, F.-S., Holland, D.S., Lehuta, S., Nye, J.A., Sun, J.C., Thomas, A.C., Wahle, R.A., (2013). Fisheries Management in a Changing Climate: Lessons from the 2012 ocean heat wave in the Northwest Atlantic. Oceanography, 26:191–195.

Mohamed, B., Abdallah, A. M., Alam El-Din, K., Nagy, H., Shaltout, M. (2019a). Inter-annual variability and trends of Sea level and Sea surface temperature in the Mediterranean Sea over the last 25 years. Pure and Applied Geophysics, 176:3787–3810.

Mohamed, B., Ibrahim, O., and Nagy, H., (2022a). Sea Surface temperature variability and marine heatwaves in the black Sea. Remote Sensing, 14:2383.

Moisan, J.R., Niiler, P.P., (1998). The seasonal heat budget of the North Pacific: net heat flux and heat storage rates (1950–1990). Journal of Physical Oceanography, 28:401–21.

Napp, J.M., Hunt, G.L., (2001). Anomalous conditions in the south-eastern Bering Sea 1997: linkages among climate, weather, ocean, and biology. Fisheries Oceanography, 10:61–68.

Olita, A., Sorgente, R., Natale, S., Gaberšek, S., Ribotti, A., Bonanno, A., Patti, B., (2007). Effects of the 2003 European heatwave on the Central Mediterranean Sea: surface fluxes and the dynamical response. Ocean Science, 3:273–89.

Oliver, E.C.J., Benthuysen, J.A., Bindoff, N.L., Hobday, A.J., Holbrook, N.J., Mundy, C.N., Perkins-Kirkpatrick, S.E., (2017). The unprecedented 2015/16 Tasman Sea marine heatwave. Nature Communications, 8:16101.

Oliver, E.C.J., Donat, M.G., Burrows, M.T., Moore, P.J., Smale, D.A., Alexander, L.V., Benthuysen, J.A., Feng, M., Sen Gupta, A., Hobday, A.J., Holbrook, N.J., Perkins-Kirkpatrick, S.E., Scannell, H.A., Straub, S.C., Wernberg, T., (2018a). Longer and more frequent marine heatwaves over the past century. Nature Communications, 9:1324.

Oliver, E.C.J., Burrows, M.T., Donat, M.G., Sen Gupta, A., Alexander, L.V., Perkins-Kirkpatrick, S.E., Benthuysen, J.A., Hobday, A.J., Holbrook, N.J., Moore, P.J., Thomsen, M.S., Wernberg, T., Smale, D.A., (2019). Projected marine heatwaves in the 21st century and the potential for ecological impact. Frontiers in Marine Science, 6:734.

Oliver, E.C.J., Benthuysen, J.A., Darmaraki, S., Donat, M.G., Hobday, A.J., Holbrook, N.J., Schlegel, R.W., Sen Gupta, A., (2021). Marine heatwaves. Annual Review of Marine Science, 13:313-342.

Overland, J.E., Bond, N.A., Adams, J.M., (2001). North Pacific Atmospheric and SST anomalies in 1997: Links to ENSO? Fisheries Oceanography, 10:69–80.

Palumbi, S.R., Barshis, D.J., Traylor-Knowles, N., Bay, R.A., (2014). Mechanisms of reef coral resistance to future climate change. Science 344:895–898.

Pastor, F., Valiente, J.A., Palau, J.L., (2017). Sea surface temperature in the Mediterranean: trends and spatial patterns (1982–2016). Pure and Applied Geophysics, 175:4017–4029.

Pastor, F., Valiente, J.A., Khodayar, S., (2020). A warming Mediterranean: 38 years of increasing sea surface temperature. Remote Sensing, 12:2687.

Pastor, F., Khodayar, S., (2023) Marine heat waves: characterizing a major climate impact in the Mediterranean. Science of the Total Environment, 861:160621.

Pearce, A.F., Lenanton, R., Jackson, G., Moore, J., Feng, M., Gaughan, D., (2011). The “marine heat wave” off Western Australia during the summer of 2010/11. Report Fisheries Research Report, 250.

Pearce, A.F., Feng, M., (2013). The rise and fall of the “marine heat wave” off Western Australia during the summer of 2010/2011. Journal of Marine Systems, 111:139–56.

Perez, T., Garrabou, J., Sartoretto, S., Harmelin, J. G., Francour, P., Vacelet, J., (2000). Mass mortality of marine invertebrates: An unprecedent event in the north occidental Mediterranean. Sciences de la Vie, 323:853–865.

Perkins-Kirkpatrick, S.E., Alexander, L.V., (2013). On the measurement of heat waves. Journal of Climate 26:4500–4517.

Perkins-Kirkpatrick, S.E., White, C.J., Alexander, L.V., Argueso, D., Boschat, G., Cowan, T., Evans, J.P., Ekstrom, M., Oliver, E.C.J., Phatak, A., Purich, A., (2016). Natural hazards in Australia: heatwaves. Climate Change 139:101–114.

Pettitt, A., (1979). A non-parametric approach to the change-point problem. Journal of the Royal Statistical Society: Applied Statistics, 28:126–135.

Philander, S.G.H., (1983). El Niño Southern Oscillation phenomena. Nature 302:295–301.

Pilo, G.S., Holbrook, N.J., Kiss, A.E., Hogg, A.M., (2019). Sensitivity of marine heatwave metrics to ocean model resolution. Geophysical Research Letters, 46:14604–12.

Pisano, A., Buongiorno Nardelli, B., Tronconi, C., Santoleri, R., (2016). The new Mediterranean optimally interpolated pathfinder AVHRR SST Dataset (1982–2012). Remote Sensing of Environment, 176:107–116.

Pisano, A., Marullo, S., Artale, V., Falcini, F., Yang, C., Leonelli, F.E., Santoleri, R., Buongiorno Nardelli, B., (2020). New evidence of Mediterranean climate change and variability from sea surface temperature observations. Remote Sensing, 12:132.

Podestá, G.P., Glynn, P.W., (2001). The 1997–98 El Niño event in Panama and Galápagos: an update of thermal stress indices relative to coral bleaching. Bulletin of Marine Science, 69:43–59.

Poulain, P.M., Cushman-Roisin, B., (2001). Circulation. In: Cushman-Roisin, B., Gacic, M., Poulain, P.M., Artegiani, A. (Eds.), Physical Oceanography of the Adriatic Sea: Past, Present and Future, 67–109.

Power, S., Delage, F., Wang, G., Smith, I., Kociuba, G., (2017). Apparent limitations in the ability of CMIP5 climate models to simulate recent multi-decadal change in surface temperature: implications for global temperature projections. Climate Dynamics, 49:53–69.

Rebert, J.P., Donguy, J.R., Eldin, G., Wyrtki, K., (1985). Relations between sea level, thermocline depth, heat content, and dynamic height in the tropical Pacific Ocean. Journal of Geophysical Research: Oceans 90:11719–11725.

Rey, J., Rohat, G., Perroud, M., Goyette, S., and Kasparian, J., (2020). Shifting velocity of temperature extremes under climate change. Environmental Research Letters, 15:034027.

Rivetti, I., Fraschetti, S., Lionello, P., Zambianchi, E., Boero, F., (2014). Global warming and mass mortalities of benthic invertebrates in the Mediterranean Sea. PloS One, 9:e115655.

Rossello´, P., Pascual, A., Combes, V., (2023). Assessing marine heat waves in the Mediterranean Sea: a comparison of fixed and moving baseline methods. Frontiers in Marine Science, 10:1168368.

Rouault, M., Illig, S., Bartholomae, C., Reason, C., Bentamy, A., (2007). Propagation and origin of warm anomalies in the Angola Benguela upwelling system in 2001. Journal of Marine Systems, 68:473–488.

Russo, A., Artegiani, A., (1996). Adriatic Sea hydrography. Scientia Marina, 60:33–43.

Ruthrof, K.X., Breshears, D.D., Fontaine, J.B., Froend, R.H., Matusick, G., Kala, J., (2018). Subcontinental heat wave triggers terrestrial and marine, multi-taxa responses. Science Reports, 8:13094.

Santora, J.A., Mantua, N.J., Schroeder, I.D., Field, J.C., Hazen, E.L., Bograd, S.J., Sydeman, W.J., Wells, B.K., Calambokidis, J., Saez, L., Lawson, D., Forney, K.A., (2020). Habitat compression and ecosystem shifts as potential links between marine heatwave and record whale entanglements. Nature Communications, 11:536.

Scannell, H.A., Pershing, A.J., Alexander, M.A., Thomas, A.C., Mills, K.E., (2016). Frequency of marine heatwaves in the North Atlantic and North Pacific since 1950. Geophysical Research Letters 43:2069–2076.

Schaeffer, A., Roughan, M., (2017). Subsurface intensification of marine heatwaves off southeastern Australia: the role of stratification and local winds. Geophysical Research Letters, 44:5025–5033.

Schiaparelli, S., Castellano, M., Povero, P., Sartoni, G., Cattaneo-Vietti, R., (2007). A benthic mucilage event in North-Western Mediterranean Sea and its possible relationships with the summer 2003 European heatwave: short term effects on littoral rocky assemblages. Marine Ecology, 28:341–353.

Schlegel, R.W., Oliver, E.C.J., Hobday, A.J., Smit, A.J., (2019). Detecting marine heatwaves with sub-optimal data. Frontiers of Marine Science, 6:737.

Schlegel, R.W., Oliver, E.C.J., Chen, K., (2021). Drivers of marine heatwaves in the Northwest Atlantic: the role of air–sea interaction during onset and decline. Frontiers of Marine Science, 8:627970.

Schoellhamer, D. H., (2001). Singular spectrum analysis for time series with missing data. Geophysical Research Letters, 28:3187–3190.

Selig, E.R., Casey, K.S., Bruno, J.F., (2010). New insights into global patterns of ocean temperature anomalies: implications for coral reef health and management. Global Ecology and Biogeography, 19:397–411.

Sen, P. K. (1968). Estimates of the regression coefficient based on kendall's tau. Journal of the American Statistical Association, 63:1379–1389.

Sen Gupta, A., McGregor, S., Van Sebille, E., Ganachaud, A., Brown, J.N., Santoso, A., (2016). Future changes to the Indonesian Throughflow and Pacific circulation: the differing role of wind and deep circulation changes. Geophysical Research Letters, 43:1669–1678.

Sen Gupta, A., Thomsen, M., Benthuysen, J.A., Hobday, A.J., Oliver, E., Alexander, L.V., (2020). Drivers and impacts of the most extreme marine heatwaves events. Science Reports, 10:19359.

Serrano, O., Arias-Ortiz, A., Duarte, C.M., Kendrick, G.A., Lavery, P.S., (2021). Impact of marine heatwaves on seagrass ecosystems. Ecosystem Collapse and Climate Change, 241:345-364.

Shanks, A.L., Rasmuson, L.K., Valley, J.R., Jarvis, M.A., Salant, C., Sutherland, D.A., Lamont, E.I., Hainey, M.A.H., Emlet, R.B., (2020). Marine heat waves, climate change, and failed spawning by coastal invertebrates. Limnology and Oceanography, 65:627–636.

Smale, D.A., Wernberg, T., (2009). Satellite-derived SST data as a proxy for water temperature in nearshore benthic ecology. Marine Ecology Progress Series 387:27–37.

Smale, D.A., Wernberg, T., (2013). Extreme climatic event drives range contraction of a habitat-forming species. Royal Society B: Biological Sciences, 280:20122829–20122829.

Smale, D.A., Yunnie, A.L.E., Vance, T., Widdicombe, S., (2015). Disentangling the impacts of heat wave magnitude, duration and timing on the structure and diversity of sessile marine assemblages. PeerJ 3:e863.

Smale, D.A., Wernberg, T., Oliver, E.C.J., Thomsen, M., Harvey, B.P., (2019). Marine heatwaves threaten global biodiversity and the provision of ecosystem services. Nature Climate Change, 9:306–312.

Smith, K.E., Burrows, M.T., Hobday, A.J., Sen Gupta, A., Moore, P.J., Thomsen, M., Wernberg, T., Smale, D.A., (2021). Socioeconomic impacts of marine heatwaves: global issues and opportunities. Science, 374:eabj3593.

Smith, K.E., Burrows, M.T., Hobday, A.J., King, N.G., Moore, P.J., Sen Gupta, A., Thomsen, M.S., Wernberg, T., Smale, D.A., (2023). Biological impacts of marine heatwaves. Annual Review of Marine Science, 15:119-145.

Sparnocchia, S., Schiano, M., Picco, P., Bozzano, R., Cappelletti, A., (2006). The anomalous warming of summer 2003 in the surface layer of the central Ligurian Sea (western Mediterranean). Annales Geophysicae, 24:443– 452.

Spillman, C., Alves, O., (2009). Dynamical seasonal prediction of summer sea surface temperatures in the Great Barrier Reef. Coral Reefs, 28:197–206.

Spillman, C., Alves, O., Hudson, D., (2013). Predicting thermal stress for coral bleaching in the Great Barrier Reef using a coupled ocean–atmosphere seasonal forecast model. International Journal of Climatology, 33:1001–1014.

Spillman, C., Smith, G.A., Hobday, A.J., Hartog, J.R., (2021). Onset and decline rates of marine heatwaves: global trends, seasonal forecasts, and marine management. Frontiers in Climate, 3:182.

Stella, J.S., Pratchett, M.S., Hutchings, P.A., Jones, G.P., (2011). Coral-associated invertebrates: diversity, ecological importance and vulnerability to disturbance. Oceanography and Marine Biology, 49:43–104.

Stocker, T.F., Qin, D., Plattner, G.K., Alexander, L.V., Allen, S.K., Bindoff, N.L., Bréon, F.M., Church, J.A., Cubasch, U., Emori, S., Forster, P., Friedlingstein, P., Gillett, N., Gregory, J.M., Hartmann, D.L., Jansen, E., Kirtman, B., Knutti, R., Krishna Kumar, K., Lemke, P., Marotzke, J., Masson-Delmotte, V., Meehl, G.A., Mokhov, I.I., Piao, S., Ramaswamy, V., Randall, D., Rhein, M., Rojas, M., Sabine, C., Shindell, D., Talley, L.D., Vaughan, D.G., Xie, S.P., (2013). Technical summary. In: Stocker, T.F., Qin, D., Plattner, G.-K., Tignor, M., Allen, S.K., Doschung, J., Nauels, A., Xia, Y., Bex, V., Midgley, P.M. (Eds.), Climate Change 2013. The Physical Science Basis. Contribution of Working Group I to the Fifth Assessment Report of the Intergovernmental Panel on Climate Change. Cambridge University Press, 33–115.

Taschetto, A.S., Sen Gupta, A., Jourdain, N.C., Santoso, A., Ummenhofer, C.C., England, M.H., (2014). Cold tongue and warm pool ENSO events in CMIP5: mean state and future projections. Journal of Climate, 27:2861–2885.

Thomsen, M.S., South, P., (2019). Communities and attachment networks associated with primary secondary and alternative foundation species; a case of stressed and disturbed stands of southern bull kelp. Diversity, 11:56.

Verdura, J., Linares, C., Ballesteros, E., Coma, R., Uriz, M.J., Bensoussan, N., Cebrian, E., (2019). Biodiversity loss in a Mediterranean ecosystem due to an extreme warming event unveils the role of an engineering gorgonian species. Science Reports, 9:5911.

Verdura, J., Santamaría, J., Ballesteros, E., Smale, D., Cefalì, M.E., (2021). Local-scale climatic refugia offer sanctuary for a habitat-forming species during a marine heatwave. Journal of Ecology, 109:1758–73.

Vergés, A., Steinberg, P.D., Hay, M.E., Poore, A.G., Campbell, A.H., (2014). The tropicalization of temperate marine ecosystems: climate-mediated changes in herbivory and community phase shifts. Proceedings of the Royal Society B, 281:20140846.

Vilibic, I., Supic, N., (2005). Dense water generation on a shelf: the case of the Adriatic Sea. Ocean Dynamics, 55:403–415.

Vogt, L., Burger, F.A., Griffies, S.M., Frölicher, T.L., (2022). Local Drivers of Marine Heatwaves: A Global Analysis With an Earth System Model. Frontiers in Climate, 4:847995.

Von Schuckmann, K., Le Traon, P.Y., Smith, N., Pascual, A., Djavidnia, S., Gattuso, J.P., (2020). Copernicus marine service ocean state report, issue 4. Journal of Operational Oceanography, 12:S1–S123.

Wernberg, T., Smale, D.A., Tuya, F., Thomsen, M.S., Langlois, T.J., De Bettignies, T., Bennet, S., Rousseaux, C.S., (2013). An extreme climatic event alters marine ecosystem structure in a global biodiversity hotspot. Nature Climate Change, 3:78–82.

Wernberg, T., Bennett, S., Babcock, R.C., Bettignies, T., de Cure, K., (2016). Climate-driven regime shift of a temperate marine ecosystem. Science, 353:169–172.

WMO (World Meteorological Organization, 2018). Guide to climatological practices. Doc. WMO-No. 100, WMO, Geneva.

Wu. L., Cai, W., Zhang, L., Nakamura, H., Timmermann, A., Joyce, T., McPhaden, M.J., Alexander, M., Qiu, B., Visbeck, M., Chang, P., Giese, B., (2012). Enhanced warming over the global subtropical western boundary currents. Nature Climate Change, 2:16.

Xu, T., Newman, M., Capotondi, A., Stevenson, S., Di Lorenzo, E., Alexander, M.A., (2022). An increase in marine heatwaves without significant changes in surface ocean temperature variability. Nature Communications, 13:7396.

Yi, S., Sneeuw, N., (2021). Filling the data gaps within GRACE missions using singular spectrum analysis. Journal of Geophysical Research: Solid Earth, 126:e2020JB021227.

Zhao, Z., Marin, M., (2019). A MATLAB toolbox to detect and analyze marine heatwaves. Journal of Open Source Software, 4:1124.